ESTIMATION OF GRAVITY TILT RESPONSE TO ATMOSPHERIC PHENOMENA AT THE FREDERICTON TILTMETRIC STATION USING A LEAST SQUARES RESPONSE METHOD

ROBIN R. STEEVES

September 1981

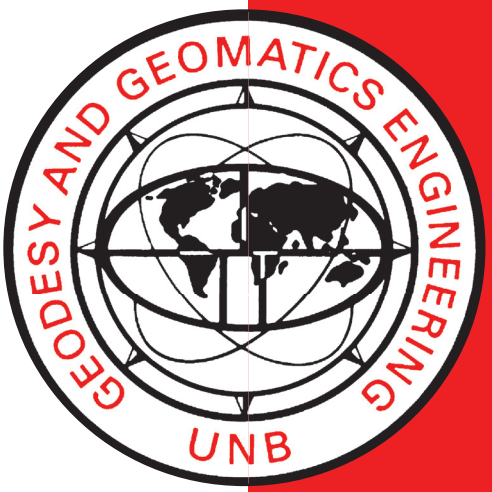

TECHNICAL REPORT
NO. 79

PREFACE

In order to make our extensive series of technical reports more readily available, we have scanned the old master copies and produced electronic versions in Portable Document Format. The quality of the images varies depending on the quality of the originals. The images have not been converted to searchable text.

ESTIMATION OF GRAVITY TILT RESPONSE TO ATMOSPHERIC PHENOMENA AT THE FREDERICTON TILTMETRIC STATION USING A LEAST SQUARES RESPONSE METHOD

BY

Robin R. Steeves

Department of Surveying Engineering

University of New Brunswick

Fredericton, N.B.

September, 1981

PREFACE

This report is an unaltered printing of the author's doctoral thesis, entitled "Estimation of Gravity Tilt Response to Atmospheric Phenomena at the Fredericton Tiltmetric Station Using a Least Squares Response Method", submitted to this Department in September, 1981.

The principle thesis advisor for this work was Dr. Petr Vanicek. Details of financial support and other assistance rendered are given in the acknowledgements.

ABSTRACT

Variations in the apparent direction of gravity, with respect to the tilting bedrock, at the Fredericton tiltmetric station have been observed, although somewhat intermittently, since 1974. Gaps in these observations account for over half of their overall time span. These tilt observations contain, among others, variations due to atmospheric pressure and surface temperature induced tilts. This work is concerned with modelling the response of the observed tilt, both for purposes of noise reduction and for understanding the phenomena themselves, to the atmospheric pressure and surface temperature variatiions, which are also observeed at this station.

As a preliminary evaluation of the collected tilt data, tidal analyses were performed for the purpose of estimating M_2 diminishing factors and testing ocean loading models which were supplied by Beaumont [1980]. This analysis also provided a means for testing the general performance of the Fredericton station and revealed a backlash effect of the recording apparatus on the recorded tilt.

Being confronted with the problem of estimating the response of an observed phenomenon to other observed phenomena, for the case of gappy and noisy data, directed this research towards the develoopment of a least squares response estimation method capable of handling such data. An evaluation of the existing techniques of cross spectral analysis and time domain convolution (see Appendix III) shows that these techniques are inadequate for our purposes. This least squares response method, developed in Chapter 4, has its basis in least

squares spectral analysis [Vanicek, 1971] which is reviewed also in Chapter 4. A statistical test of significance of peaks in the least squares spectrum was also derived during this work.

Application of the least squares response method to the Fredericton station data is discussed and summarized in Chapter 5. The results of this analysis indicates that more study is required in interpreting the response estimates in physical terms. However, apparently valid results for tilt response to surface temperature andatmospheric pressure are generated by the least squares response method from the very noisy data of the Fredericton station. In particular it is shown that atmospheric pressure induced tilts have magnitudes in excess of tidal tilts. Recommendations regarding future work at the Fredericton station are made.

TABLE OF CONTENTS

LIST OF TABLES

LIST OF FIGURES

ACKNOWLEDGEMENTS

This research was financially supported in part by the National Research Council of Canada (NSERC grant #A8300), the University of New Brunswick and the Maritime Provinces Higher Education Commission, to all of whom I am grateful.

I am deeply indebted to Dr. Petr Vanicek, my supervisor during this study, for his unfailing support and advice. I have benefited immensely from many enlightening discussions with Dr. Vanicek and for this I am truly grateful.

I also thank Dr. Don Bower, of the Earth Physics Branch, Energy, Mines and Resources, for his many discussions and especially his help with understanding the digitized data used in this research.

Discussions with many people have benefited this work; I would especially like to thank: Dr. Christopher Beaumont, of the Oceanography Department at Dalhousie University, who also kindly provided ocean loading data; Dr. Tony Lambert of the Earth Physics Branch, Energy, Mines and Resources; Dr. J.C. Harrison of the University of Colorado; Dr. Ken Burke of the Geology Department at U.N.B.; Dr. Dave Wells of the Surveying Engineering Department at U.N.B.; Dr. Charles Merry of the University of Natal, South Africa; Mr. Jack Gibson of the Data Acquisition Division, Canada Centre for Remote Sensing.

I would like to acknowledge the capable assistance of Mr. Burton Shaw and Mrs. Laura Mills for their help in data management and programming. I thank also the U.N.B. Computing Centre staff for their full cooperation during this work.

My sincere thanks are extended to Mrs. Debbie Smith whose typing, even under severe time constraints, was expertly and efficiently performed. Also I thank Teet Vahi for his excellence in the drawing of the figures.

Last, but certainly not least, I am deeply appreciative of the love and understanding given me by Mary-Lee, Jason and Jody to whom I dedicate this thesis. Without their support this study would not have been possible.

CHAPTER ONE

INTRODUCTION

Temporal variations of gravity, both in magnitude and direction, along witth the superimposed tilting of bedrock, have been observed and studied systematically at various centres around the world for several decades now. These variations are caused by various dynamic physical phenomena whose effects presently have varying degrees of understanding. The best understood variations are the direct tidal variations caused by the relative motions of the Sun-Earth-Moon system and to some extent the indirect tidal variations caused by the tidal loading of the oceans on the continental shores [Melchior, 1978]. Several other more localized phenomena, which will be briefly discussed in Chapter 2 of this report, also cause significant temporal variations of the local gravity vector. It is primarily these local phenomena and their effect on the apparent direction of the gravity vector which are studied here as they pertain

to the Fredericton tiltmetric station. By changes in the apparent direction of "gravity" or simply "direction of the local gravitty vector" we will hereafter mean the combined variations of the gravity vector ittself and the tilting of the bedrock on which our measuring instruments are situated.

These temporal variations or "tilts" of the direction of the local gravity vector have been observed, although somewhat intermittently, since 1974 at the Fredericton station. This station consists of a near surface vault of the type described by Beaumont et al [1970] in which two orthogonal Verbaandert-Melchior horizontal pendulums [Melchior, 1978] are operating. As well, measurements of local temperature and atmospheric pressure are continuously recorded.

A more detailed description of the station and its collected observations is given in Chapter 3 where we will see that the tilt observations are subject to various "noise" sources. By "noise" is meant a variation in the observations which is not of direct interest in a particular analysis. The word "signal" will be used to mean a variation which is of direct interest; see also Chapter 4. From a point of view of studying the ocean loading effect, for example, the variation of tilt caused by atmospheric pressure changes is considered as noise. As an example of the effect of atmospheric pressure and temperature on tilt, Figures 1.1 and 1.2 illustrate typical sections of these observations in which the tilt-pressure and tilt-temperature correlations are apparent. However, atmospheric pressure loading effects on tilt can be interesting from the geophysical point of view also [e.g. Beaumont & Lambert, 1972] and for purposes of their study, these effects become our signal. Both of these views are considered

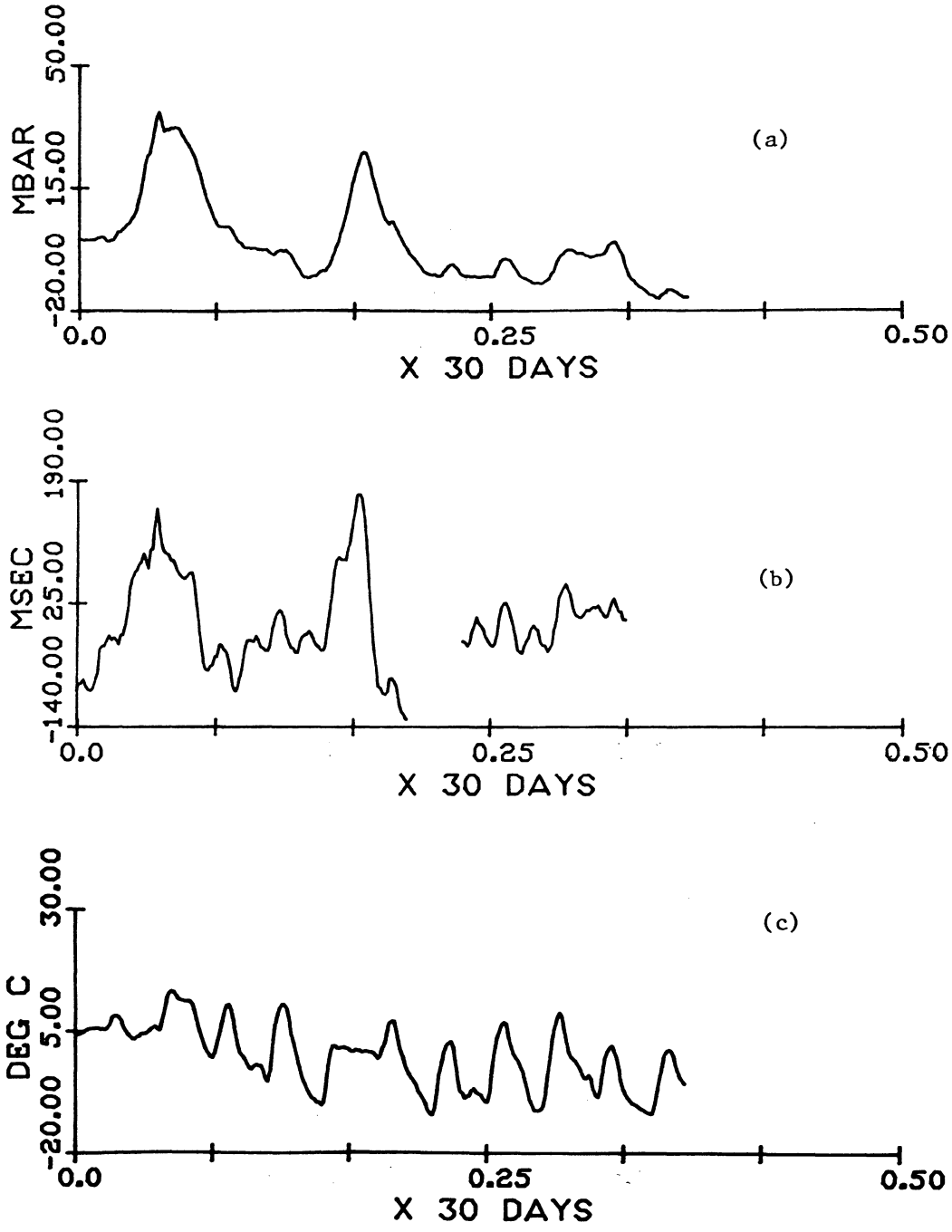

Figure 1.1. Plots of (a) atmospheric pressure (b) tilt and (c) surface temperature showing the effects of pressure and temperature on tilt. Time origin is Jan. 25, 1975. Pendulum azimuth is 118 degrees clockwise from north.

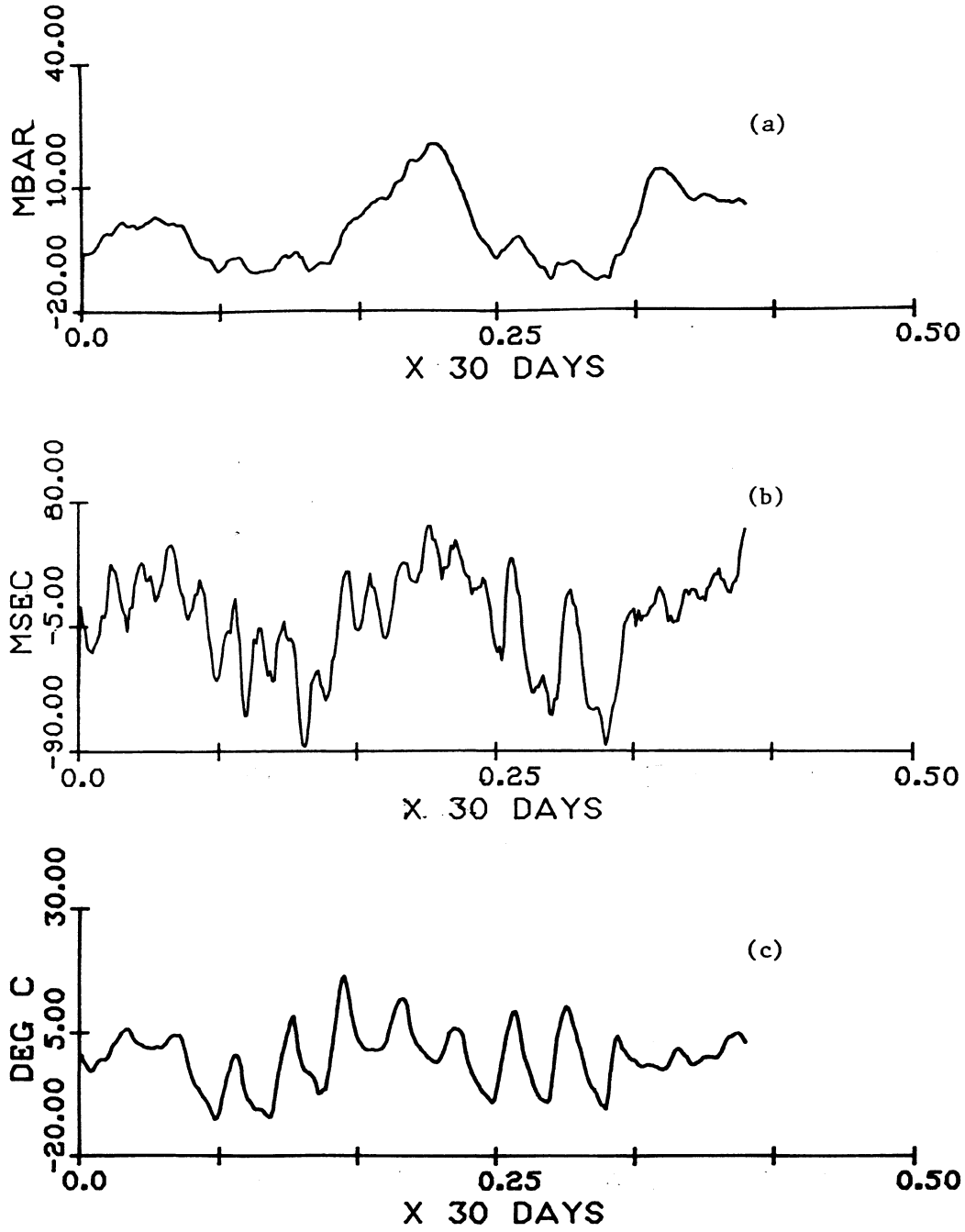

Figure 1.2. Plots of (a) atmospheric pressure, (b) tilt and (c) surface temperature showing the effects of pressure and temperature on tilt. Time origin is March 25, 1975. Pendulum azimuth is 208 degrees clockwise from north.

in this work with the emphasis on attempting to model the tilt variations caused by observed local atmospheric pressure and surface temperature variations, for purposes of understanding and quantifying these interactions themselves. The so determined model is then used in an attempt to enhance the signal to noise ratio for purposes of acquiring better estimates of other effects. This is in following the suggestion by Lennon and Baker (1973) that we should attend more closely to studying the local effects which instrumentation and techniques have shown themselves to be sensitive, rather than the global concept.

A major concern here is therefore a mathematical modelling of the "response" of an observed phenomenon, tilt, in our case, to certain observed forcing physical phenomena (e.g., atmospheric pressure variations). It is natural to model these physical interactions as a function of the frequency composition of the forcing phenomena (see Chapter 4). There are basically two types of existing methods, namely the cross spectral analysis and convolution in the time domain (see Appendix III) for performing such an analysis for the case in which there is no observation noise on the "input" forcing functions. These methods also require equally spaced data and continuous records. However, in our case we are dealing with observed input phenomena (i.e., with observational errors) and have to deal with gappy records and therefore may question the applicability of the existing methods for our purposes. This led to the development of an alternative approach based on assumptions in agreement with the actual characteristics of the data from which we wish to estimate the response charcteristics. This method, which we will call the "least

squares response method" has its basis in the method of least squares spectral analysis [Vanicek, 1971] and is presented in Chapter 4 along with a numerical example demonstrating its application.

In the remainder of this introductory chapter a brief general overview of motivations and aims of understanding observed tilt variations is used as a framework for discussing the context and contributions of this study.

1.1 Motivations and Aims of Understanding Observed Tilt Variations

Understanding observed tilt and problems associated with gaining this understanding can be of interest from at least three points of view, namely: geodetical, geophysical and mathematical.

The geodetic interest in observed tilt arises basically from the fact that these variations are perturbations of Earth's gravity field. These perturbations are affecting the geometry of the space in which geodetic observations are made and therefore corrections for these effects must be made. Even though tilts are only in the order of a few tens of milli-arcseconds, ignoring these effects, either in very precise geodetic work such as high order astronomical latitude and longitude determinations or in geodetic networks over extensive areas, can have serious systematic distorting effects. Although the direct body tidal effects are well enough understood so that analytical models for them may be used in correcting geodetic observations (e.g. Vanicek [1980a]), effects from other sources are not.

From the geophysical point of view, observed tilt can be used to learn more about the Earth's crustal and upper mantle elastic properties through estimating the tilt response to dynamic surface loads such as ocean tides, atmospheric pressure, precipitation,

changes in lake and reservoir levels, and recent changes in ice loads (Beaumont and Lambert [1972]). From this point of view the response of the Fredericton tiltmetric station to ocean loading and atmospheric pressure loading may provide valuable information.

From a mathematical modelling point of view, the problem of making a meaningful analysis of noisy, gappy data, making full use of all available auxilary data, is of interest in its own right. The Fredericton tilt data is of this variety, as is much of the data collected in experiments in other physical sciences, and has thus provided impetus for developing a response modelling technique capable of handling such data.

1.2 General Context and Contributions of this Study

This study represents the first documented, systematic analysis (including sorting and testing) and evaluation of at least part of the data collected at the Fredericton tiltmetric station; only preliminary analyses were performed previously (Bower [1980], Vanicek [1980b]). Therefore a contribution is made both to the experiment itself and to the collection of published results of similar studies.

As mentioned earlier, the present understanding of variations of tilt caused by local phenomena is not yet satisfactory, for either the purpose of understanding these interactions in their own right or for the purpose of noise reduction to allow more meaningful studies of other hidden phenomena of interest. Methods used in previous studies of this kind (see Chapter 2) have had varying degrees of success. In this work an alternative approach, using a least squares response method, is developed thus contributing another possible tool for this type of analysis especially in the case of noisy, gappy data.

A contribution is also made in a recasting of the method of least squares spectral analysis, as developed by Vanicek [1971], to include the consideration of an arbitrary covariance matrix of the time series (see Chapter 4). Also a statistical test of significance of peaks in the least squares spectrum was derived during this work (Steeves [1981]).

Another contribution is made by a combined testing of the Fredericton installation performance, testing of ocean loading models supplied by Beaumont [1980] and the computation of diminishing factors (see Sections 2.2 and 3.4) for the M_2 frequency at Fredericton.

In terms of improving our presently poor understanding of effects of local phenomena on observed tilt, especially for atmospheric pressure loading and temperature variations, a contribution is made by estimating at least preliminary models for these effects at the Fredericton station. Seemingly valid results for tilt response to temperature and pressure are generated by the least squares response analysis from very noisy data.

Finally, so that the modelling technique developed here can be applied easily by others the FORTRAN computer program which was developed during this work has been documented and is readily available from the Department of Surveying Engineering at U.N.B.

CHAPTER TWO

REVIEW OF THE PRESENT STATUS OF TILT OBSERVATIONS AND THEIR UNDERSTANDING

In this chapter an overview of the present status of tilt measurements and their understanding in terms of various physical forcing phenomena is given so that this study can be seen in a proper perspective. A brief summary of the best understood causes of tilt variations is given which leads naturally to a discussion of the present problems in interpreting the actually observed variations.

2.1 An Overview of the Present Status of Tilt Measurements

The publication by Lord Kelvin in 1863 of his theory on the tidal deformation of Earth marks the real beginning of Earth tides research but in 1954 the theory of earth tides was still more advanced than experiments in this field [Lecolazet, 1977]. During the International Geophysical year of 1957 worldwide research in Earth tides was organized and one year later the Permanent Commission on

Earth tides was formed with headquarters at the Royal Observatory of Belgium. Although important experimental work was carried out before this time, the bulk of experimental data has been collected in the last few decades. There are presently many globally scattered centres performing both theoretical and experimental work in Earth tides as is witnessed by the bulk of scientific and technical publi- cations on this and related subjects (see especially the bibliography in Melchior [1978]). However, as pointed out by Lennon and Baker [1973] "we have now experienced a significant application of effort to the discipline at more than 300 observing stations, but the facts are that the output is confusing and disappointing".

It is considered beyond the scope of this report to give a comprehensive account of the many types of installations and instruments used for measuring tilt; we only briefly mention some of these here so that the description in Chapter 3 of the Fredericton station will be seen in a general perspective.

Classically, tilt measurements are made in derelict mines with horizontal pendulums mounted in niches in tunnel walls; variations in this basic design are numerous [Melchior, 1978]. Installations of this type were particularly designed for the study of tidal effects on observed tilt and thus were placed in fairly deep tunnels so that atmospheric effects were minimized. The accuracy of a single reading in these installations is in the order of one milli-arcsecond.

More recently, a near surface installation was designed by Beaumont et al [1970] especially for the purpose of observing the ocean loading effect on tilt in Nova Scotia. Advantages of this design are that it is relatively inexpensie to install and is not

dependent on the availability of existing underground tunnels. This is the design followed in constructing the Fredericton station and will be described in Chapter 3.

A longer baseline hydrostatic tiltmeter was developed by Bower [1973] for observing tilting of the crust due to Earth and ocean tides in Britain and for monitoring secular tilting due to dam reservoir loading in Canada. This type of tiltmeter appears to have a sensitivity approximately equal to that of the short baseline horizontal pendulums and has the advantage of less sensitivity to very localized tilting. Other tiltmeter designs are the vertical pendulum installed in boreholes at various depths and mercury level tiltmeters of varying baselength (Stacey et al [1969]; Peters [1977]) the latter of which have high practical sensitivities and operating ranges. This is by no means a complete list of instruments for measuring tilt. We note however, that the present development of tiltmeters makes possible tilt measurements of a precision beyond the modelling capabilities our present understanding allows.

2.2 Causes of Tilt and Their Present Understanding

One of the major causes of observed variations in the direction of the local gravity vector is the direct luni-solar tidal effect. This so-called "body tilt" for a rigid Earth can be parameterized in terms of the position of the terrestrial point in question and the orbital ephemerides of the Moon and Sun (see Melchior [1978] for details). The resulting tilt as a function of mean solar time can be, and has been, decomposed into several hundred sinusoidal constituents which have been classified and named by Doodson [1921];

examples of which are a lunar semi-diurnal constituent M_2, a solar semi-diurnal constituent S_2, a lunar diurnal constituent O_1, etc. Computer programs are available for generating this theoretical rigid body tilt such as a program written by Harrison [1971] which was used in this study (see Chapter 3).

Since Earth is not in reality rigid, but displays elastic properties, the tidal tilt is diminished because of the corresponding tidal uplift of the crust (of the order of 50 cm in range). This resulting tilt attenuation can be expressed in the form of a "diminishing factor" D which has been shown to have the relation D = 1+k-h with the Love numbers h and k (eg. Melchior [1978]). These Love numbers, and therefore the diminishing factor, are a function of both the elastic properties of Earth and the frequency of excitation. For semi-diurnal tides, D is approximately equal to 0.7 (Melchior [1978]). The theoretical rigid body tilt multiplied by D gives the theoretical elastic body tilt which is the direct tidal tilt we should ideally observe.

Another major cause of tilt variations is the loading of the ocean tides on Earth's crust; the so-called indirect effect. This loading effect consists of three parts: tilt directly due to the deformation of Earth's surface, tilt caused by the gravitational attraction of the tidal waters and tilt caused by a change in the gravitational potential due to the Earth's deformation. The resulting total loading tilt is thus a function of the ocean tides and the physical properties of Earth's crust and upper mantle and can be modelled in an azimuth θ at a point on the Earth's surface with position vector r by (Baker, [1979])

$$L(r, t) = \rho \iint_{\text{oceans}} \cos \alpha(r', t)\, G(|r-r'|)\, H(r')\, dA \qquad (2.1)$$

where ρ is sea water density, $H(r')$ is the complex amplitude of the ocean tide over the surface area dA at position r', $G(|r-r'|)$ is the tilt loading Green's function describing the elastic and gravitational effects of a point mass load and $\alpha(r', t)$ is the azimuth of the load at r'. Such models have been computed for Maritime Canada by Beaumont and Lambert [1972] and more recently improved by Beaumont and Boutilier [1978]. Their results for the M_2 and O_1 tidal frequencies were made available for the Fredericton station by Beaumont [1980] and used in our analysis (see Chapter 3).

Air pressure induced tilts can be much larger in magnitude than the tidal tilts (Zschau [1976], Zschau [1977]). Previous studies have proposed different mechanisms for this effect: rigid tilt of tectonic plates, elastic deformation of the regional crust, local deformations of the observation site and deformations of the measuring instruments themselves. Herbst [1979] has analysed the deformation of Earth's surface caused by the changing load of the air masses and by the gravitational effect of the changing air mass distribution using the finite element method. For an air pressure change of 50 mbar he finds a maximum combined tilt of 9.4 milliarcseconds (the gravitational effect is approximately 40% of the combined effect). However, one may question the reliability of these results in view of the suggestions in Bower and Heaton [1976] that the tilt response to air pressure variations in a porous media is dependent on the rate of change of air pressure, i.e. it is a function of frequency. Generally a satisfactory modelling of atmospheric pressure induced tilts has not been made.

Thermoelastic tilts have been investigated especially by Harrison and Herbst [1977] who show that these tilts can be significant for shallow installations. They also conclude that topography is an important factor here. They point out also that their analytical treatment of this effect is too simple and that freezing and precipitation can produce important effects. Herbst [1979] also points out that his analytical model using a homogeneous half-space assumption is not suited to the actual complexities involved.

Other important effects on tilt are ground water variations which are presently being investigated by Bower [1981], geological effects and the cavity effect (e.g. Harrison, [1976]). It is expected that ground water variations and possibly geological heterogenities may have an effect on tilt at the Fredericton station. (The cavity effect does not apply here since there is no cavity; tilt is being measured on the surface of the undisturbed bedrock). However, these effects have not been considered in this work.

CHAPTER THREE

TILTMETRIC OBSERVATIONS IN FREDERICTON AND THEIR LOCAL PERTURBANCES

The primary objective of this study is to model the tilt observations of the Fredericton tiltmetric station. In this chapter we therefore give a description of this station and its collected data along with a summary of its local sources of observed tilt variations. As a preliminary evaluation of the observed tilt, results of a least squares fit of the M_2 and O_1 tidal constituents to this data are also presented.

3.1 Description of the Fredericton Station

The Fredericton tiltmetric station was constructed in 1973 after an extensive search for a suitable site using the seismic refraction and electrical resistivity methods [Burke, 1972] and some test drillings. Another station was constructed near Clarendon, New Brunswick but has been abandoned because of severe water effects and is not considered further in this study.

The Fredericton station is located in the University of New Brunswick woodlot, near highway 101, at a north latitude of $45^{o}54'20"\pm3"$ and a west longitude of $66^{o}40'26"\pm3"$ (these coordinates were scaled from a 1:25,000 topographical map, the indicated accuracies are thus approximate standard deviations). It is at an elevation (above sea level) of approximately 100 $\pm$5 metres above sea level (interpolated from 25 foot contour lines).

As mentioned in the Introduction, the station was constructed according to the design introduced by Beaumont et al [1970]. The main characteristics of the station are illustrated in Figure 3-1. A 6.1 metre long corrugated cylindrical 10 gauge steel pipe of 1.8 metre diameter was placed on the exposed Pennsylvanian siltstone bedrock with a portion of the bedrock exposed through a rectangular (1.2 m by 0.6 m) hole at one end of the pipe. (The bedrock was initially exposed by excavating two to three metres of glacial till overburden). The hole was sealed with concrete, butyl rubber caulking compound and asphalt. A vertical access pipe of 0.8 metre diameter was then attached over a flange in the horizontal pipe. This apparatus was then covered with approximately 6 metres of gravel fill and landscaped to provide for free water run-off. A small (3.6 m by 2.7 m by 2.4 m high) access building was then constructed over the partially exposed vertical pipe. A hinged hatch cover was installed at the top of the vertical pipe. Later a second hatch cover was installed at the lower end of the vertical pipe in order to affect a better damping of thermal convection. This second hatch visibly improved the quality of subsequent tilt recordings.

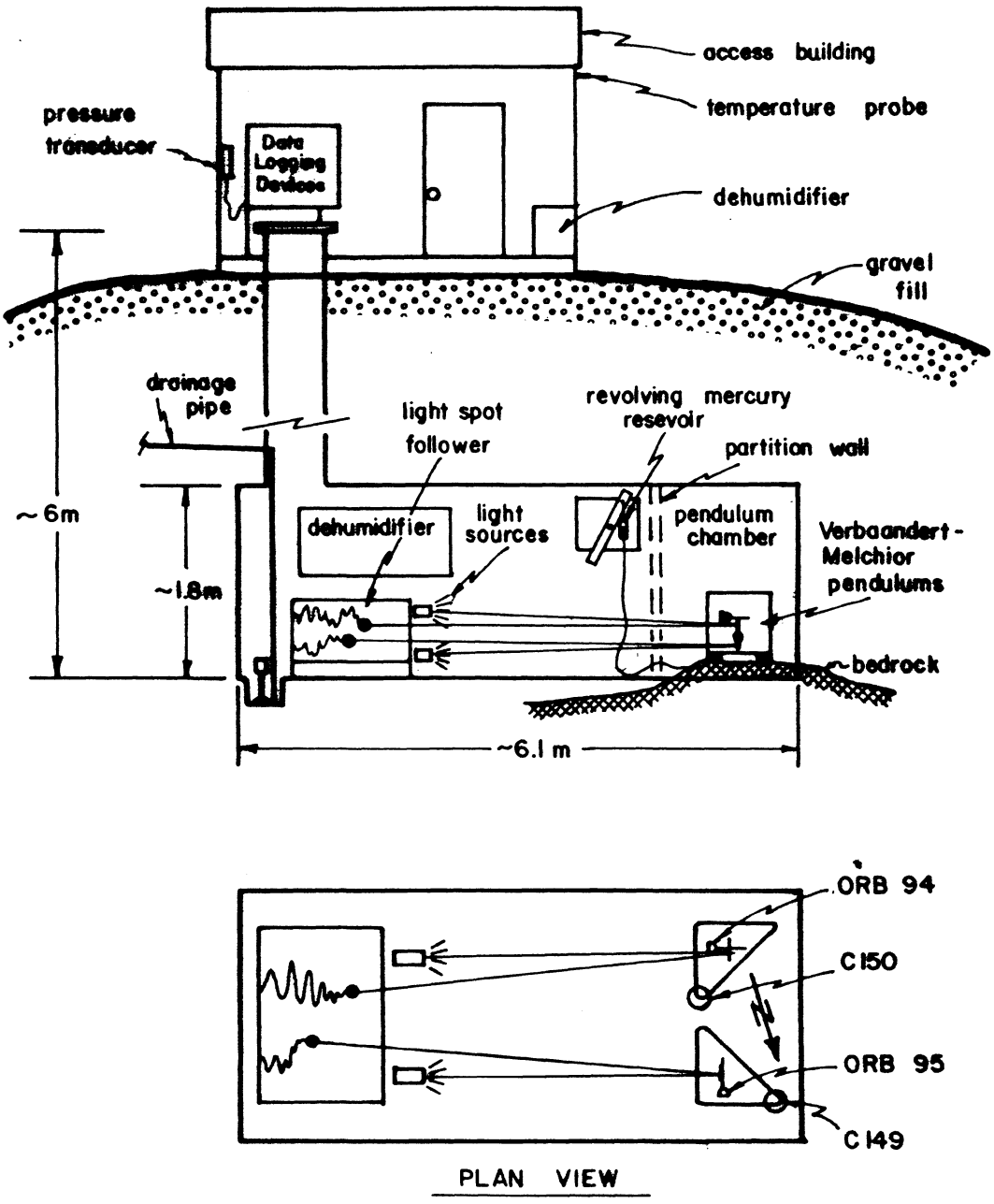

Figure 3.1 Section and Plan Schematic Views of the Fredericton Tiltmetric Station

Six 3 cm diameter holes were drilled to a depth of approximately 4 cm in the exposed bedrock and 2.5 cm diameter stainless steel pins were cemented in these holes with epoxy glue. These pins serve as supports for the two Verbaandert-Melchior quartz horizontal pendulums (numbers ORB 94 and ORB 95 of the Observatoire Royal de Belgique (O.R.B), Bruxelles). Stainless steel expandable bearing plates (crapaudine dilatables) were placed under the drift screw of each pendulum for providing calibration of the recordings [Melchior, 1978]. Crapaudines C150 and C149 are used with pendulums ORB 94 and ORB 95 respectively. (See section 3.2 for more detail on the calibration).

Pendulum motions are magnified by an optical lever of 5 m length (see Figure 3.1). A focused light spot is reflected by a mirror attached to the pendulum shaft to a Sefram model PH 2D 158 light spot follower. These motions were recorded on a strip chart by electrostatic pens attached rigidly to the photo cell followers. A provision is made for analogue to digital conversion by means of sliding potentiometers. However, until late 1980 a digital recording system was not made available and thus it was necessary to manually digitize the analogue records before this time. The manual digitization was performed at the Earth Physics Branch, Department of Energy, Mines and Resources, in Ottawa under the direction of Dr. D.R. Bower.

As well as tilt of the two pendulums, temperature at three locations and surface atmospheric pressure measurements are recorded on a strip chart recorder situated in the surface access building. (The surface temperature record on these charts was also digitized in

Ottawa at the Earth Physics Branch). The temperature measurements are made continuously by thermistors located in the exposed bedrock, in the pendulum chamber and external to the access building. We note however that only the surface temperature measurements are presently in digitized form. However, even if the bedrock and pendulum chamber temperature measurements were digitized, only short sections have been recorded since these measurements were out of the recording range most of the time. This has been corrected by the addition of new recording instruments (see next paragraph). The pressure measurements are made with the use of an Ametek pressure transducer. Hourly time marks on both analogue strip chart recorders were provided by signals from a Venner signal timer (a synchronous electric clock).

The bulk of data gathered to date (see section 3.2) has been procured using the above instrumentation. In late 1980 the station recording system was updated by the addition of a Fluke 2240B datalogger, and IBM compatible Kennedy 1600/360 magnetic tape recorder and a Phillips PM8236 multi-point strip chart recorder. The continuously recording strip chart recorder is connected in parallel with the datalogger. The datalogger is presently digitizing the tilt (2 channels), temperature (3 channels), and atmospheric pressure (1 channel) measurements at 20 minute intervals including an "on the hour" recording. The datalogger has a built-in digital clock which is maintained within $\pm$ 10 seconds of Greenwich Mean Time; the actual sampling times from this clock are recorded automatically. The datalogger also has a paper tape printer which prints a backup copy of the digitized results.

3.2 Collected Data, Its Calibration and Local Noise Sources

Actual computer plots of the data collected at the Fredericton station to date are presented in Figures 3.2 to 3.7. (Note that the removal of linear trend refers to one trend for the entire series throughout this work). The most striking characteristic of the observed tilt is the preponderance of gaps. The longer gaps are due to recording equipment failures; the more common shorter gaps are due to the limited recording range of the horizontal pendulums. Of particular interest in this work are the data collected during 1974 and 1975. Since we are primarily interested in modelling the tilt response to temperature and pressure, the tilt collected during 1977-1980 will not be considered further here since digitized temperature and pressure records are not yet digitized for this period.

The surface temperature and atmospheric pressure recordings r (in units of millivolts) are transformed to degrees Celsius or millibars, x, respectively using

$$x = c_1 + (r-\theta).c_2 \qquad (3.1)$$

where θ is the zero offset of the recording and c_1 and c_2 are supplied by the calibration performed at U.N.B. These constants are given in Table 3.1 where constant c_2 has been multiplied by 10^{-3} accounting for the fact that there are 10^3 digitizing units per millivolt. The constants given in Table 3.1, along with equation (3.1), therefore give the direct transformation from digitizer units (d.u.) to degrees Celsius or millibars.

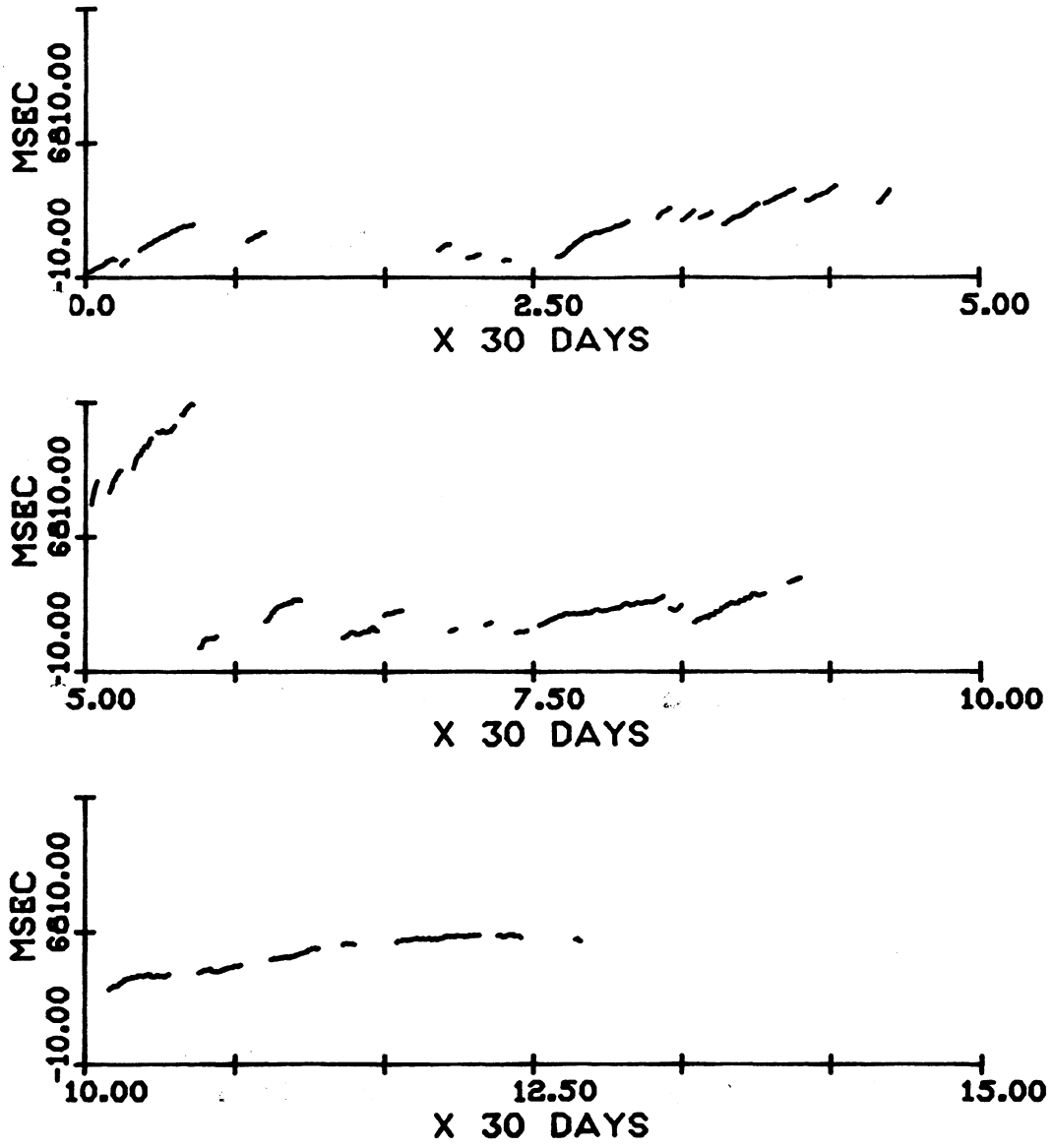

Figure 3.2(a). Tilt observations, ORB 95. Time origin is day 197 (July 16), 1974.

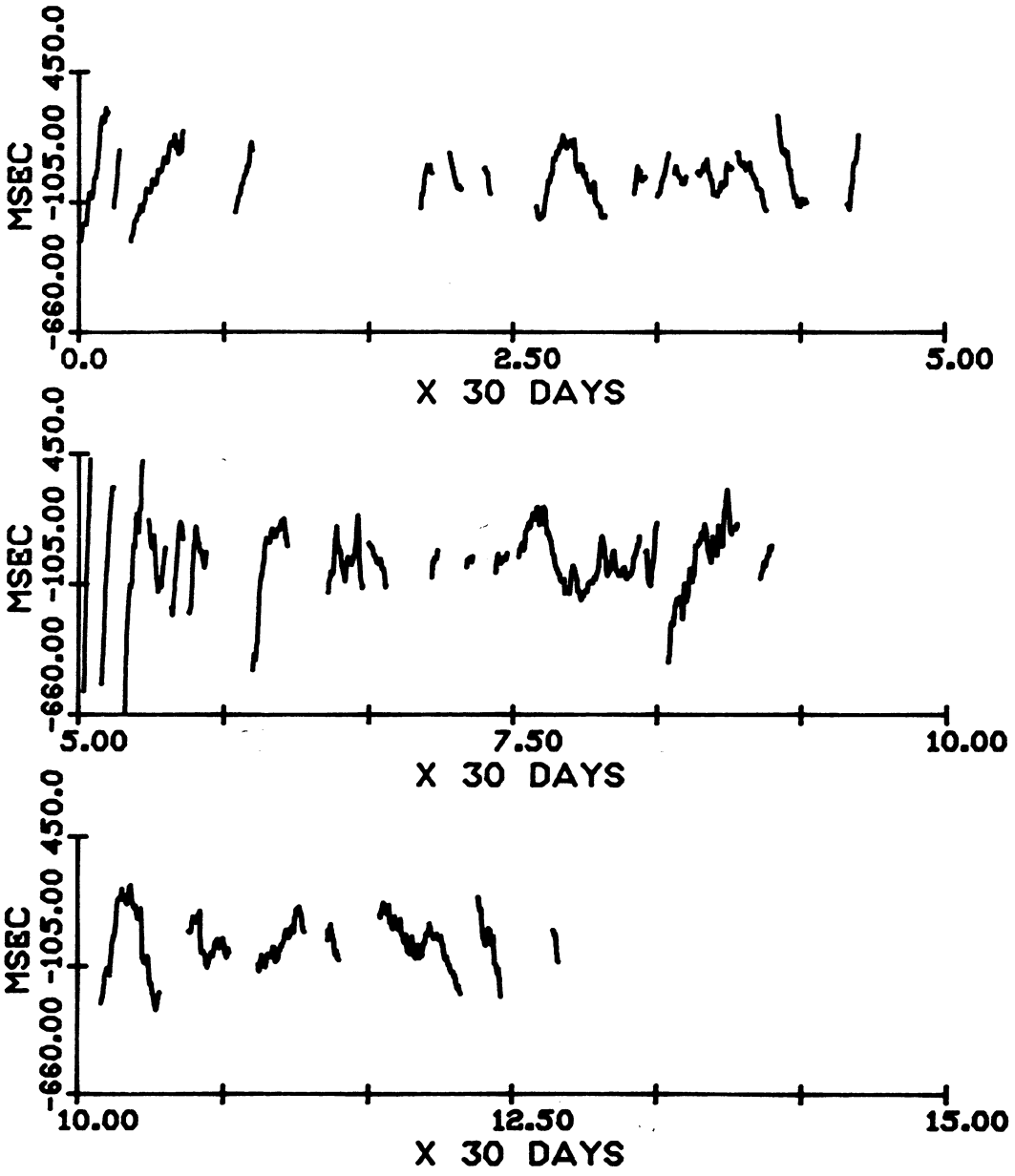

Figure 3.2(b). Tilt observations, ORB 95, with least squares estimates of linear trend and datum biases removed. Time origin is day 197, 1974.

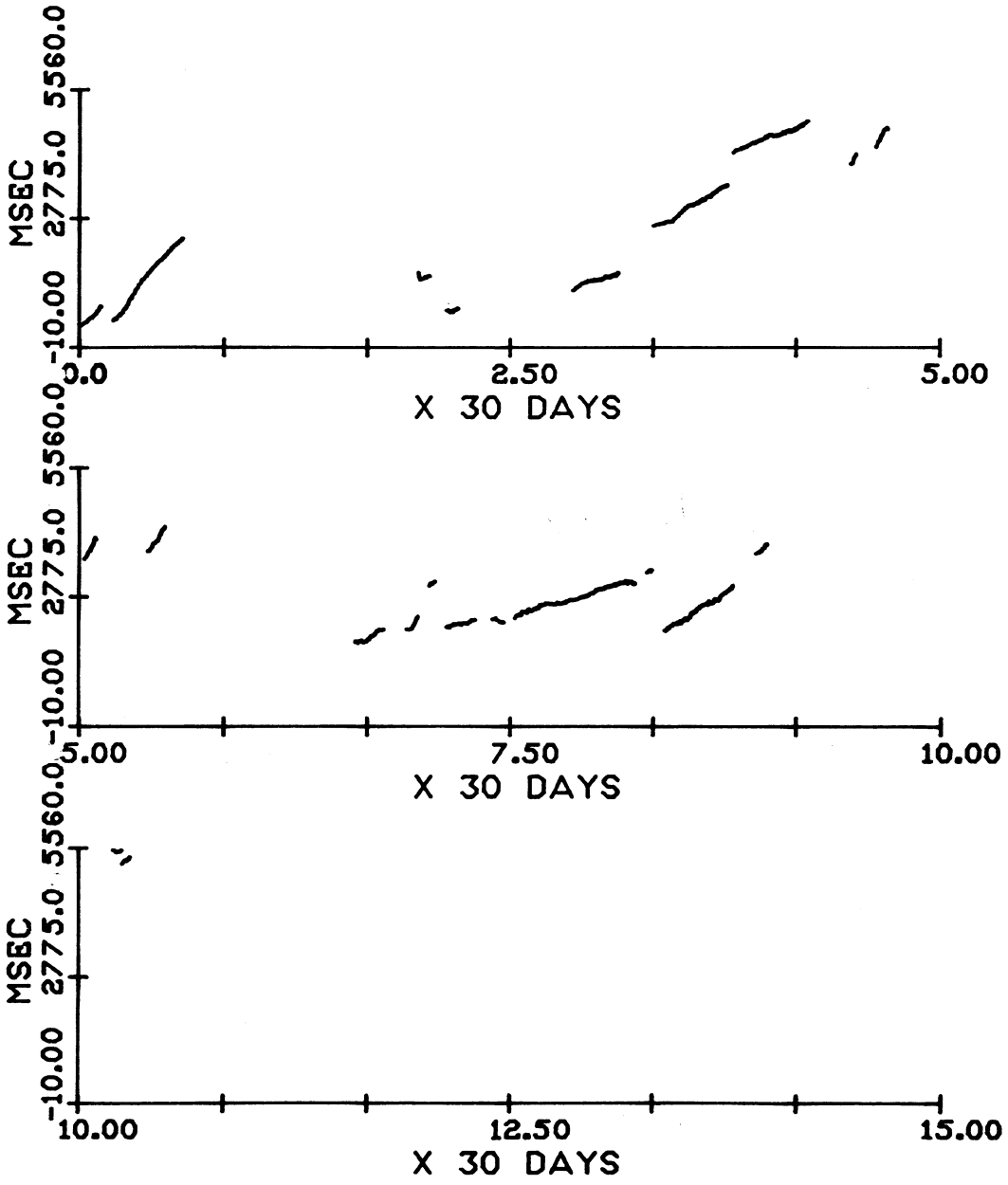

Figure 3.3(a). Tilt observations, ORB 94. Time origin is day 197, 1974.

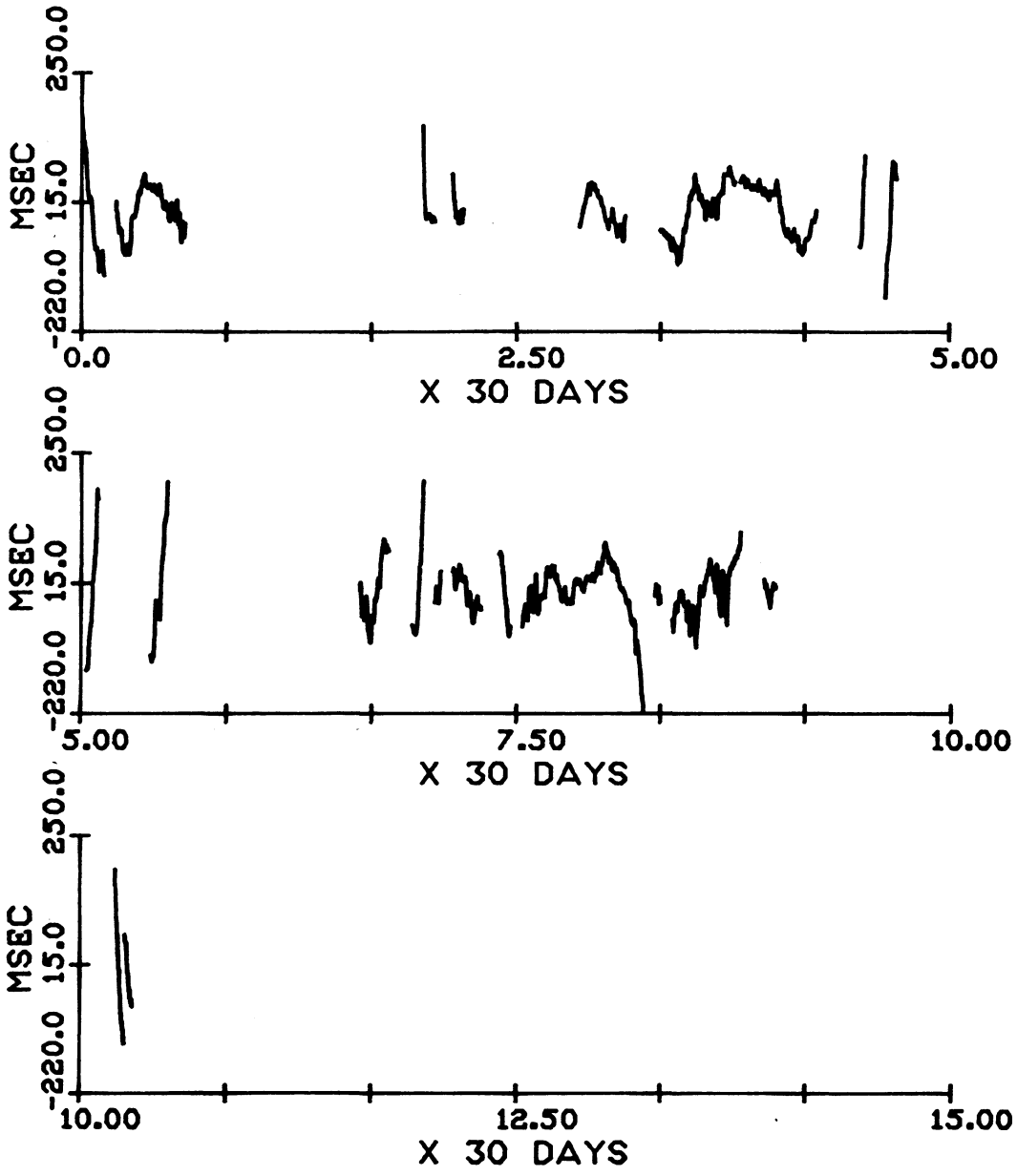

Figure 3.3(b). Tilt observations, ORB 94, with least squares estimates of linear trend and datum biases removed. Time origin is day 197, 1974.

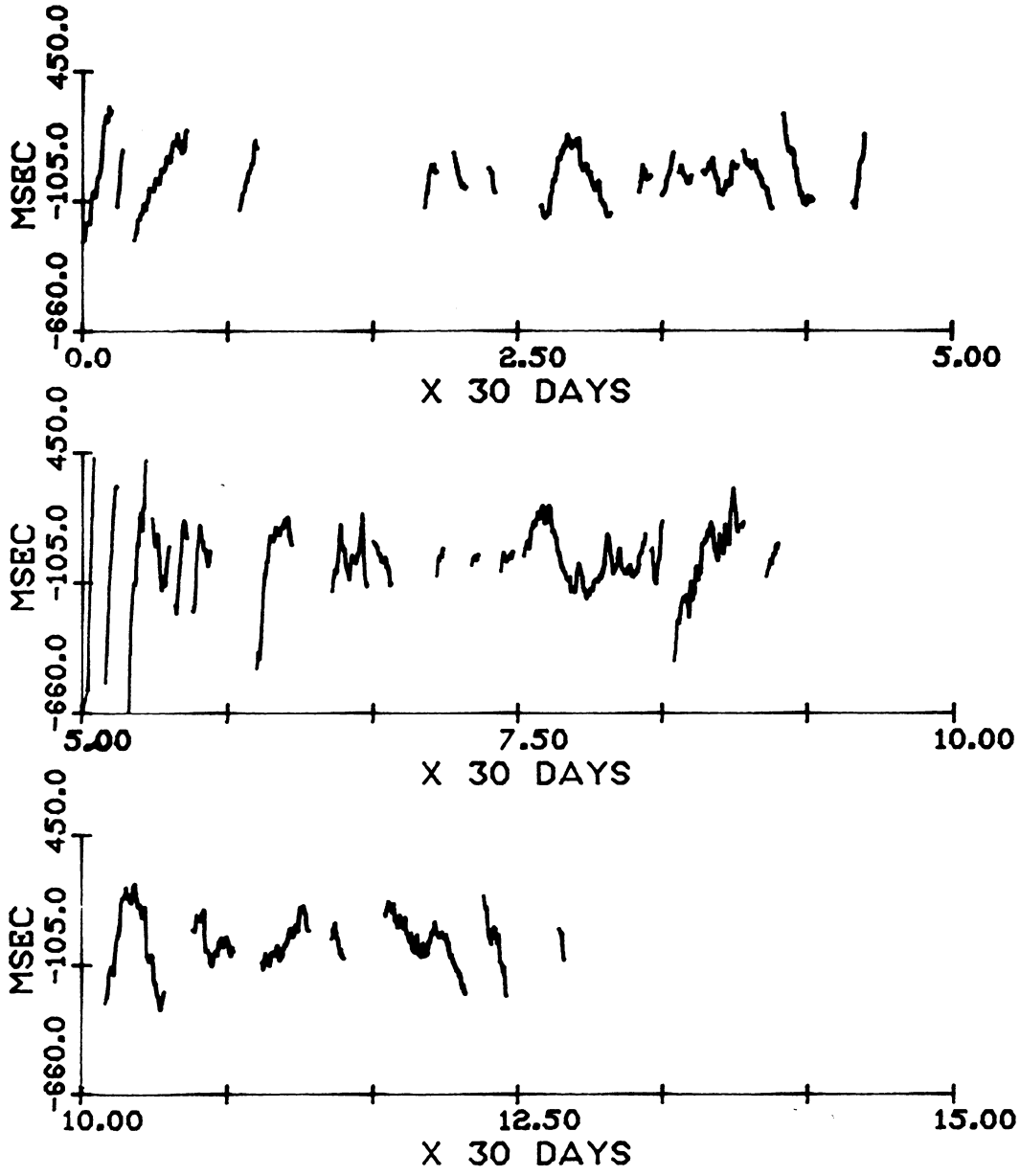

Figure 3.4. Tilt observations, ORB 94, in approximate msec units, with least squares estimates of linear trend and datum biases removed. Time origin is day 292, 1977.

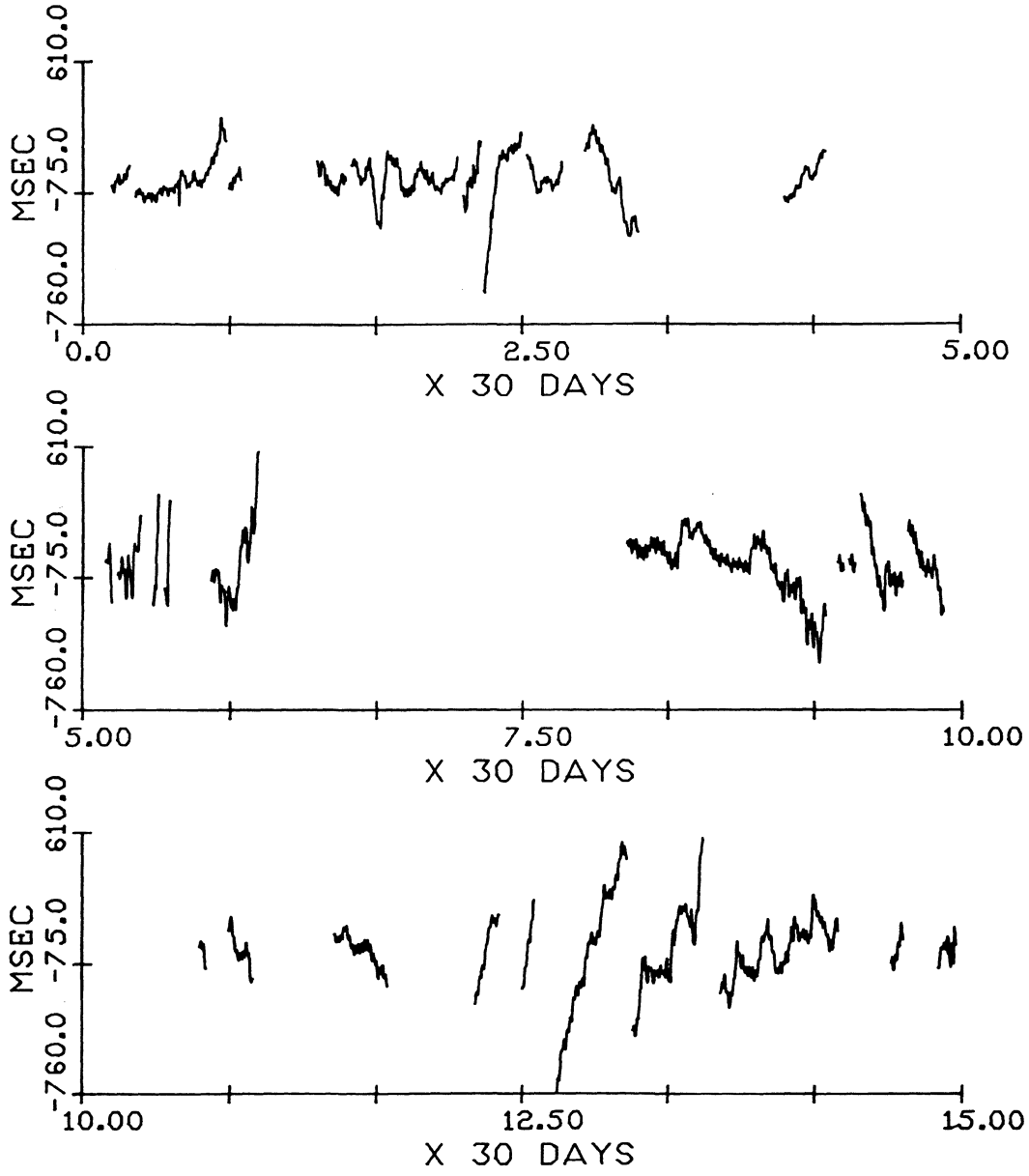

Figure 3.5. Tilt observations, ORB 95, in approximate msec units, with least squares estimates of linear trend and datum biases removed. Time origin is day 297, 1977.

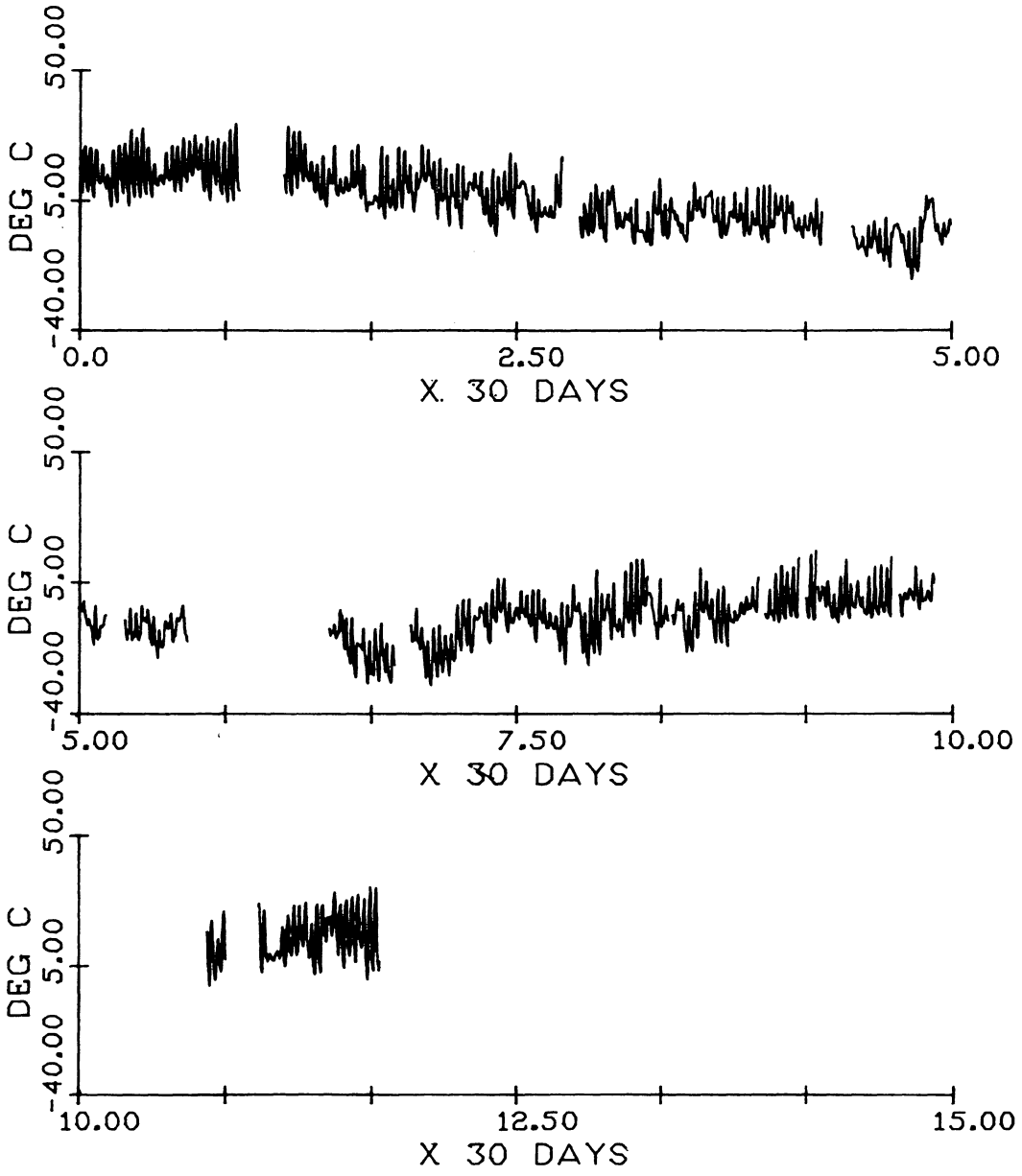

Figure 3.6. Surface temperature observtions. Time origin is day 197, 1974.

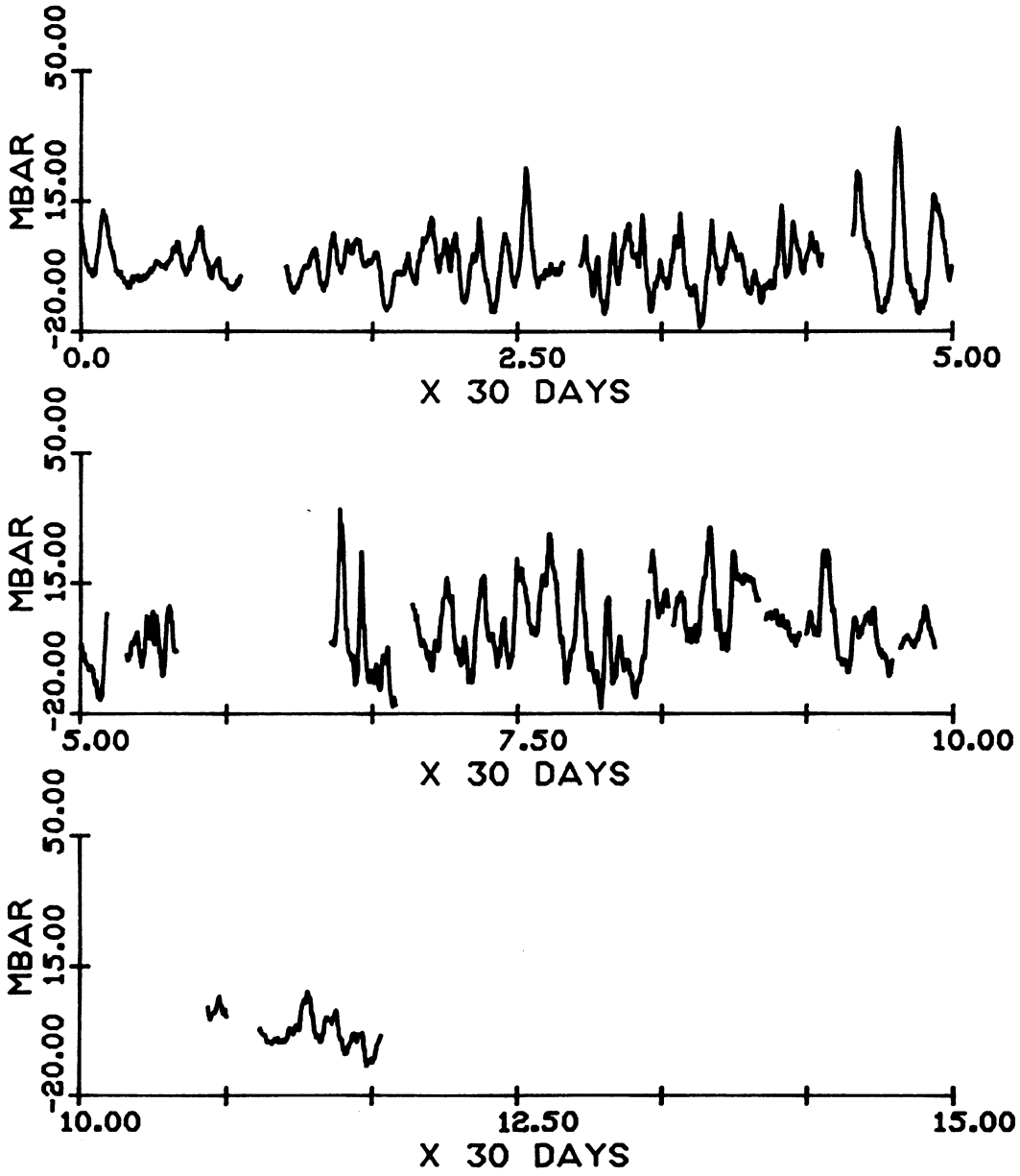

Figure 3.7. Atmospheric Pressure observations. Time origin is day 197, 1974.

Recording	c_1	c_2
Surface Temperature	41.18 ^{o}C	-0.09026 ^{o}C/d.u.
Atmospheric pressure	947.3 mbar	0.100 mbar/d.u.

Table 3.1 Calibration Constants for Temperature and Pressure Observations

As mentioned in the previous section, the observed tilt was calibrated using the calibrated stainless steel crapaudines which were provided by the O.R.B. The crapaudine is simply a hollow disk with a thin upper surface. A small flexible hose is attached to an opening in the side of the disk; the other end of the hose is attached to a small resevoir which is partially filled with mercury. The mercury is allowed to completely fill the hose and crapaudine by bleeding air through a small screw hole in the crapaudine. The resevoir is attached to a rotating arm whose rotation is controlled by a special clock. At the Fredericton station, one rotation, which takes 3 hours, is performed automatically twice a week. In each rotation the arm rotates first through 180 degrees, which takes approximately 10 minutes, remains there for approximately 2 1/2 hours and then completes the full 360^{o} rotation. During rotation of the arm the mercury head with respect to the crapaudine is changed by a known amount. An increase in the head this way causes the crapaudine to expand by bending the thin upper surface upwards. This in turn tilts the base of the tiltmeter by a precisely known amount since the

relationship between the change in thickness Δt of the crapaudine and the change in head ΔH is precisely determined in a laboratory using an interferometric method [Melchior, 1978]. This relationship is also linearly affected by the mean head $\bar{H}$ and thus the laboratory calibration supplies the constants c_1 and c_2 in

$$\Delta H = c_1 + c_2\bar{H} \quad \text{cm} \tag{3.2}$$

which is the head change, for a given $\bar{H}$, resulting in a crapaudine thickness change of $\Delta t = 0.273037 \times 10^{-4}$ cm. This is the half wavelength of the green line of the mercury spectrum [Melchior, 1978]. The constants c_1, c_2 for crapaudines C149 and C150 (used with pendulums ORB95 and ORB94 respectively) are given in Table 3.2 as supplied by the O.R.B.

Crapaudine No.	c_1 (cm)	c_2 (unitless)
C149	+42.22	$+3.0 \times 10^{-4}$
C150	+39.38	-1.5×10^{-4}

Table 3.2. Crapaudine constants.

With known (measured) $\bar{H}$ and drift screw base b we can then easily calculate the angle of "artificial tilt" induced on the tiltmeter base during a revolution of the mercury reservoir. At the Fredericton Station we have $\bar{H}$ = 98.8 cm and the drift screw bases of pendulums ORB94 and ORB95 are b_{94} = 27.435 cm and b_{95} = 27.112 cm respectively. These give the artificial tilts α in milliarcseconds (msec) as listed in Table 3.3 for head changes of 30.00 and 40.00 cm.

Head change (cm)	α_{94}(msec)	α_{95}(msec)
30.00	156.442	147.496
40.00	208.589	196.661

Table 3.3. Artificial tilts induced by the crapaudine calibration device.

Before mid 1978 the head change was set at 40.00 cm, since then it has been set at 30.00 cm when the operating characteristic periods of the pendulums were increased from approximately 30 seconds to between 45 to 60 seconds. The periods were increased in order to increase the sensitivity (and thus the recording amplitudes); the head change then had to be decreased in order to decrease the amplitude of the calibration pulses so that they would not extend beyond the recording range.

3.3 Local Noise Sources at the Fredericton Station

We now turn to a brief discussion of various local noise sources at the Fredericton station. This discussion will lead us naturally to a preliminary evaluation of the tilt data in section 3.4 by computing least squares estimates of some tidal constituents.

In Figure 1.1 and 1.2 continuous sections of tilt are plotted along with the observed atmospheric pressure and surface temperature for the same periods. The influence of pressure on tilt is obvious. However a direct least squares regression of tilt on observed pressure results in a very poor modelling of this effect. That is, the estimated coefficients were zero (as ± 0.1) and therefore the residual tilt variance was equal to the variance of the original

tilt series. This is apparently because of the frequency dependence of tilt response to pressure which was mentioned earlier in this chapter. The failure of this simplified approach thus directed this research towards a modelling technique which considers the frequency dependence of the response (see chapters 4 and 5).

An effect of observed surface temperature on tilt is also visually apparent. Again straightforward regression results were poor and a frequency dependent modelling is attempted in Chapter 5.

The effects of precipitation and ground water variations on tilt at the Fredericton station may be significant but are not considered in this work since the primary objective here is to model such responses using observed inputs and these observations are not yet available for the station itself (equipment for mesuring precipitation at the station has not yet been procured). Observations of precipitation at the Fredericton airport, some 15 kilometres from the Fredericton station, are available which may or may not be representative of the precipitation at the station itself. (For possible future work a short period (e.g. a few months) of precipitation measurements at the station could be compared with the airport measurements to test how represeentative the latter are).

Another loading effect may result at the Fredericton station due to its proximity to highway 101. This two-lane highway, which has moderate traffic loads, runs approximately in a north-south direction and is approximately 50 metres from the station at its nearest point. A simplified model of assumed daily traffic patterns (assuming peaks in traffic at 8 a.m. and 5 p.m.) was generated and its frequency composition determined using the least squares spectral analysis

technique (see Chapter 4). Although periodic constituents of near 12 and 24 hours were predominant in this model, it is dangerous to estimate responses using these results in lieu of actual traffic patterns. Since actual traffic data are not available, this effect is not considered further in this work.

Still another loading effect may result from the fluctuations in water level of the nearby (approximately 5 km) St. John river. However, because of water partially flooding the station during the spring months, at the same time as significant water level changes occur in the river, it has not yet been possible to observe this effect.

The Fredericton station is situated on a gently sloping (approximately a 3% slope) wooded terrain. As well a circular mound approximately 15 metres in diameter and 1 to 2 metres high is situated directly over the station on which the surface building of the station sits. It is expected therefore that there may be a topographic effect on thermoelastic tilts (Harrison [1976], Harrison and Herbst [1977]). This effect has not yet been evaluated for the station. However, a digital terrain model is being constructed for the area so that a finite element modelling of this effect may be attempted.

At least two other sources of systematic error affect our tilt measurements. First there is the uncertainty in recording azimuths of the pendulums and second there is a "backlash" effect resulting from a slight freedom of movement of the light spots across the photocells of the light spot followers.

The latter effect is described and evaluated analytically in Appendix II. Its associated flattening effect on the recorded tilt signal is actually visible on some portions of the charts. The actual effect on amplitude and phase determination for the M_2 frequency is evaluated in the following section. With this effect superimposed on the recorded tilt (which can be different for the two pendulums since the two photocells are independent in this respect) it is unlikely that precise conclusions about especially the phases of the tidal constituents can be made (see section 3.4). Although a provision to adjust the photocells is provided with the instrument, it is felt that the necessary precision to which this adjustment must be made so that only insignificant phase and amplitude distortions occur, is not possible. A precision of 0.01 mm in adjusting the width of the "free area" on the photo cell to zero still results in a possible phase shift of 2.5 degrees and an amplitude distortion of $< 0.1\%$ (see Appendix II).

Finally, we consider now the effect of uncertainties in the recording azimuths. In February 1975 the azimuths of the drift screw bases for each pendulum were determined. The method used is illustrated in Figure 3.8 in which the azimuth Az_{AC} was determined with a WILD GAK1 gyroscope attachment mounted on a WILD T2 theodolite.

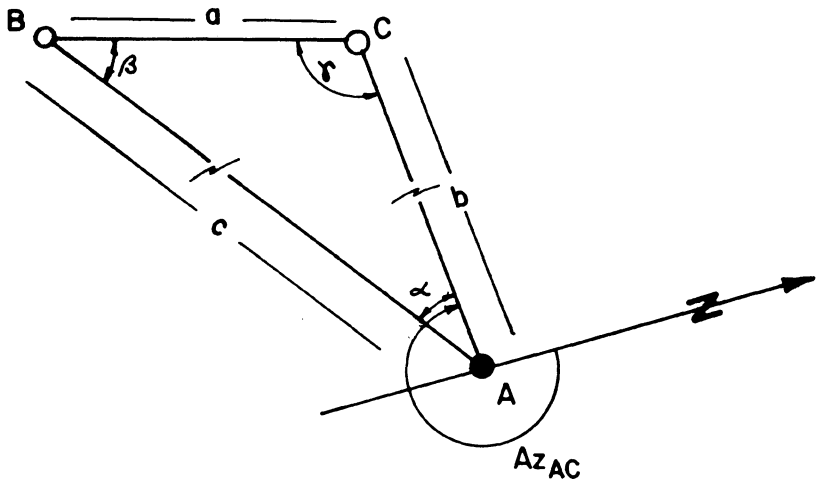

Figure 3.8 Method of Determining Recording Azimuth of Pendulum.

The horizontal angle α was also measured with the WILD T2 theodolite. (The theodolite and WILD targets were mounted on WILD tripods; centering of these instruments over the points was done using adjusted optical plummets in the tribrach mounts). Distances a, b and c were measured with a steel tape. A least squares adjustment was then performed to determine the coordinates (in a local plane coordinate system) of points B and C with respect to point A. From the adjusted coordinates angle γ was computed which allowed computation of the azimuth Az_{CB} from

$$Az_{CB} = Az_{AC} + \gamma - 180^{\circ} \qquad (3.2)$$

The so determined recording azimuths along with their estimated standard deviations are 118° 01' $\pm$10' and 207° 58' $\pm$10' for pendulums

ORB95 and ORB94 respectively (see Figure 3.1). In practice, however three sources of systematic effects in using these azimuths must be considered. The first is the initial assumption that the drift screw base is perpendicular to the effective longitudinal axis of the pendulum. This can be affected in practice using the method described by Skalsky [1969] as was done in the case of the Fredericton station. A second major source of systematic effect is the fact that the pendulum cases are not restricted to rotate in a horizontal plane on their supporting pins. A very slight nudge by the attendant or removing and replacing the pendulums can thus change the recording azimuths significantly: A total horizontal rotation of the instruments of approximately 4 degrees is possible in this way. This freedom of motion could be restrained by inserting circular rings in the tops of the supporting legs. Finally we should consider the variations of the recording azimuths due to the pendulum motions caused by the tilting which we wish to observe. This variation can have a maximum of approximately 0.7 degrees but can be easily monitored via the observed ordinates of the recorded tilt record.

Because of the uncertainties in whether and how much the pendulums were actually rotated on their base since the azimuth measurement, it is difficult to assign a meaningful error bar to the determined recording azimuths. It appears that an uncertainty of about 2 to 3 degrees can be ascribed to them. A systematic difference of 3 degrees in recording azimuths results in M_2 amplitude and phase distortions respectively of 2.8% and 1.2 degrees for ORB95 and 6.1% and 2.5 degrees for ORB94. These were computed by comparing the results of projecting the predicted M_2 tilt on azimuths of 118° and

208° and azimuths 3 degrees different than these (see section 3.4 and Appendix I). A visual interpretation of this sensitivity of the M_2 tilt to azimuth variations is given in Figure 3.9.

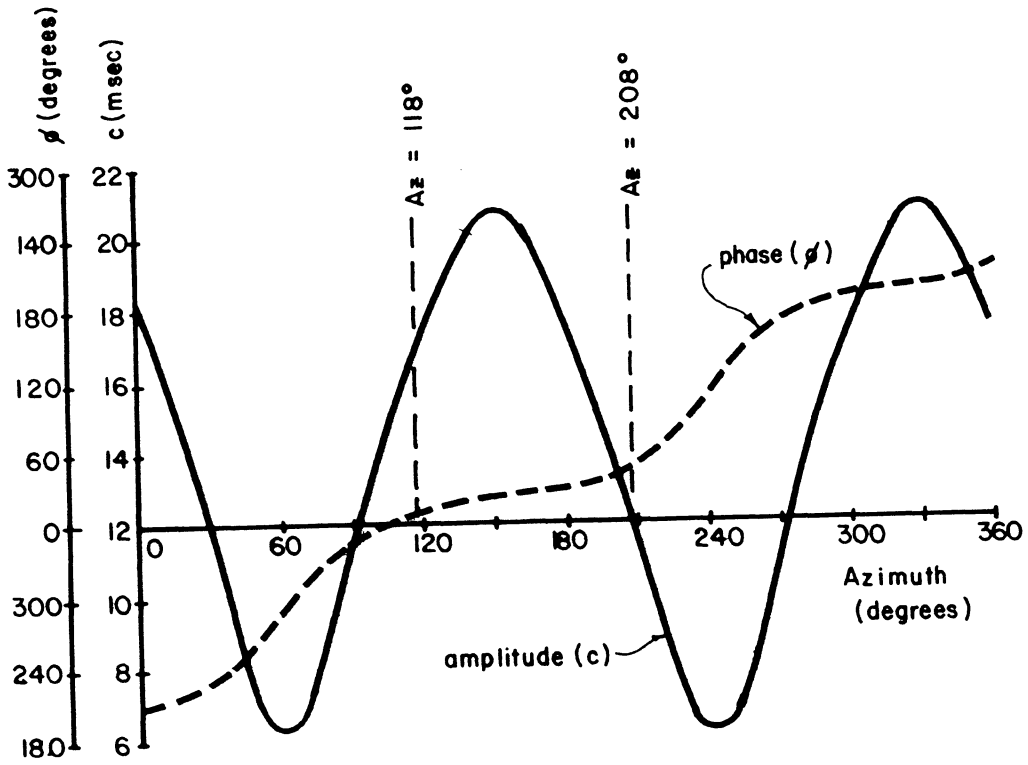

Figure 3.9 **Variation of M_2 Tilt Amplitude and Phase with Recording Azimuth.**

3.4 Preliminary Evaluation of the Tilt Observations

The results of a least squares fit of the M_2 and O_1 tidal constituents to the observed tilt is presented here along with comparisons of the estimated M_2 and O_1 constituents with their

predicted amplitudes and phases. By "predicted" is meant the vector sum of the theoretical elastic body tilt and the ocean loading effect as determined by Beaumont [1980]. Other effects (such as atmospheric pressure loading and temperature effects) are completely ignored in this section.

The ocean loading induced tilts at Fredericton as supplied by Beaumont (op cit) are given in Table 3.4 for M_2 and Table 3.5 for O_1 for four Earth models. The Atlantic Coast A (ACA) and Gulf of St. Lawrence (GOSL) models are described in Beaumont and Lambert [1972]; the Farrell Harkrider Continental (FHC) and Farrell Gutenburg Bullen (FGB) models in Farrell [1972].

Model	North Tilt		East Tilt	
	amplitude (msec)	phase lag (degrees)	amplitude (msec)	phase lag (degrees)
FHC	14.106	-106.7	3.831	63.3
GOSL	13.550	-107.5	3.679	60.4
ACA	14.524	-105.6	4.065	66.8
FGB	14.397	-105.8	4.006	66.4

Table 3.4. M_2 Ocean Loading Tilt at Fredericton as Supplied by Beaumont [1980]. (Phase lags are Greenwich phase lags).

Theoretical elastic (diminishing factor equal to 0.7) body tilt was computed by fitting (using least squares) the four main seemi-diurnal and four main diurnal tidal constituents (including M_2 and O_1) to the tilt generated by Harrison's [1971] computer program

for the Fredericton station. (A series of 9168 hourly values in azimuths 118° and 208° were generated beginning on day 197, 1974; the same time span as the observed tilt we will analyse). The so

Model	North Tilt		East Tilt	
	amplitude (msec)	phase lag (degrees)	amplitude (msec)	phase lag (degrees)
FHC	1.228	-27.4	0.530	-108.9
GOSL	1.207	-27.3	0.523	-109.6
ACA	1.233	-26.5	0.523	-109.9
FGB	1.228	-26.6	0.522	-109.8

Table 3.5. O_1 Ocean Loading Tilt at Fredericton as Supplied by Beaumont [1980]. (Phase lags are Greenwich phase lags).

determined constituents were added vectorially to the ACA model ocean loading tilt (concluded to be best representing the crust in this area by Beaumont and Boutilier [1978]) after transforming the loading tilt to azimuths 118° and 208° and transforming both to "local phase lags" (with respect to 2300 hours, day 196, 1974 GMT; for the procedure used see Appendix I). The resulting predicted tilt is given in Table 3.6. These are thus the tilts we should observe ideally, with a diminishing factor of 0.7, in the absence of other effects.

Constituent	Azimuth (degrees)	Amplitude (msec)	Local phase lag (degrees)
M_2	118 208	17.742 12.164	11.2 48.7
O_1	118 208	2.361 2.610	100.7 288.9

Table 3.6. Predicted (Body + Ocean Loading) Tilt at Fredericton for M_2 and O_1.

The least squares estimates of the M_2 and O_1 tilts constituent in the observed tilt of 1974-75 (see Figure 3.2) are given in Table 3.7. (The four main semi-diurnal and four main diurnal tidal constituents were forced). These results are based on 4200 hourly observations, with intermittent gaps, over a period of 9192 hours for pendulum ORB 95 (azimuth = 118^{o}) and 2782 hourly values (with gaps) over a period of 7416 hours for pendulum ORB 94 (azimuth = 208^{o}). The ORB 95 record during this period is thus composed of 54% gaps; that of ORB 94 being 62% gaps.

Constituent	Azimuth	Amplitude (msec)	local phase lag (degrees)
M_2	118 208	17.543 ± 3.555 12.033 ± 3.613	19.2 ± 11.6 59.8 ± 17.2
O_1	118 208	5.634 ± 3.560 0.728 ± 3.627	82.8 ± 36.2 344.7 ± 104.6

Table 3.7. Least Squares Estimates of M_2 and O_1 Constituents Using 1974-75 Observed Tilt. (Dispersion estimates are least squares estimates of the standard deviations).

It is clear that the O_1 constituents are poorly determined as indicated by the estimated standard deviations of their phase lags. This is apparently because of the diurnal effects of temperature and possibly traffic which we attempt to remove in Chapter 5.

The M_2 constituents are better determined both because of their larger amplitudes and that we expect less contamination by other effects in the lunar semi-diurnal band. There are however, significant systematic differences between these observed constituents and the predicted counterparts of Table 3.6. These differences, for each ocean loading model, are summarized in Table 3.8 and can apparently be explained by the backlash effect of the light spot followers. In Appendix II we have shown that a freedom of movement of the light spot across the light spot follower of $\Delta h = 0.5$ mm results in a systematic phase shift of 13 degrees and an amplitude distortion of -1 per cent.

Loading Model Used	Azimuth (degrees)	Amplitude difference (per cent)	Phase Lag difference (degrees)
FHC	118 208	+ 1.1 + 1.2	9.1 11.0
GOSL	118 208	+ 3.5 +4.7	10.2 10.3
ACA	118 208	- 1.1 -1.1	8.0 11.1
FGB	118 208	-0.5 -0.6	8.1 11.1

Table 3.8. Differences in M_2 amplitudes and phasee lags; observed minus predicted.

It appears that the FGB loading model is the best fitting to our observed tilt. However, we must note that the estimated standard deviations of these differences are approximately 20 per cent for amplitude and approximately 20 degrees for phase. We see that the differences of the amplitude and phase differences in Table 3.8 are

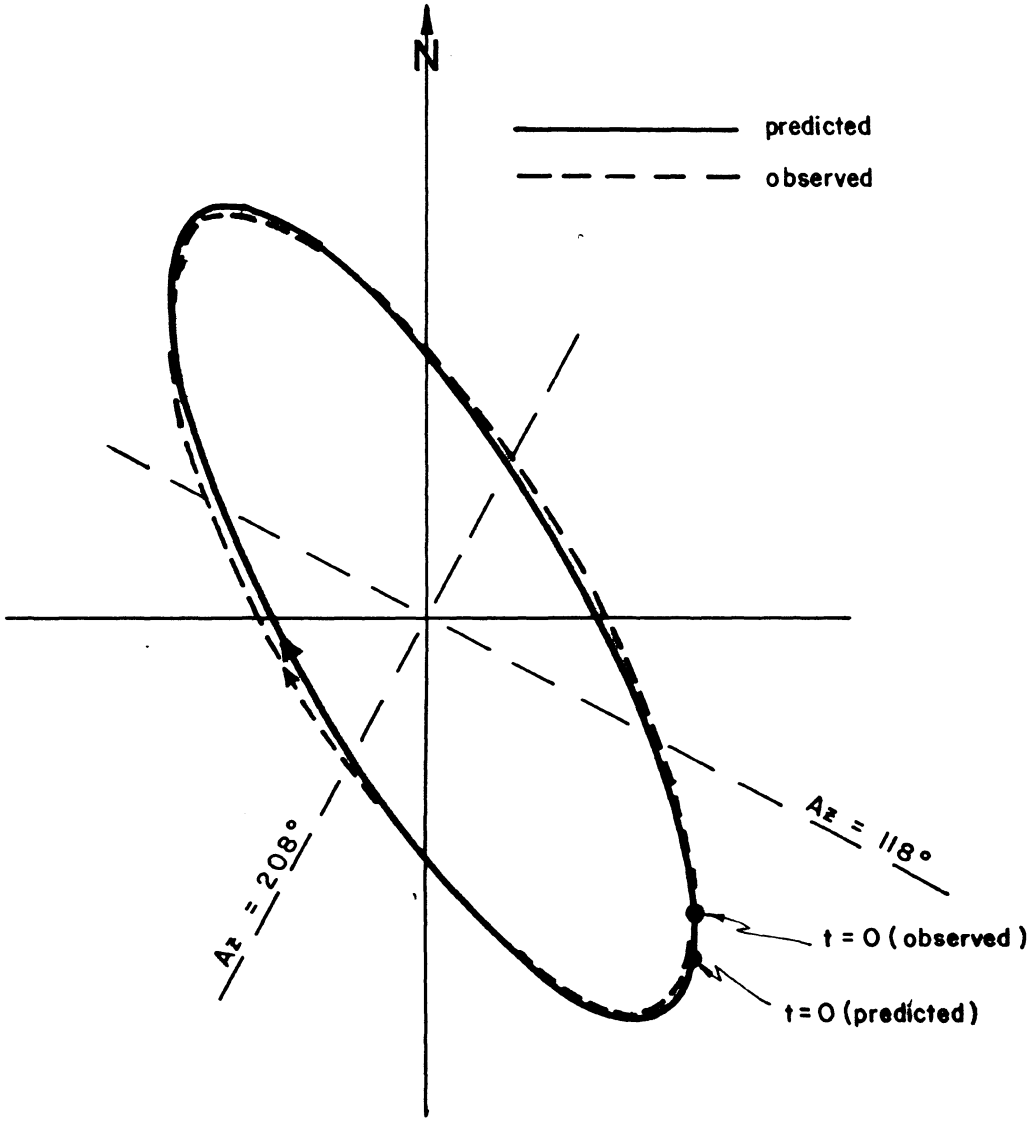

Figure 3.10 M_2 Hodographs for Predicted and observed Tilt at Fredericton. (t = 0 corresponds to 2300h, day 196, 1974)

not statistically significant. A visual presentation, in the form of a hodograph (see Appendix I), of the comparison of the predicted M_2 tilt (using the ACA loading model) and that which is observed (not corrected for the back-lash effect is given in Figure 3.10. In the above comparisons of predicted and observed M_2 tilt we have assumed diminishing factors of 0.7. We will now compute diminishing factors for the north and east directions based on our observations. We do this by first subtracting the predicted ocean loading effect (using any one of the available models) and then we form the ratio of the amplitude of the remainder and the amplitude of the rigid body tilt as well as the phase difference. The results are summarized in Table 3.9. The standard deviations of these estimates are approximately 0.2 for the diminishing factors and 20 deegrees for

Loading Model Used	Direction	Computed Diminishing Factor	Computed Phase Lag Difference (degrees)
FHC	East North	0.713 1.000	12.8 17.2
GOSL	E N	0.725 1.041	14.2 13.7
ACA	E N	0.696 0.956	10.8 19.8
FGB	E N	0.701 0.966	11.1 18.9

Table 3.9. Computed M_2 Diminishing Factors and Phase Lag Differences for thee Four Ocean Loading Models.

the phase differences. Assuming that the diminishing factors are actually 0.700, we see that the FGB model gives a better east/west diminishing factor than the ACA model. However, the difference between these diminishing factors is not statistically significant. The north/south diminishing factors are consistently high, possibly due to neglected local effects such as the topographical effect. However this has not been studied further here.

CHAPTER FOUR

LEAST SQUARES RESPONSE ESTIMATION

In this chapter a least squares method for modelling observed output of a physical system in terms of various observed inputs is developed. In attempting to model the tilt response to various dynamic physical phenomena at the Fredericton tiltmetric station, incentive for developing this least squares method arose from consideration of the following two fundamental points.

First we must recognize that, whenever we deal with the reaction of a physical system to time varying forces acting on the system, the characteristics of the reaction or deformation of the system are generally dependent not only on the magnitudes and spatial characteristics of the applied forces but also on the temporal

characteristics or time rates of change of these forces. That is, the response of the physical system is in geneeral dependent on all spatial and time derivatives of the forcing phenomena. In this work we consider only the first time derivative but find in Chapter 5 that at least the first spatial derivative must be considered also. This dependence on temporal characteristics of the applied forces is, as is well known, directly related to the physical characteristics (e.g. size, shape, strength of inter-molecular forces, etc.) of the system being forced. Also well known is the fact that the response of forced physical systems is more pronounced, or resonant, to temporal variations commensurate with the characteristic frequencies of that system. It is clear therefore that frequency has a fundamental relationship with the character of the physical system and is thus an important parameter in describing the system response to time varying forcing phenomena.

Also of fundamental importance to the specific problem of modelling the response of tilt to various forcing phenomena is the actual character of the observed time series from which we wish to attempt to estimate these models. A summary in this chapter (section 4.1) of these observation characteristics forms a basis which is used to show where the existing cross-spectral analysis and time domain convolution techniques are inadequate for our purposes.

The least squares response estimation technique we develop in this chapter (section 4.3) has its basis in the method of least squares spectral analysis [Vanicek, 1971] which is reviewed in section 4.2. In section 4.4 a numerical example is given to illustrate the application of the least squares response method.

Although we will deal specifically with the Fredericton station in our discussion it must be noted that the method developed here is more widely applicable. Thus both the specific Fredericton tilt and the more general time series analysis problems are addressed.

4.1 Characteristics of Observations at the Fredericton Station; Inadequacies of Other Response Estimators for Our Purposes.

Development of a response estimation technique capable of giving meaningful estimates of response from observed discrete time series representations of system inputs and output must perforce consider the characteristics of these observations. These characteristics which specifically apply to tilt observations collected at the Fredericton station are reviewed now.

Our observed time series are non-stationary, i.e. their statistical properties are time varying (eg. Bendat and Piersol, [1971]). This is obvious for especially the observed tilt which contains for example a pronounced secular trend as well as a significant response to observed atmospheric pressure variations.

We must also recognize the fact that our observed time series are noisy, that is, the time series contain variations due to phenomena which are not of direct interest in a specific analysis. For example, in estimating the response of tilt to atmospheric pressure variations we must recognize the fact that tidal variations of tilt are also present. Also the presence of "observational noise" on both the observed inputs and output must be recognized.

Another major consideration is that our collected time series are invariably gappy, i.e. there are intervals of time for which we

have no observations. In order to extract the maximum information from our observations about, for example, long period or secular terms we must be capable of handling these gaps.

The time series at the Fredericton station are digitized at equally spaced (hourly) times. However, in some cases in practice observations are made at unequally spaced times and thus an analysis method able to handle unequally spaced observations would be of significant practical importance.

On the basis of the above data characteristics we can now objectively discuss existing techniques and their applicability to our specific purposes.

There are two fundamentally different existing approaches for the estimation of physical system response as a function of frequency: 1) estimation of gain and phase characteristics in the frequency domain using cross-spectral analysis and 2) estimation of impulse resonse in the time domain (Jenkins and Watts [1968]; Bendat and Piersol [1971]). These methods are briefly described in Appendix III.

Both of these techniques are based on the assumption that the time series representations of input and output (see Appendix III) are stationary. This is not the case for our data, and although, for example, a mean and trend can be removed from the data before proceeding with a response analysis, we must always be concerned about the effect of this prior removal on the response estimates in each specific application.

These techniques also both assume that observational noise is not present on the inputs. This is also not the case in our specific application and the poor results in applying these methods to cases

with noise on the inputs (as well as on the output) have been demonstrated numerically by Merry and Vanicek [1981]; see Appendix III.

Finally these two approaches are obviously not suited for handling gappy and/or unequally spaced data. In the case of the Fredericton station we do have equally spaced observed time series but gaps are commonplace.

4.2 Review of Least Squares Spectral Analysis

The suitability of least squares spectral analysis as developed by Vanicek [1971] for analysis of time series with the characteristics summarized in the previous section makes it particularly attractive as a basis for a response method. For the sake of completeness we give here a review of least squares spectral analysis following the development given by Steeves [1981].

Consider an observed time series which we will represent by a vector f of values f_i, i = 1, 2, ..., n observed at respective times t_i, i = 1, 2, ..., n not necessarily equally spaced and which may contain gaps of arbitrary length. We may also have an estimate of the accuracy of f in the form of a non-singular covariance matrix C_f. (We note here that in the case of the Fredericton tilt data only estimates of precision can be reliably estimated since this data is extremely noisy. We therefore, in our analyses, assume an identity matrix as weight matrix for our time series and estimate the covariiance matrix of constituents from equation (4.17)). We wish to detect unknown periodic constituents of f in an optimal manner especially in the case that f contains various systematic variations of unknown magnitude

whose functional forms are known. Since these systematic variations are a nuisance from the point of view of detecting the unknown periodic signal, we call them "systematic noise". We call the unknown periodic constituents of f "systematic signal".

Least squares spectral analysis is based on a least squares estimation of the magnitudes of the systematic noise constituents (examples of which may be unknown constant terms (datum biases), linear (or other) trends, trigonometric terms of the form $a_N \cos \omega_N t + b_N \sin \omega_N t$ with known angular frequency ω_N and unknown magnitudes a_N and b_N, etc., along with the coefficients a_S and b_S in the trigonometric term $a_S \cos \omega_S t + b_S \sin \omega_S t$ where here ω_S (frequency) is the argument of the least squares spectrum (as defined below). That is we determine the simultaneous least squares estimates of a_S and b_S along with the systematic noise magnitudes. Because of this simultaneous estimation, the least squares estimates of a_S and b_S, and thus the spectrum, will not be distorted by the presence of the systematic noise constituents [Taylor and Hamilton, 1972].

We thus attempt to model the time variations of the observed time series f by

$$\tilde{f} = A_N x_N + A_S x_S \qquad (4.1)$$

where A_N (dim (A_N) = (n, m), $m < n+2$) is the Vandermonde matrix of functional values of the systematic noise with unknown magnitudes x_N (dim x_N = m) and A_S (dim A_S = n, 2)) is the Vandermonde matrix of functional values (cos $\omega_S t_i$ and sin $\omega_S t_i$, i = 1, 2, ..., n) of the systematic signal with unknown magnitudes $x_S = [a_S, b_S]^T$. (Superscript $(^T)$ denotes matrix transposition and $(^{-1})$ will denote matrix inversion). Defining the residual vector

$$r = \tilde{f} - f \tag{4.2}$$

and minimizing the quadratic form $r^T C_f^{-1} r$ with respect to $x = [x_N \; x_S]^T$ yields the least squares estimator

$$\hat{x} = (A^T C_f^{-1} A)^{-1} A^T C_f^{-1} f \tag{4.3}$$

where we have let $A = [A_N \vdots A_S]$. We assume $A^T C_f^{-1} A$ is non-singular which in practice has to be confirmed in each specific case in practice. The least squares estimate of the residual vector r is then given by

$$\hat{r} = f - A^T \hat{x} \; . \tag{4.4}$$

Similarly we get

$$\hat{x}_p = (A_N^T \, C_f^{-1} \, A_N)^{-1} A_N^T \, C_f^{-1} f \tag{4.5}$$

for the least squares estimates of the systematic noise magnitudes x_N with the systematic signal ignored; the corresponding residual vector estimate is given by

$$\hat{r} = f - A_N^T \, \hat{x}_p \; . \tag{4.6}$$

The quadratic form $\hat{r}_p^T C_f^{-1} \hat{r}_p$ is thus a measure of the variance of f which is not modelled by the systematic noise. The difference

$$s^*(\omega_S) = \hat{r}_p^T C_f^{-1} \hat{r}_p - \hat{r}^T C_f^{-1} \hat{r} \tag{4.7}$$

is thus a measure of the variance of f absorbed by the trigonometric term represented by $A_S x_S$. In other words $s^*(\omega_S)$ is a measure of the maximum (since $\hat{r}^T C_f^{-1} \hat{r}$ is minimized) contribution of $A_S x_S$ to the variance of f. Since $s^*(\omega_S)$ takes values in the interval $[0, \; \hat{r}_p^T \, C^{-1}{}_f \hat{r}_p]$ we can define the normalized least square spectrum, whose values lie in the interval [0, 1],

$$s(\omega_S) = \frac{\hat{r}_p^T C_f^{-1} \hat{r}_p - \hat{r}^T C_f^{-1} \hat{r}}{\hat{r}_p^T C_f^{-1} \hat{r}_p} \; , \; \hat{r}_p^T C_f^{-1} \hat{r}_p \neq 0 \tag{4.8}$$

or

$$s(\omega_S) = 1 - \frac{\hat{r}^T C_f^{-1} \hat{r}}{\hat{r}_p^T C_f^{-1} \hat{r}_p} \tag{4.9}$$

We see that $100.s(\omega_S)$ is thus a measure of the percentage of the variance of f not accounted for by $A_N x_N$ that is accounted for by $A_s x_s$.

It can be shown that the computation of the least squares spectrum does not require the explicit computation of equation (4.3) since the spectrum is given explicitly by Steeves, [1981].

$$s(\omega_S) = \frac{\hat{r}_p^T C_f^{-1} A_S \left(N_{SS} - N_{SN} N_{NN}^{-1} N_{NS}\right)^{-1} A_S^T C_f^{-1} \hat{r}_p}{\hat{r}_p^T C_f^{-1} \hat{r}_p} \tag{4.10}$$

where we have let $N_{ij} = A_i^T C_f^{-1} A_j$; i, j = N, S). This has been detailed further for computer implementation by Wells and Vanicek [1978].

The question of statistical significance of peaks in the least squares spectrum has been addressed from two points of view by Jeudy [1981] and Steeves [1981]. We discuss now the results of these two investigations which differ in the initial selection of a statistical null hypothesis.

The null hypothesis selected by Jeudy is

$$H_o^J: \hat{r}_p \sim N_n(0, I) \tag{4.11}$$

(where "~" is read "has the underlying probability density function") i.e. that the estimated residual vector $\hat{r}_p$ has a multivariate normal distribution with mean zero and the identity matrix (I) as covariance matrix. His resulting critical value, above which spectral peaks are accepted as statistically signficiant, is given by [Jeudy, 1981]

$$c^J = \frac{1}{(1 + \frac{n-m-2}{m+2} F(n-m-2,\ m+2,\ 1-\alpha))} \qquad (4.12)$$

where F denotes the central Fisher distribution (with n-m-2 and m+2 degrees of freedom) and α is the significance level. Steeves [1981], on the other hand, selected as null hypothesis

$$H_o^S:\ f \sim N_n(0,\ I) \qquad (4.13)$$

which results in a critical value given by (op cit)

$$c^S = \frac{1}{(1 + \frac{n-m-2}{2} F(n-m-2,\ 2,\ \alpha))} \quad . \qquad (4.14)$$

A graphical comparison of these two critical values (for m+2 = 10, a typical case, and α = 0.05) against log (n-m-2) is presented in Figure 4.0. We see that for typical n-m-2, usually greater than 100 (in our case several thousand), the two critical values rapidly approach one another. However, for lower degrees of freedom (υ = n-m-2) the two values diverge with c^S approaching 100 much more rapidly than c^J. That the critical value should approach 100 quickly for low degrees of freedom agrees with the realization that, for zero degrees of freedom, any frequency (trigonometric term) will account for 100% of the variation in the time series.

We see that the basic philosophies of these two approaches differ significantly. Jeudy is taking the approach which basically assumes that a complete modelling of systematic variation in the time series will be reached at which point the residual series will contain only uncorrelated random noise. Steeves, however, following Vanicek

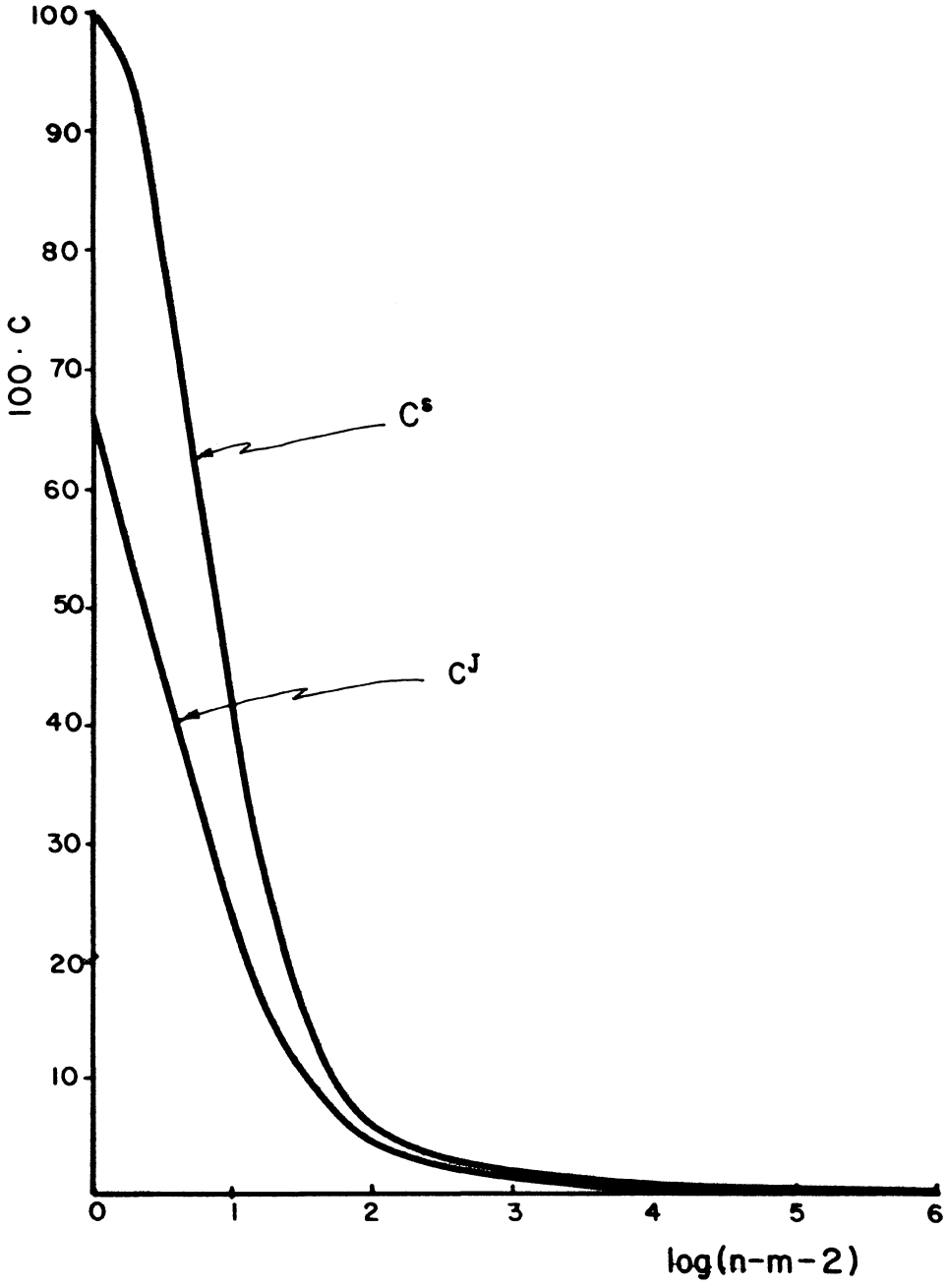

Figure 4.0 95% Critical Values C^s and C^J.

[1971], is basically examining the response of the least squares spectrum to random noise, which is independent of the status of modelling of the systematic variations of the time series (op cit).

In view of the fact that the critical values of these two approaches converge rapidly towards each other for degrees of freedom greater than 100, it may seem simply a matter of personal choice when choosing which to use in practice. However we should also point out that, for non-zero degrees of freedom (υ), the null hypothesis H_o^J: $\hat{r}_p \sim N_n(0, I)$ is never fulfilled since the covariance matrix $C_{\hat{r}_p}$ of $\hat{r}_p$ has rank υ [Mikhail 1976, p. 119]. That is, at best we can have υ diagonal elements of $C_{\hat{r}_p}$ equal to unity with all other elements equal to zero. Especially for low degrees of freedom this is a major flaw in the basic assumptions of Jeudy's approach.

For the above reasons, the critical value used in this present study for examining statistical significance of spectral peaks is c^S (equation 4.14) which can be written more simply as [Steeves, 1981]

$$c^S = (1 + (\alpha^{-2/\upsilon} - 1)^{-1})^{-1} \qquad (4.15)$$

4.3 Development of a Least Squares Response Estimation Method

We consider first the estimation of the response gain and phase (see Appendix III), as a function of frequency, of an observed physical linear system output to a single observed forcing input phenomenon. We later generalize the approach for handling multiple inputs.

We consider an input observed time series which we represent by a vector g, dim (g) = n_g, of values g_i, i = 1, 2, ..., n_g not necessarily equally spaced and which may contain gaps. Also we consider the corresponding output observed time series which we

represent by a vector f, dim (f) = n_f, of values $f_i = 1, 2, \ldots, n_g$ not necessarily equally spaced and may contain gaps (not necessarily the same spacing or gaps as in g). We assume that each of f and g may contain system- atic noise constituents. The procedure proposed for response estima- tion as a function of frequency is as follows.

First of all we must have some assurance, based on some physical understanding of the situation we are considering, that the observed output f of the physical system is indeed being caused, at least in part, by the observed input g. Otherwise the estimation of response of f to g may be physically meaningless. With this assurance we proceed by identifying periodic constituents of the input series g using least squares spectral analysis.

We should, if possible, attempt to relate the identified periodic constituents with any physical understanding we have of the process in question. If this is possible we will be able to eliminate the effect of shifting of corresponding spectral peaks. Otherwise shifting of peaks can not in general be detected.

We successively incorporate any identified statistically significant components into the systematic noise and search for further hidden periodicities in g until a large portion of g is modelled by the so determined periodic components. This results in identifying a set of frequencies ω_i, $i \in I \equiv \{1, 2, \ldots, m_g\}$ constituent in g and provides least squares estimates of the magnitudes a_i^g, b_i^g, $i \in I$ of the corresponding trigonometric terms

$$a_i^g \cos \omega_i t + b_i^g \sin \omega_i t, \quad i \in I. \tag{4.16}$$

The estimated covariance matrix of these coefficients is also determined from, using the notation of section 4.2,

$$C_{\hat{x}_N} = \hat{\sigma}_o^2 \, (A_N^T C_f^{-1} A_N)^{-1} \tag{4.17}$$

where

$$\hat{\sigma}_o^2 = \frac{\hat{r}_p^T C_f^{-1} \hat{r}_p}{n-m} \quad . \tag{4.18}$$

For each pair $\hat{a}_i^g$, $\hat{b}_i^g$ of these estimated coefficients we can compute the corresponding amplitudes and phases from

$$\hat{c}_i^g = \{(\hat{a}_i^g)^2 + (\hat{b}_i^g)^2\}^{1/2} \tag{4.19}$$

and

$$\hat{\phi}_i^g = 2.\arctan \frac{\hat{b}_i^g}{\{\hat{a}_i^g + \hat{c}_i^g\}} \tag{4.20}$$

$i \in I$. Applying the covariance law [Mikhail, 1976] to equations (4.19) and (4.20), and denoting the estimated covariance matrix of the coefficients $\hat{a}_i^g$, $\hat{b}_i^g$ by

$$\hat{C}_i = \begin{bmatrix} \hat{\sigma}^2_{a_i} & \hat{\sigma}_{a_i b_i} \\ \hat{\sigma}_{a_i b_i} & \hat{\sigma}^2_{b_i} \end{bmatrix} \tag{4.21}$$

which is extracted from $\hat{C}_{\hat{x}_N}$ (equation 4.17), we have

$$\hat{\sigma}_{c_i^g} = \frac{1}{\hat{c}} \{\hat{a}_i^2 \sigma^2_{a_i} + 2\hat{a}_i \hat{b}_i \hat{\sigma}_{a_i b_i} + \hat{b}_i^2 \hat{\sigma}^2_{b_i}\}^{1/2} \tag{4.22}$$

and

$$\hat{\sigma}_{\phi_i^g} = \frac{1}{\hat{c}_i^2} \{ \hat{b}_i^2 \hat{\sigma}_{a_i}^2 - 2\hat{a}_i \hat{b}_i \hat{\sigma}_{a_i b_i} + \hat{a}_i^2 \hat{\sigma}_{b_i}^2 \}^{1/2} \qquad (4.23)$$

The set of frequencies $\{\omega_i, i \in I\}$ is then forced as systematic noise constituents in the output series f thus determining least squares estimates of the magnitudes a_i^f and b_i^f, $i \in I$, of these trigonometric terms as they are constituent in f. The estimates of amplitudes c_i^f and phases ϕ_i^f, $i \in I$, and their estimated standard deviations are then determined (equations 4.19, 4.20, 4.22 and 4.23 with "g" replaced by "f"). It must be noted that any other systematic noise, besides the successively determined periodic constituents, is always included in the estimation of the constituents of both f and g so that we minimize the distortion of the determined amplitudes and phases of the periodic constituents.

We now estimate the gain of the response at each frequency ω_i, $i \in I$ using

$$\hat{G}_i = \frac{\hat{c}_i^f}{\hat{c}_i^g} \quad , \qquad \hat{c}_i^g \neq 0 \qquad (4.24)$$

and the corresponding response phase

$$\hat{\Phi}_i = \hat{\phi}_i^f - \hat{\phi}_i^g \ . \qquad (4.25)$$

Application of the covariance law to equations (4.24) and (4.25) results in

$$\hat{\sigma}_{G_i} = \left[\frac{(\hat{c}_i^{f\,2})}{\hat{c}_i^{g\,4}} \hat{\sigma}_{c_i^g}^2 + \frac{1}{\hat{c}_i^{g\,2}} \hat{\sigma}_{c^f}^2 \right]^{1/2} \qquad (4.26)$$

and

$$\hat{\sigma}_{\Phi_i} = [\, \hat{\sigma}^2_{\phi_i f} + \hat{\sigma}^2_{\phi_i g}\,]^{1/2} \qquad (4.27)$$

as estimates of the standard deviations of $\hat{G}_i$ and $\hat{\Phi}_i$ respectively.

Since we may expect that these response estimates will be distorted somewhat depending on the effect on these estimates of the unmodelled variations of both input and output, and since we should expect usually a smooth response function for a well behaved physical systems, we should now smooth the estimated responses (see section 4.4 and Chapter 5). These smoothed estimates $\tilde{G}_i$, $\tilde{\Phi}_i$, $i \in I$ can then be used for generating the smoothed output response,

$$\tilde{f}^g(t) = \sum_{i \in I} \tilde{c}^g_i . \tilde{G}_i . \cos\,(\omega_i t - (\hat{\phi}^g_i + \hat{\Phi}_i)) \qquad (4.28)$$

As a check on this model we can then force $\tilde{f}^g(t)$, as a numerical function, in g, along with other systematic noise constituents. We should expect that the so determined coefficient $\hat{\tilde{c}}_f$ will be close (within, say, its 95% confidence interval) to unity.

The approach is easily extended to handle several input functions. We simply decompose each input function separately into its constituent periodic components using least squares spectral analysis. All so determined frequencies (except frequencies common to two or more inputs which are forced only once) are then forced in the output series (as systematic noise). The response estimates of gain and phase corresponding to each input are then formed as before while those estimates at common frequencies are interpolated from the

smoothed response functions. Numerical functions (equation (4.28)) can then be generated and forced in the output (simultaneously) and the resulting estimated coefficients of these numerical functions should again be close to unity.

We now demonstrate the application of this method with a simple numerical example.

4.4 Numerical Example of Least Squares Response Estimation

For our numerical example we will consider a case with three input forcing functions, each composed of four periodic constituents with the first and third having linear trends. All three inputs as well as the output are gappy and are considered to have unknown datum biases. As well all these generated time series are superimposed with pseudo random noise which was generated with a random number generator of the UNB FORTRAN library. Specifics of the constituents of these series are tabulated in Tables 4.1-4.4 (on pages 61 - 64) and are plotted along with their least squares spectra below these tables in Figures 4.1-4.4. The response functions used for generating the output from the three inputs are illustrated in Figure 4.5 and the corresponding gains and phases are listed in Table 4.5. (These functions are not meant to be physically meaningful; we take purely an empirical approach).

Periodic constituents			Data Intervals		
Period (hrs.)	Amplitude (^{o}C)	Phase (degrees)	from (hrs.)	to (hrs.)	bias (^{o}C)
12.0	20.0	120.0	1	250	5.0
24.0	10.0	60.0	325	550	-5.0
150.0	5.0	230.0	600	720	2.0
200.0	15.0	170.0			

linear trend: 0.05 mbar/hr.
range of pseudo random noise: 2 ^{o}C

Table 4.1. Input #1 constituents.

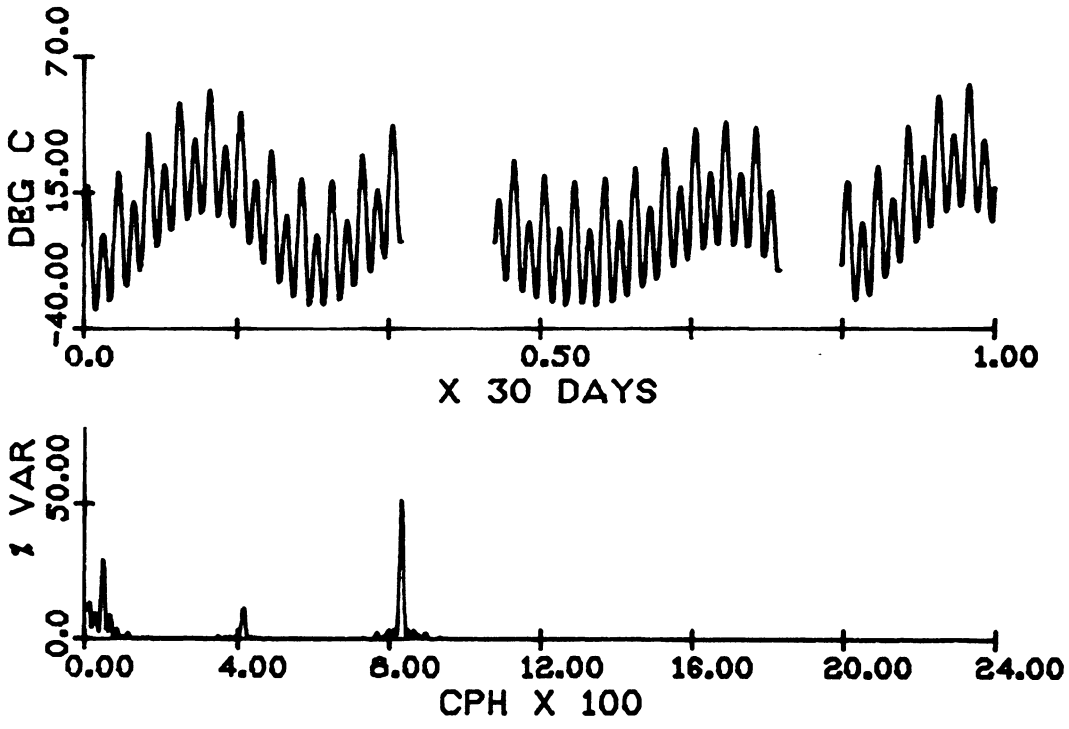

Figure 4.1. Input #1 series and least squares spectrum.

Periodic Constituents			Data Intervals		
Period (hrs)	Amplitude (mbar)	Phase (degrees)	from (hrs.)	to (hrs.)	bias (mbar)
5.0	5.0	75.0	25	250	3.0
24.0	7.0	150.0	200	450	8.0
100.0	6.0	30.0	500	720	-2.0
175.0	4.0	200.0			

range of pseudo random noise: 1 mbar

Table 4.2 Input #2 constituents

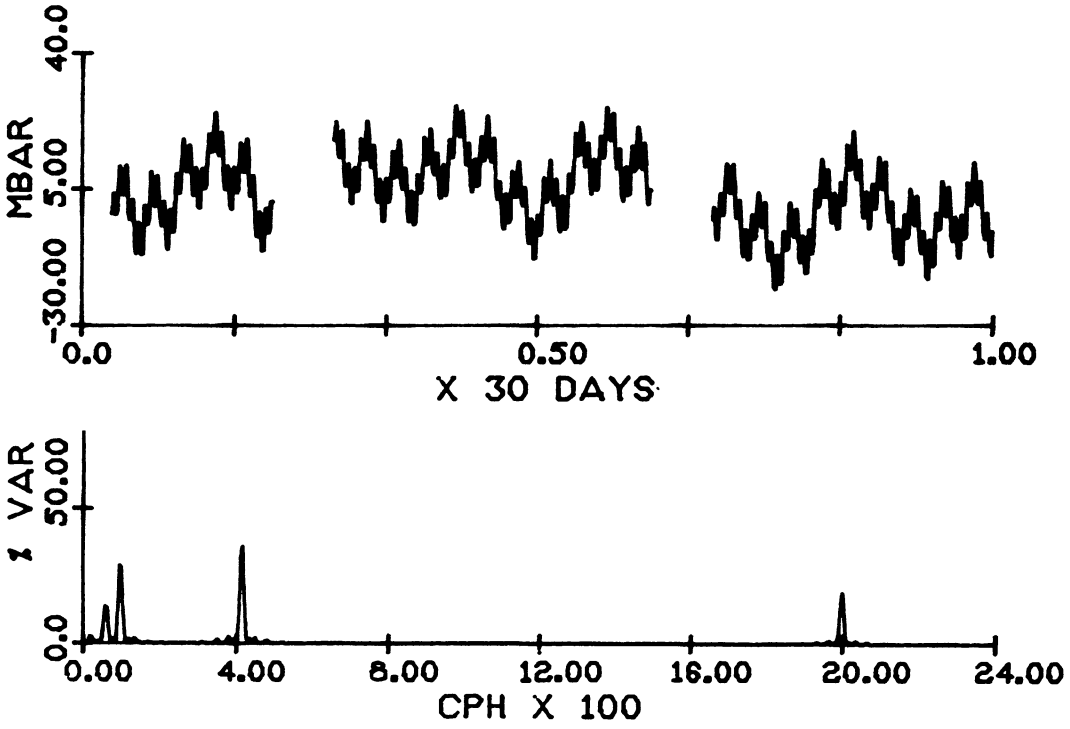

Figure 4.2. Input #2 series and least squares spectrum

Periodic constituents			Data Intervals		
Period (hrs.)	Amplitude (cm)	Phase (degrees)	From (hrs)	To (hrs)	Bias (cm)
20.0	10.0	340.0	1	100	10.0
50.0	15.0	210.0	150	500	0.0
125.0	10.0	35.0	550	720	5.0
235.0	15.0	110.0			

linear trend: 0.10 cm/hr.
range of pseudo random noise: 2 cm.

Table 4.3. Input #3 constituents

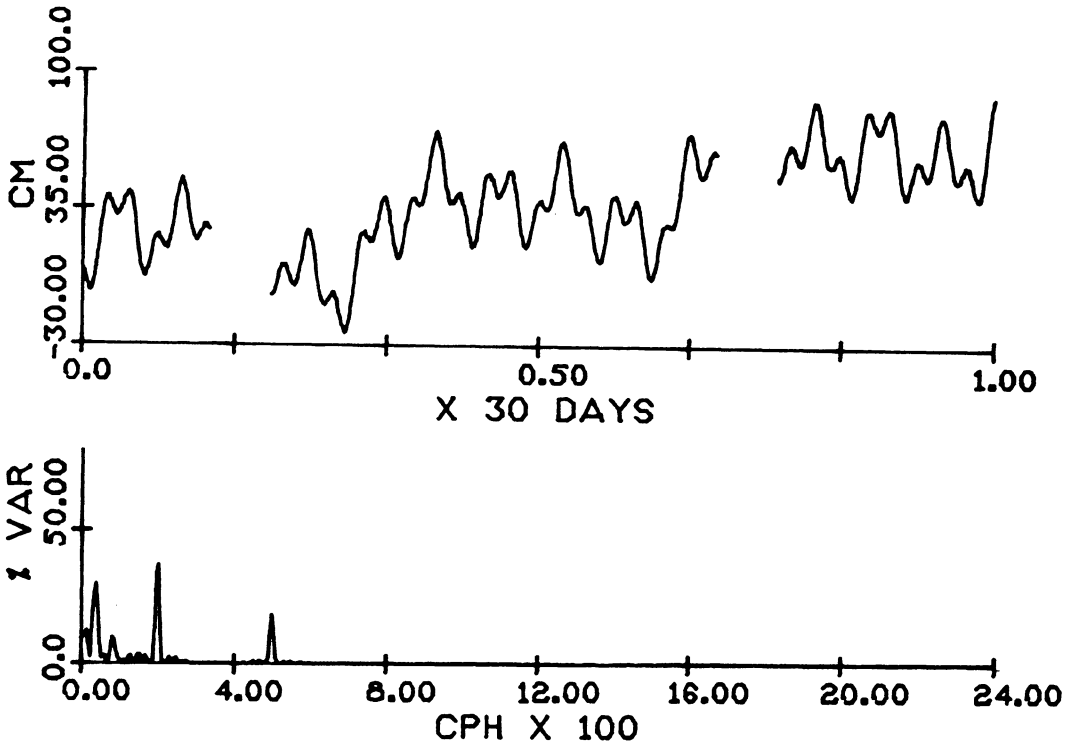

Figure 4.3. Input #3 Series and least squares spectrum

Periodic Constituents			Data Intervals		
Period (hrs)	Amplitude (msec)	Phase (degrees)	From (hrs)	To (hrs)	Bias (hrs)
12.0	20.0	0.0	20.0	30.0	340.0
24.0	11.0	300.0	50.0	45.0	210.0
150.0	17.5	170.0	125.0	30.0	35.0
200.0	84.0	250.0	235.0	45.0	110.0
			Data Intervals		
5.0	12.5	125.0	From (hrs)	To (hrs)	Bias (cm)
24.0	19.6	210.0			
100.0	36.0	130.0	1	275	10.0
175.0	24.8	320.0	325	600	0.0
			650	720	5.0
			linear trend 0.15 msec/hr. range of pseudo random noise: 3.0 msec.		

Table 4.4 Output constituents

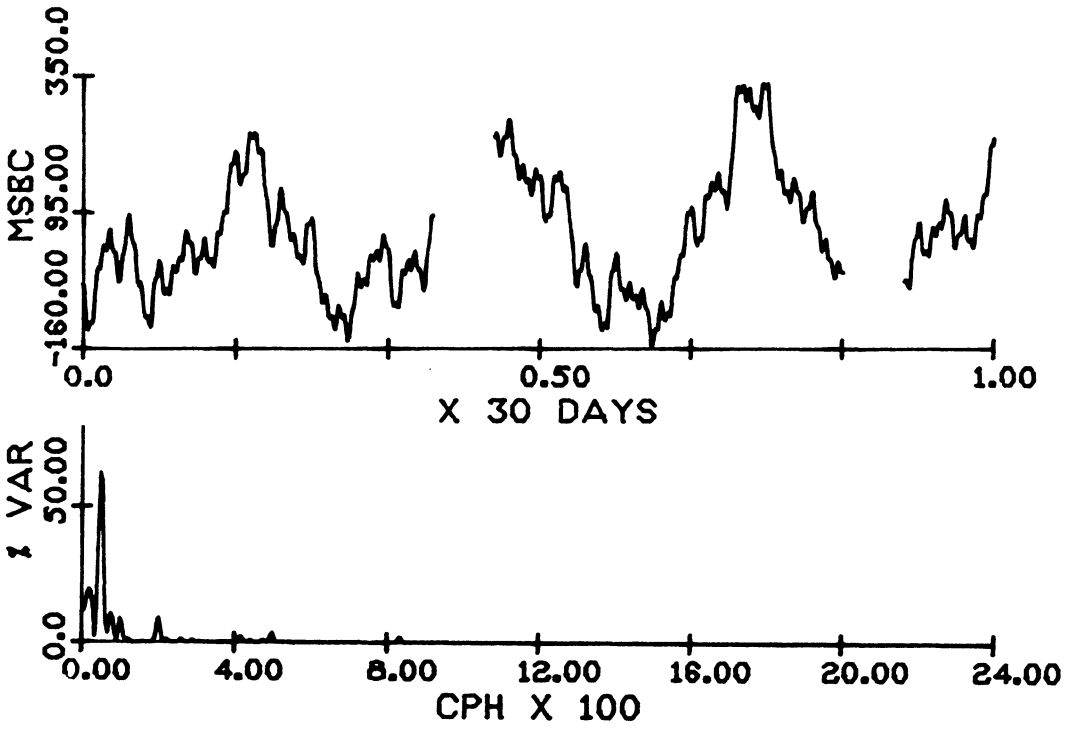

Figure 4.4. Output series and least squares spectrum.

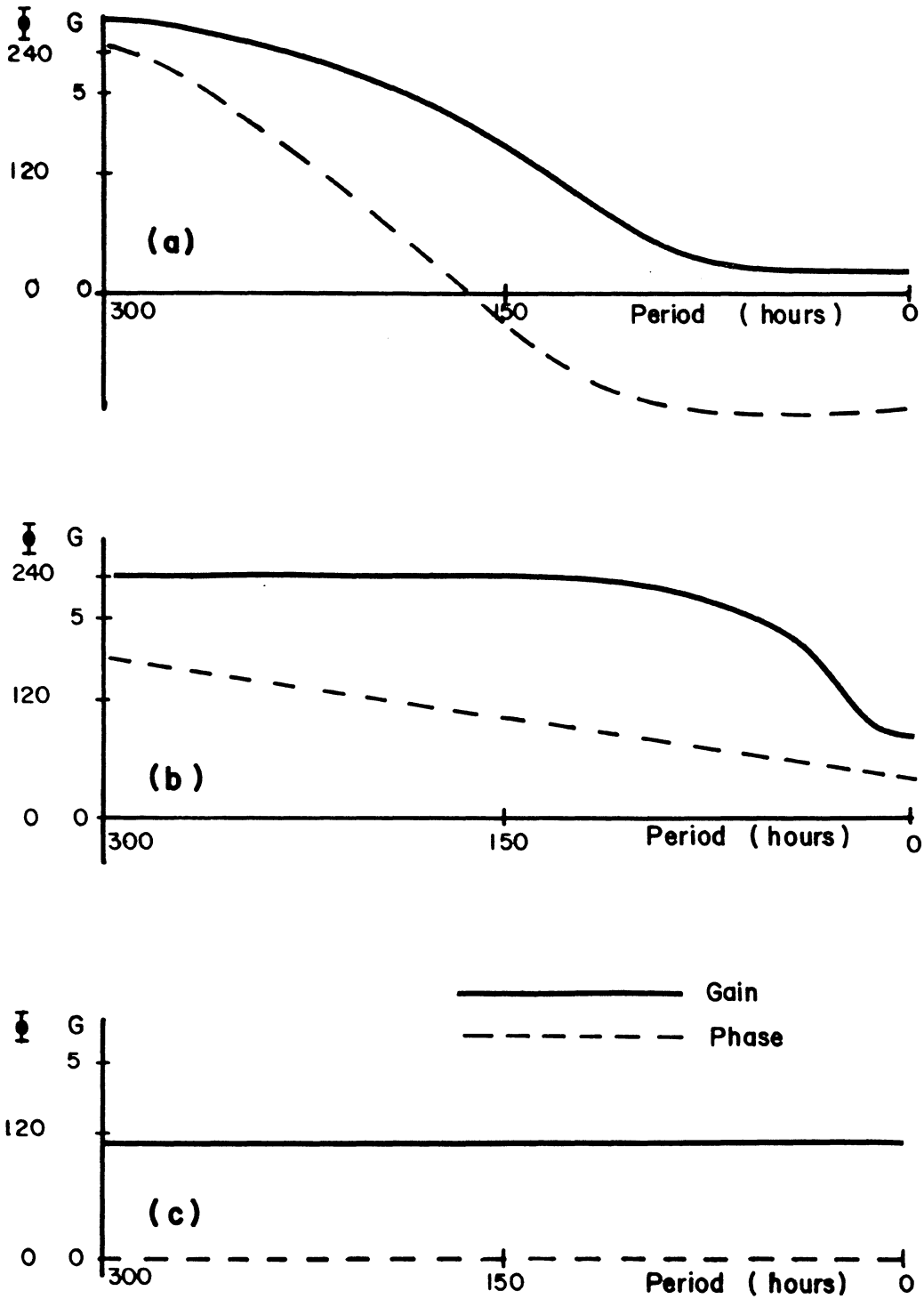

Figure 4.5 Gain (G) and Phase (Σ in degrees) for Response to (a) Input *1 (b) Input *2 and (c) Input *3.

Time Series	Period (hours)	Response Gain	Response Phase (degrees)
Input #1	12.0	1.0	240.0
	24.0	1.1	240.0
	150.0	3.5	300.0
	200.0	5.6	80.0
Input #2	5.0	2.5	50.0
	24.0	2.8	60.0
	100.0	6.0	100.0
	175.0	6.2	120.0
Input #3	20.0	3.0	0.0
	50.0	3.0	0.0
	125.0	3.0	0.0
	235.0	3.0	0.0

Table 4.5 Assumed Gains and Phases of the Input Time Series.

We demonstrate now the decomposition of one of the input functions into its periodic constituents using least squares spectral analysis. Let us consider input #3. In Figure 4.3 the least squares spectrum of input #3 is shown with no forced periodic constituents (only linear trend and datum biases were forced) in which peaks are present at periods of 20.0, 50.0 and approximately 260 hours. We begin the decomposition then by first forcing periods 20.0 and 50.0 hours whose peaks are narrow and well separated. Figure 4.6 demonstrates the successive identification and removal (forcing as systematic noise) of further periodic constituents. Figure 4.6(a) is the spectrum after forcing 20.0 and 50.0 hour periods in which the 260.0 hour period peaks. Figure 4.6(b) shows the spectrum after forcing 20.0, 50.0 and 260.0 hour periods; a peak at 124.0 hours

appears. Figure 4.6(c) is the spectrum after forcing 20.0, 50.0, 124.0 and 260.0 hour periods in which a peak occurs at 235.0 hours. Including this 235.0 hour period in the systematic noise resulted in the 260.0 hour period having a very small (0.4) poorly determined (σ = 9.5) amplitude. Since this indicates that the initial 260.0 hour period was actually the 235.0 hour period showing up but shifted, the 260.0 hour period was then replaced by this 235.0 hour period. Figure 4.6(d) is the spectrum when periods of 20.0, 50.0, 124.0 and 235.0 hours were forced as systematic noise; a peak at a period of 125.0 hours emerges. This again resulted in the 124.0 hour period being eliminated. Finally in Figure 4.6(e) the spectrum when forcing periods of 20.0, 50.0, 125.0 and 235.0 hours is shown. This final spectrum is relatively flat with highest peaks at 1.0 percent variance which is equal to the 95 percent critical value c^S for this case; we conclude therefore that there are no further statistically significant periodic constituents in the time series. (Note that the pseudo random noise generator which was used here has the desired flat spectrum characteristic of noise).

The practical use of the least squares spectral analysis has been demonstrated here. Specifically its capability of reducing (in this simple case completely removing) the systematic distortion of estimated systematic noise constituents caused by unmodelled variations in the time series has been demonstrated.

The estimated amplitudes and phases of identified periodic constituents of input #3, along with those of inputs #1 and #2, are given in Table 4.6. These periods of all three inputs, except the

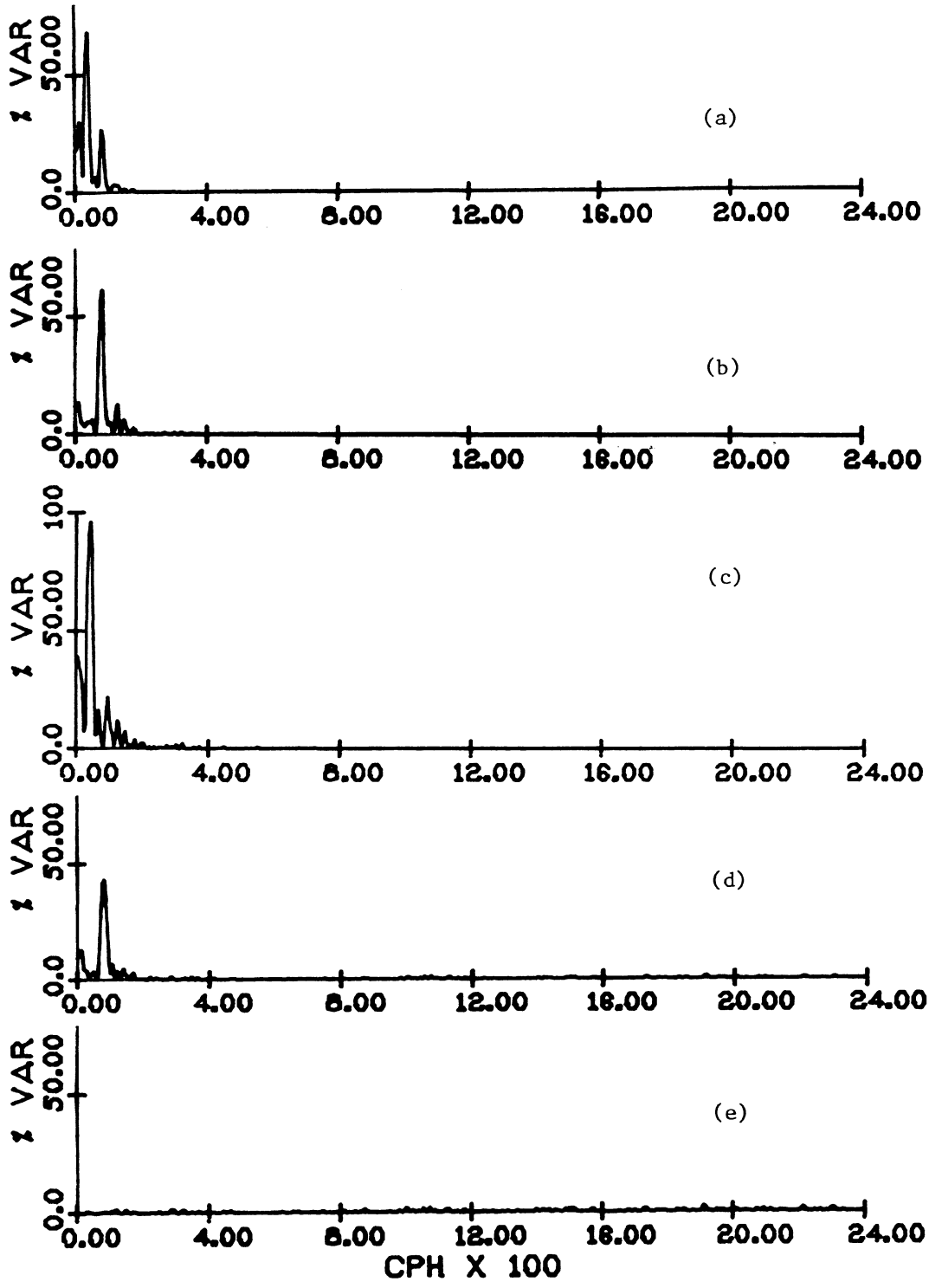

Figure 4.6. Least squares spectra during decomposition of input #3.

Time series	Period (hours)	Amplitude	Phase (degrees)
Input #1	12.0	20.00 ± 0.03°C	120.0 ± 0.1
	24.0	10.03 ± 0.03°C	59.9 ± 0.2
	150.0	4.98 ± 0.04°C	229.8 ± 0.4
	200.0	15.03 ± 0.04°C	170.0 ± 0.1
Input #2	5.0	5.01 ± 0.02 mbar	75.3 ± 0.2
	24.0	6.99 ± 0.02 mbar	149.9 ± 0.1
	100.0	6.01 ± 0.02 mbar	29.9 ± 0.2
	175.0	3.99 ± 0.02 mbar	200.2 ± 0.2
Input #3	20.0	10.00 ± 0.03 cm	340.3 ± 0.2
	50.0	15.00 ± 0.03 cm	209.7 ± 0.1
	125.0	9.95 ± 0.03 cm	35.0 ± 0.2
	235.0	15.03 ± 0.04 cm	109.9 ± 0.1

Table 4.6 Estimated periodic constituents of the Input time series.

24.0 hour period which inputs #1 and #2 have in common, were then forced simultaneously as systematic noise in the output series. The gain and phase of the response of the output to these inputs were then computed for each of these input periods according to equations (4.25)

Time Series	Period (hours)	Response Gain $\hat{G}$	Response Phase $\hat{\Phi}$ (degrees)
Input #1	12.0	1.00 ± 0.04 msec/°C	240.2 ± 2.6
	150.0	2.73 ± 0.53	294.3 ± 10.4
	200.0	5.27 ± 0.46	70.5 ± 6.3
Input #2	5.0	2.51 ± 0.18 msec/mbar	50.0 ± 4.2
	100.0	6.22 ± 0.18	98.2 ± 1.6
	175.0	6.97 ± 1.85	143.5 ± 11.0
Input #3	20.0	2.84 ± 0.09 msec/cm	358.9 ± 1.8
	50.0	2.99 ± 0.06	358.7 ± 1.2
	125.0	3.01 ± 0.13	357.3 ± 2.7
	235.0	2.86 ± 0.15	12.1 ± 8.6

Table 4.7 Estimated Response Gains and Phases and Their Estimated Standard Deviations.

to (4.27). These estimates are given in Table 4.7 and plotted in Figure 4.7 in which we have drawn smooth curves through these estimates. These smoothed response estimates (determined graphically) are then used for determining the response gain and phase at the 24.0 hour period for inputs #1 and #2. Table 4.8 lists these estimates and we see that they are in close agreement with the assumed gains and phases of Table 4.5.

Time Series	Period (hours)	Response Gain	Response Phase (degrees)
Input #1	24.0	1.0	240.0
Input #2	24.0	3.0	60.0

Table 4.8 Interpolated Response Gains and Phases for the 24 hour period

By forming the smoothed output response $\tilde{f}$, using equation (4.28), and forcing it as a numerical function in the output time series we get $c_f = 1.0 \pm 0.03$.

We have thus demonstrated the applicability of the least squares response method to a simple case. We have taken a purely empirical approach with no reference to whether our results are physically meaningful.

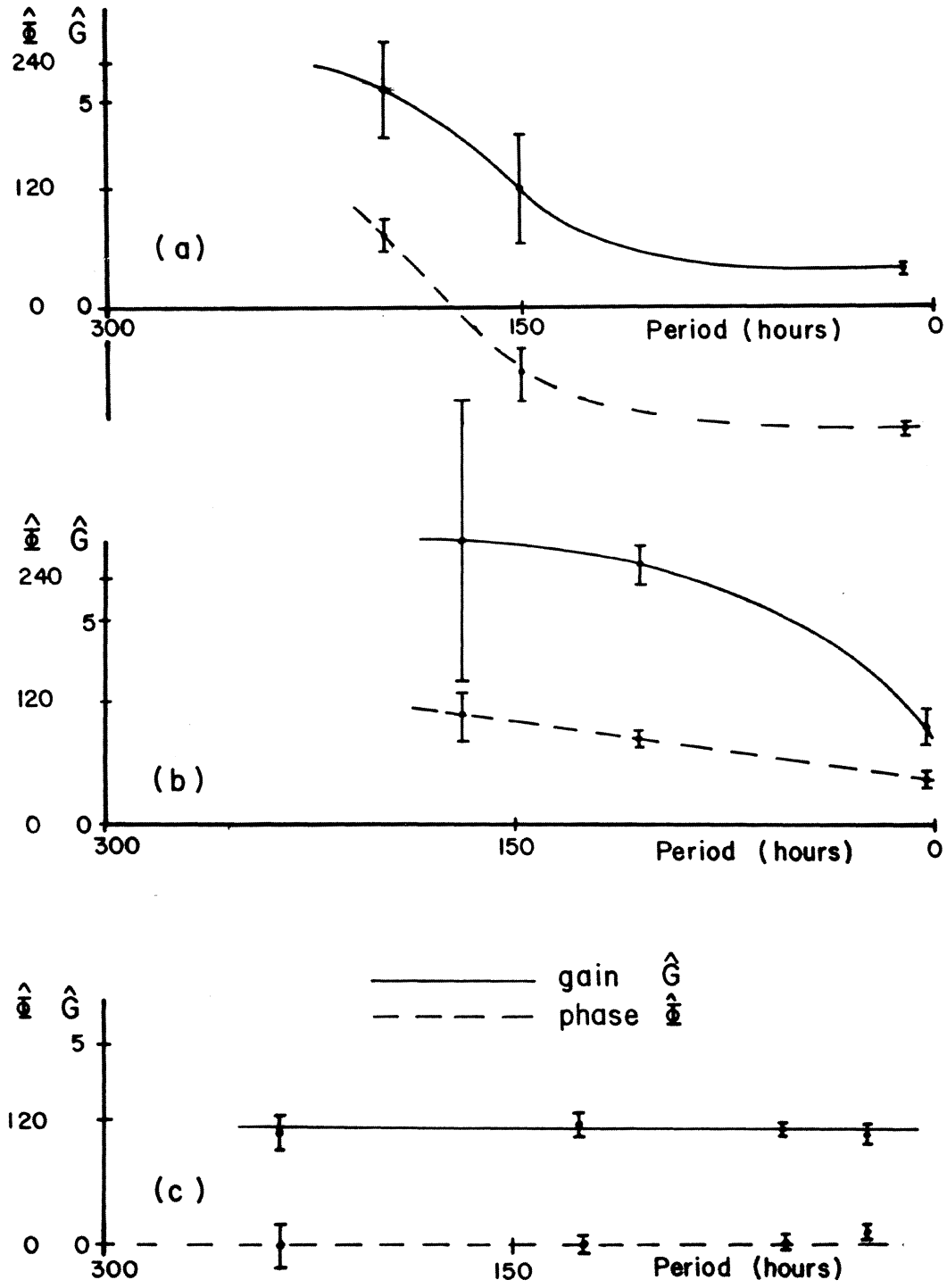

Figure 4.7 **Estimated Response Gain and Phase for Inputs 1(a), 2(b), and 3(c).** (Error b are at 95% confidence intervals).

CHAPTER FIVE

LEAST SQUARES ESTIMATION OF TILT RESPONSE TO SURFACE TEMPERATURE AND ATMOSPHERIC PRESSURE AT FREDERICTON

In this chapter we apply the least squares response method to observations collected at the Fredericton station. We consider only surface temperature and atmospheric pressure as inputs since these data are all that are presently available in digitized and calibrated form. This will result in other phenomena having possible distortional effects on the estimated responses; in this sense this analysis is preliminary. Also we take a purely empirical approach for this first attempt. We will see that our modelling is preliminary also in this regard and that further investigations should attempt to interpret the results of this analysis in physical terms as will become clear presently.

5.1 Frequency Decomposition of Observed Surface Temperature and Atmospheric Pressure

We first discuss the decomposition of the surface temperature into its periodic constituents. This process is illustrated in Figure 5.1. In Figure 5.1(a) the least squares spectrum is illustrated for the case with no forced periods; only a datum bias was forced at this stage. A 24 hour period was significant and was forced as systematic noise; the resulting spectrum is shown in Figure 4.1(b). We see that the spectrum at this stage is dominated by long periodic constituents. Therefore the solar annual and semi-annual periods were then also forced resulting in the spectrum of Figure 5.1(c), in which a period of 951.4 hours was predominant. We note that the 95% critical value c^S (see Chapter 4) for these spectra was equal to 0.1%; all peaks identified during the decomposition of both the temperature and pressure were at least 10 times this critical value, i.e. greater than 1% of the variance of the residual series (see Chapter 4).

Figure 5.1(d) is the spectrum after adding the 951.4 hour period to the systematic noise. At this stage a peak occurred at a period of 2538.0 hours; this was forced giving the spectrum of Figure 5.1(e). Successively, periods of 12.0, 237.9, 566.7, 639.5, 23.93 and both 82.1 and 190.7 were forced. Figure 5.1(k) shows the spectrum for the case with all 12 of these aforementioned periods forced. These periods are apparently due to "weather" variations and could not be attributed to the motion of the sun. At this stage the spectrum has many peaks of equal intensity, more than is apparent in the figure. The decomposition was stopped here. Although statistically

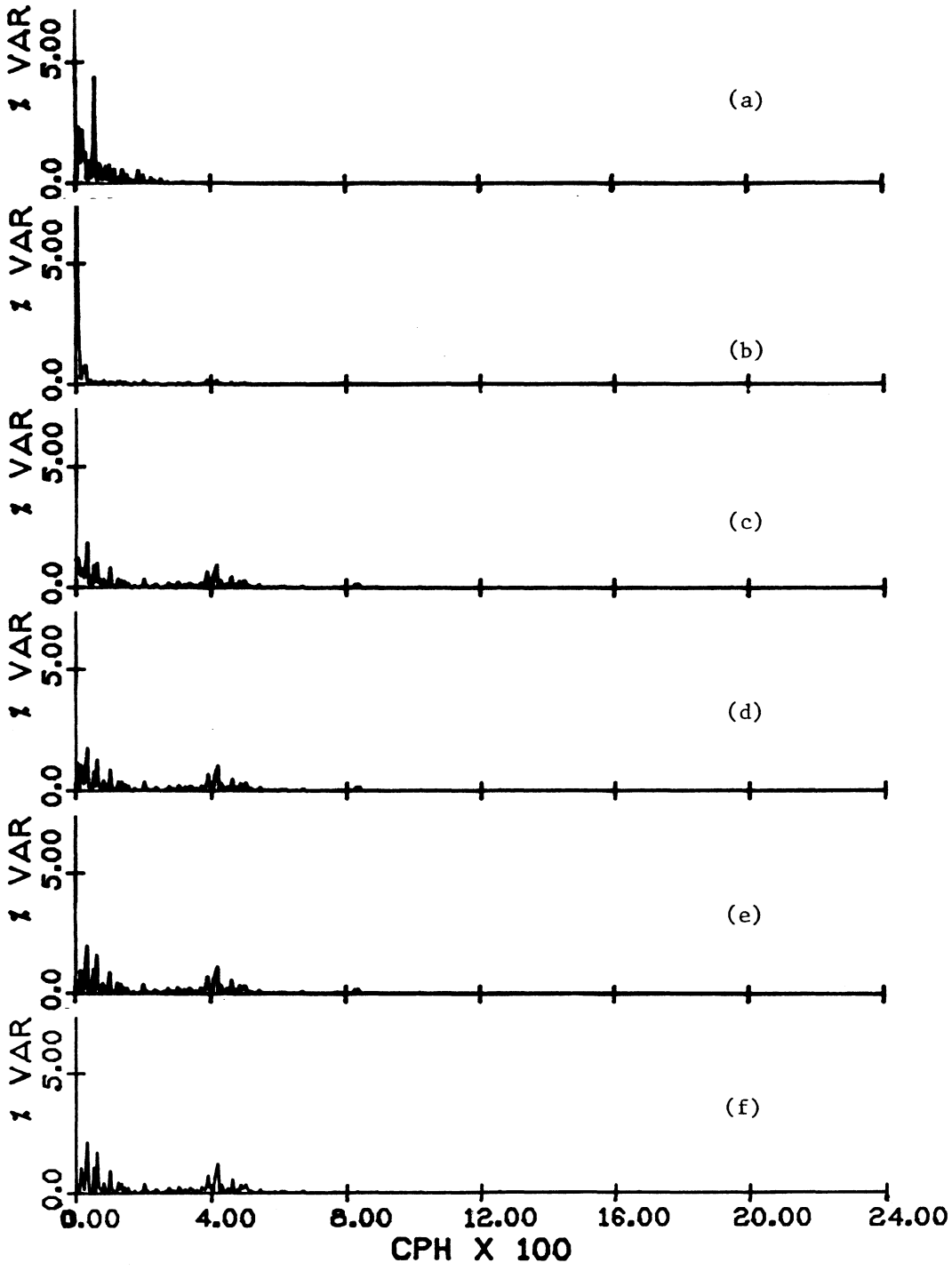

Figure 5.1 (A). Least Squares Spectra During Temperature Decomposition

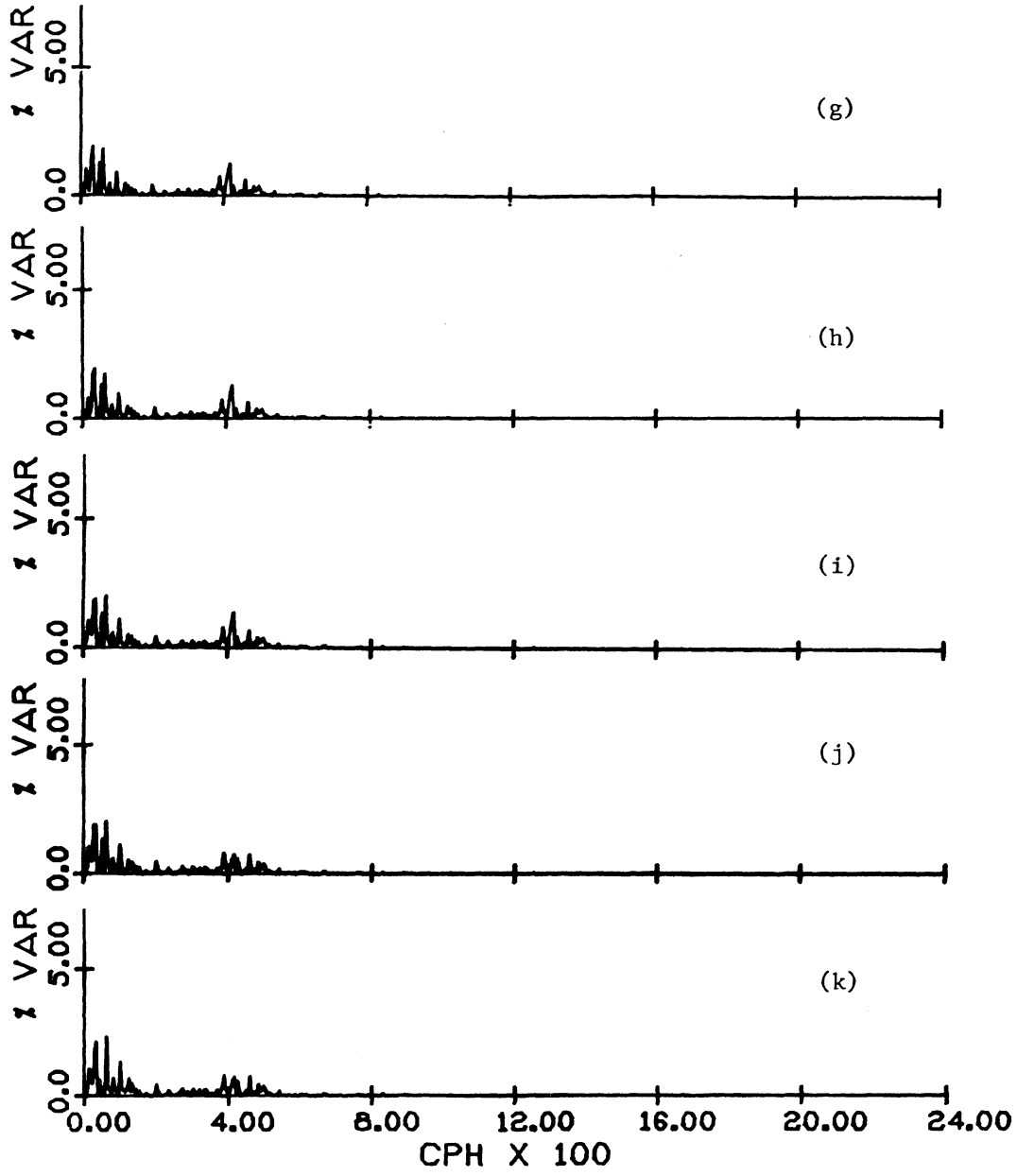

Figure 5.1 (B) Least Squares Spectra During Temperature Decomposition (continued)

signficant peaks were still present in the spectrum it was felt that the 12 most significant periodic constituents of the temperature series will represent the major portion of its variations during its time span. The least squares estimates of the amplitudes and phases (with respect to the beginning of the time series) of these periodic constituents are given in Table 5.1. Note that the 23.93 hour constituent is not included since an interference with the 24.00 hour period was suspected.

Period		Amplitude	Phase
(hours)	mean (solar days)	(^{o}C)	(degrees)
12.00	0.5	1.46 ± 0.07	209.7 ± 2.9
24.00	1.0	5.62 ± 0.07	302.8 ± 0.8
82.10	3.42	0.90 ± 0.07	358.5 ± 4.7
190.70	7.94	0.92 ± 0.07	167.4 ± 4.6
237.90	9.91	1.03 ± 0.08	321.3 ± 4.1
566.70	23.61	1.09 ± 0.08	138.6 ± 4.2
639.50	26.64	1.13 ± 0.08	114.6 ± 3.8
951.40	39.64	1.63 ± 0.08	289.9 ± 2.6
2538.00	105.75	2.52 ± 0.09	103.0 ± 1.8
4382.92	182.62	0.43 ± 0.08	222.2 ± 11.0
8766.16	365.25	14.59 ± 0.08	7.3 ± 0.3

Table 5.1 Least Squares Estimates of Amplitudes and Phases of Periodic Constituents of Temperature. Dispersion measures are estimated standard deviations.

A similar procedure was taken in the decomposition of the pressure series. The spectra during this decomposition are illustrated in Figure 5.2. Figure 5.2(a) shows the pressure spectrum with only a datum bias forced as systematic noise. Long period constituents were predominant in this first spectrum and therefore annual and semi-annual constituents were forced; the resulting

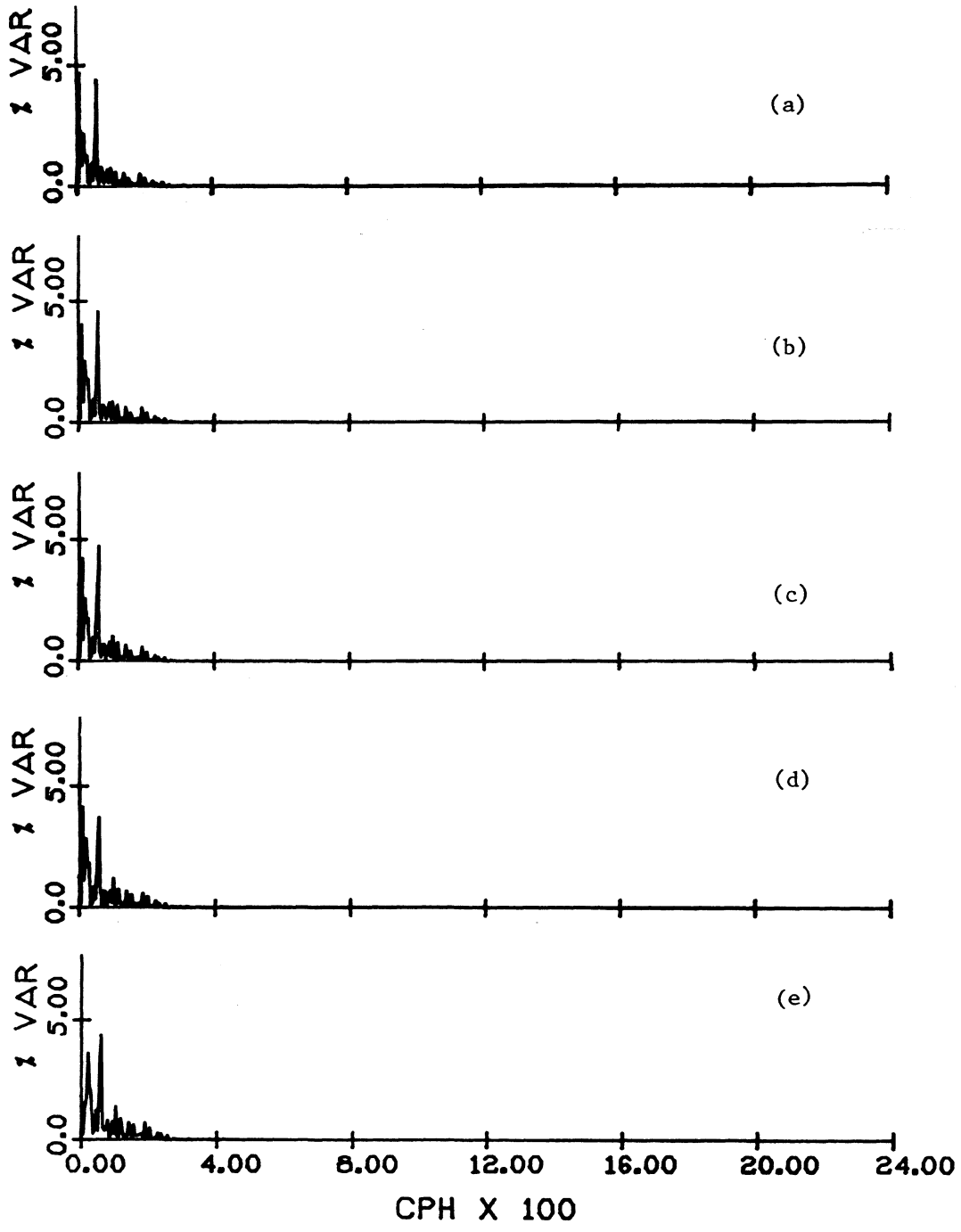

Figure 5.2 (A). Least Squares Spectra During Pressure Decomposition

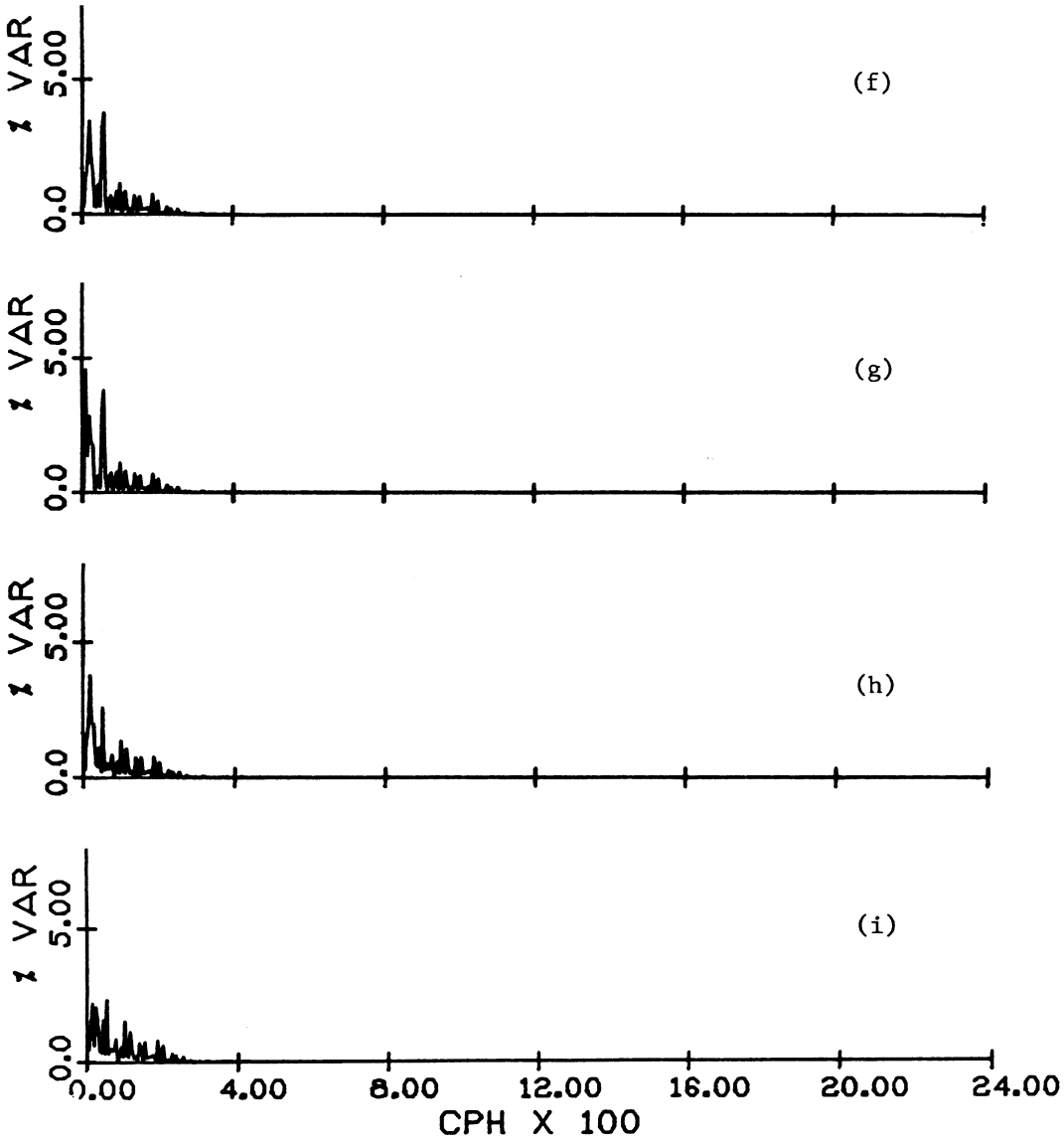

Figure 5.2 (B). Least Squares Spectra During Pressure Decomposition.

spectrum is shown in Figure 5.2(b). Further periods of 97.1, 156.4, 218.5, 1079.0, 144.2, 174.1 and 513.3 hours were identified and forced as systematic noise. Again the final spectrum, Figure 5.2(i), was composed of many peaks of near equal intensity and it was felt that the 9 predominant constituents represent the major variations of the pressure series during its time span. The estimated amplitudes and phases of the identified constituents are given in Table 5.2. We note here that a previous study by Petrie and Lively [1979] has shown that a period of 96 hours was dominant in the spectrum of atmospheric pressure variations observed off the Nova Scotia coast. These measurements were made during 1976-77; we observe a similar period (97.1 hours) in our pressure measurements.

Period		Amplitude (mbar)	Phase (degrees)
(hours)	mean solar days		
97.10	4.04	1.73 ± 0.12	329.4 ± 4.0
144.20	6.00	2.21 ± 0.12	142.7 ± 3.2
156.40	6.52	2.07 ± 0.12	227.9 ± 3.4
174.10	7.25	2.31 ± 0.12	165.0 ± 3.1
218.50	9.10	2.84 ± 0.12	144.2 ± 2.5
512.30	21.34	2.05 ± 0.12	313.8 ± 3.4
1079.00	44.96	2.44 ± 0.12	334.0 ± 3.0
4382.92	182.62	1.81 ± 0.15	202.9 ± 4.8
8766.16	365.27	5.40 ± 0.25	252.2 ± 1.5

Table 5.2 Least Squares Estimates of Amplitudes and Phases of Periodic Constituents of Pressure. Dispersion measures are estimated standard deviations.

5.2 Response Estimates

The identified periodic constituents at non-tidal frequencies of the temperature and pressure series were forced simultaneously in the tilt series of both ORB 94 and ORB 95. Along with these periods the four main semi-diurnal and four main diurnal tidal constituents were forced as well as a linear trend and datum biases. Response estimates were formed, according to the formalism described in Chapter 4. The least squares estimates of response gain G and phase Φ are given in Tables 5.3 and 5.4 and graphically displayed in Figures 5.3 to 5.6. In these figures also we have estimated smoothed response functions (graphically) with the smooth dashed lines. We will now evaluate these response estimates.

5.3 Discussion of Response Estimates

Let us first evaluate the gain estimates for tilt response to pressure and temperature from the plots of the short sections of data in Figures 1.1 and 1.2. Although these will be crude estimates they will give us a check on at least the order of magnitude. By scaling the amplitudes of the variations where there is apparent correlation we get the following estimates. From Figure 1.1 we get a gain for pressure induced tilt of approximately 6 msec/mbar; from Figure 1.2 we get approximately 5 msec/mbar, both for a period of approximately 90 hours. These are in order of magnitude agreement with our least squares estimates of gain near this period (see Table 5.4). Similarly for the tilt response to temperature we get, by scaling in both Figures 1.1 and 1.2, a gain of approximately 3 msec/^{o}C, again in rough

Pendulum	Period (hours)	Gain ($\hat{G}$) (msec/^{o}C)	(Phase ($\hat{\Phi}$) (degrees)
ORB 95	82.1	13.15 ± 2.63	186.9 ± 11.9
	190.7	36.60 ± 4.53	68.0 ± 6.8
	237.9	73.48 ± 6.72	147.6 ± 5.1
	566.7	193.68 ± 15.15	169.5 ± 4.6
	639.5	129.90 ± 11.44	322.5 ± 5.1
	951.4	62.05 ± 7.25	335.8 ± 6.8
ORB 94	82.1	10.63 ± 2.08	34.2 ± 11.3
	190.7	31.76 ± 3.54	62.0 ± 6.1
	237.9	76.78 ± 6.75	114.0 ± 4.9
	566.7	91.20 ± 9.64	153.6 ± 5.5
	639.5	149.70 ± 14.9	270.2 ± 4.8
	951.4	153.59 ± 8.53	302.4 ± 3.4

Table 5.3 Estimated Response of Tilt to Surface Temperature (Error bars are estimated standard deviations).

Pendulum	Period (hours)	Gain ($\hat{G}$) (msec/mbar)	Phase ($\hat{\Phi}$) (degrees)
ORB 95	97.1	3.56 ± 1.34	77.3 ± 21.3
	144.2	9.67 ± 1.40	109.9 ± 8.1
	156.4	3.18 ± 1.42	236.0 ± 23.8
	174.1	5.93 ± 1.32	328.0 ± 13.2
	218.5	8.24 ± 1.21	138.0 ± 8.5
	513.3	37.01 ± 3.35	350.6 ± 5.5
	1079.0	137.87 ± 8.42	352.2 ± 3.3
ORB 94	97.1	7.47 ± 1.13	301.1 ± 8.7
	144.2	18.98 ± 1.40	93.7 ± 4.4
	156.4	11.22 ± 1.22	302.4 ± 6.2
	174.1	18.82 ± 1.33	340.9 ± 4.1
	218.5	6.67 ± 1.17	71.2 ± 8.4
	513.3	77.30 ± 6.14	321.7 ± 3.9
	1079.0	35.29 ± 5.34	253.2 ± 5.5

Table 5.4 Estimated Response of Tilt to Atmospheric Pressure. (Error bars are Estimated Standard Deviations).

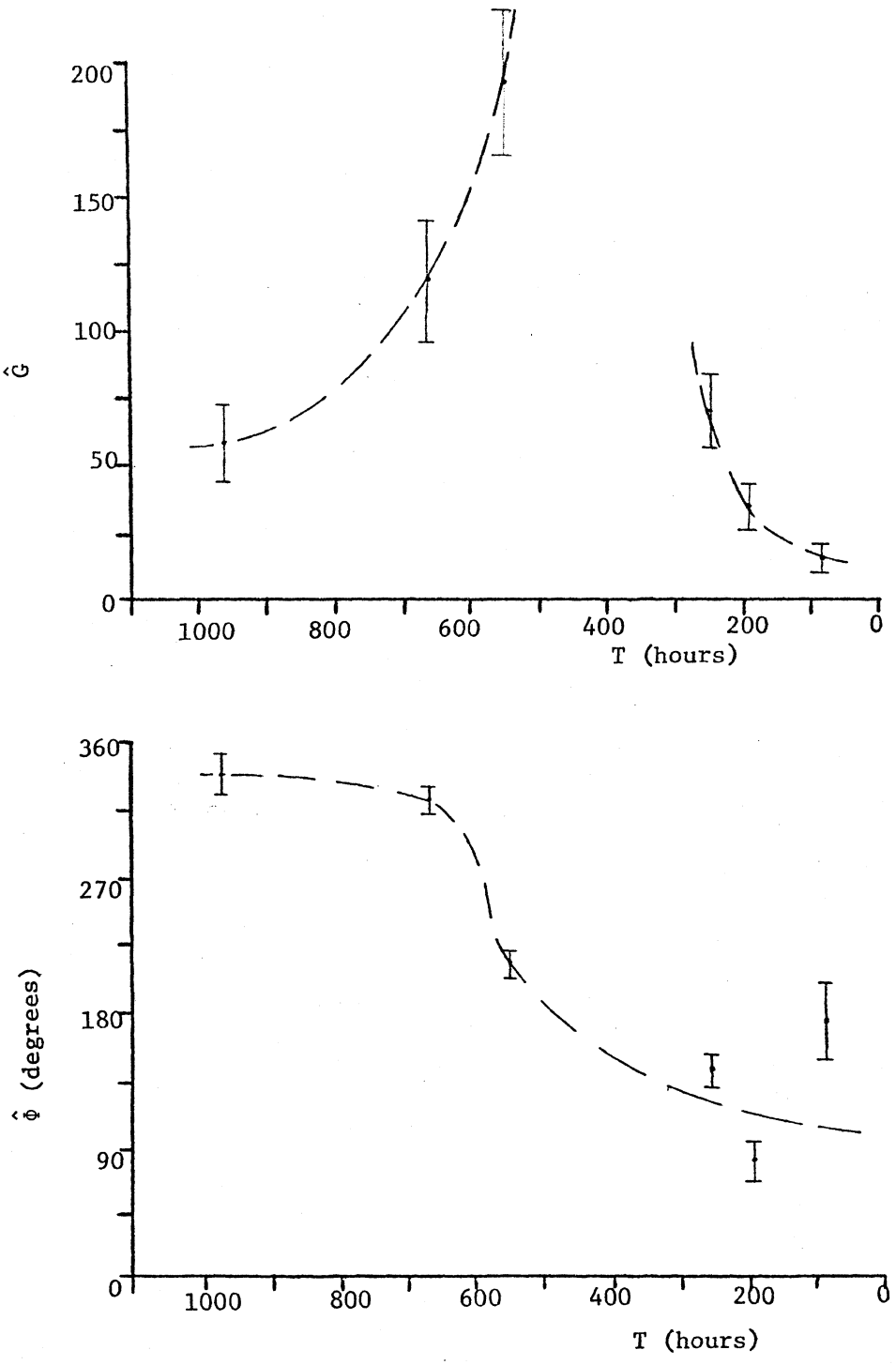

Figure 5.3 Estimates of ORB 95 Tilt Response To Temperature with 95% Confidence Intervals.

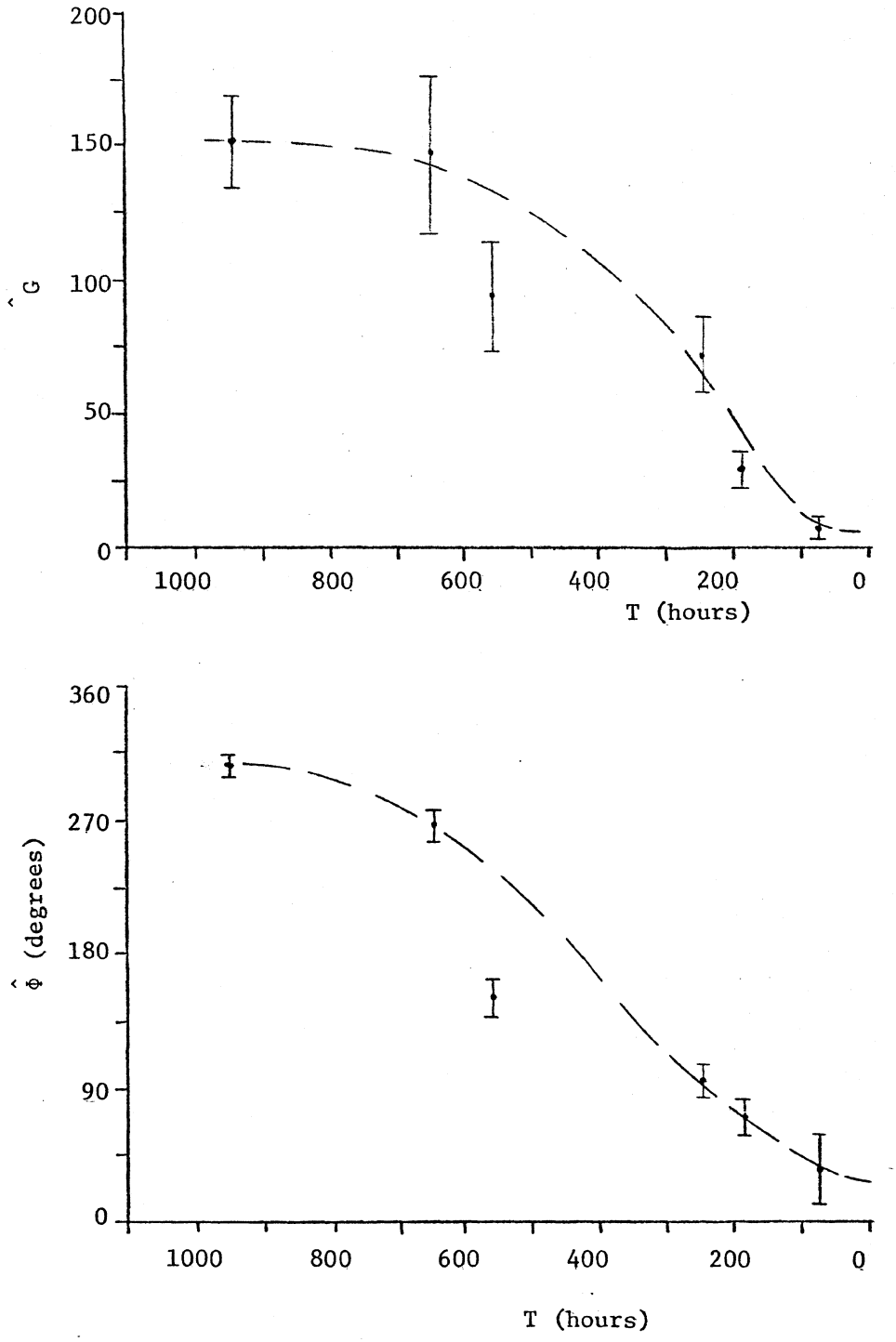

Figure 5.4 Estimates of ORB 94 Tilt Response To Temperature with 95% Confidence Intervals.

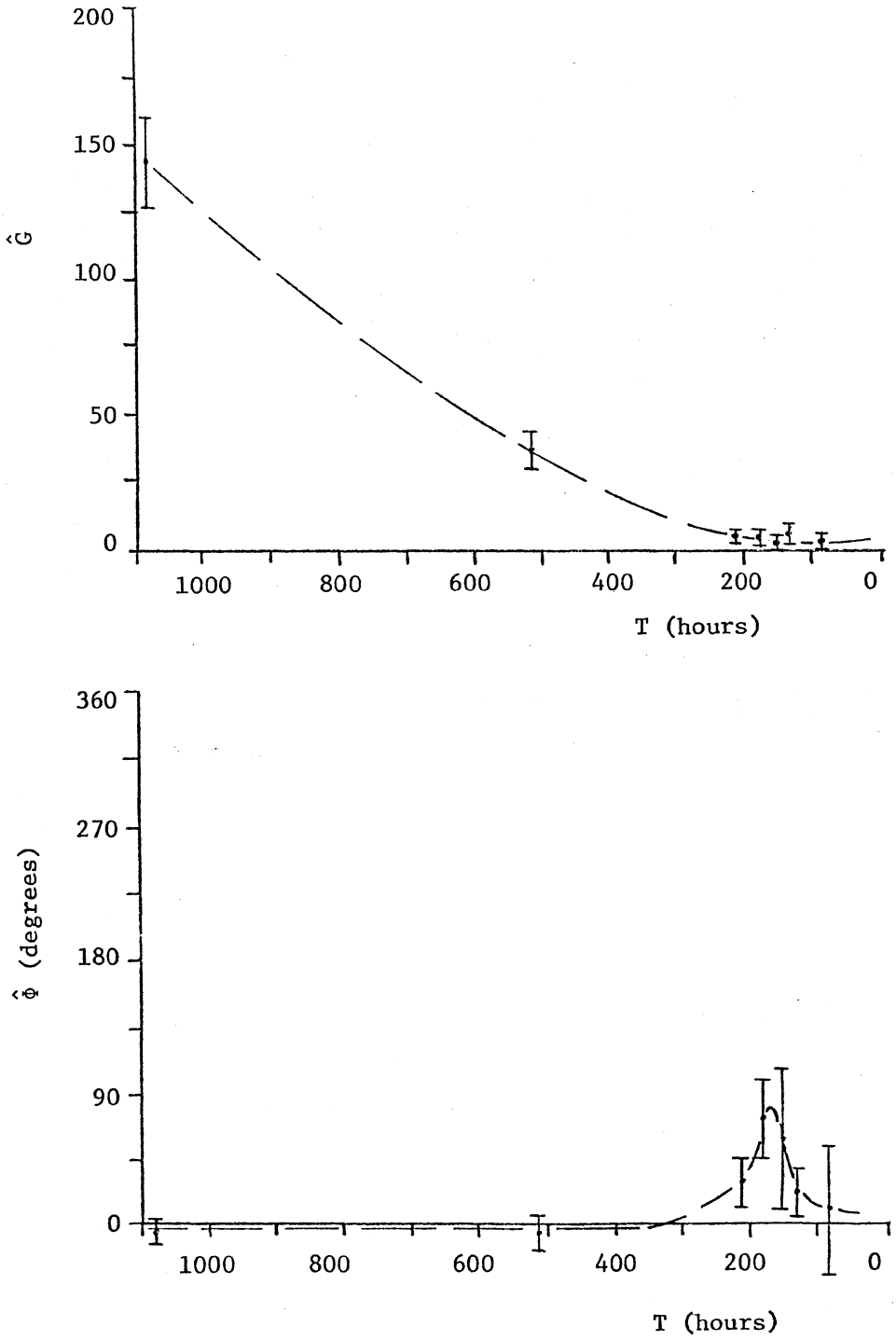

Figure 5.5 Estimates of ORB 95 Tilt Response To Atmospheric Pressure with 95% Confidence Intervals.

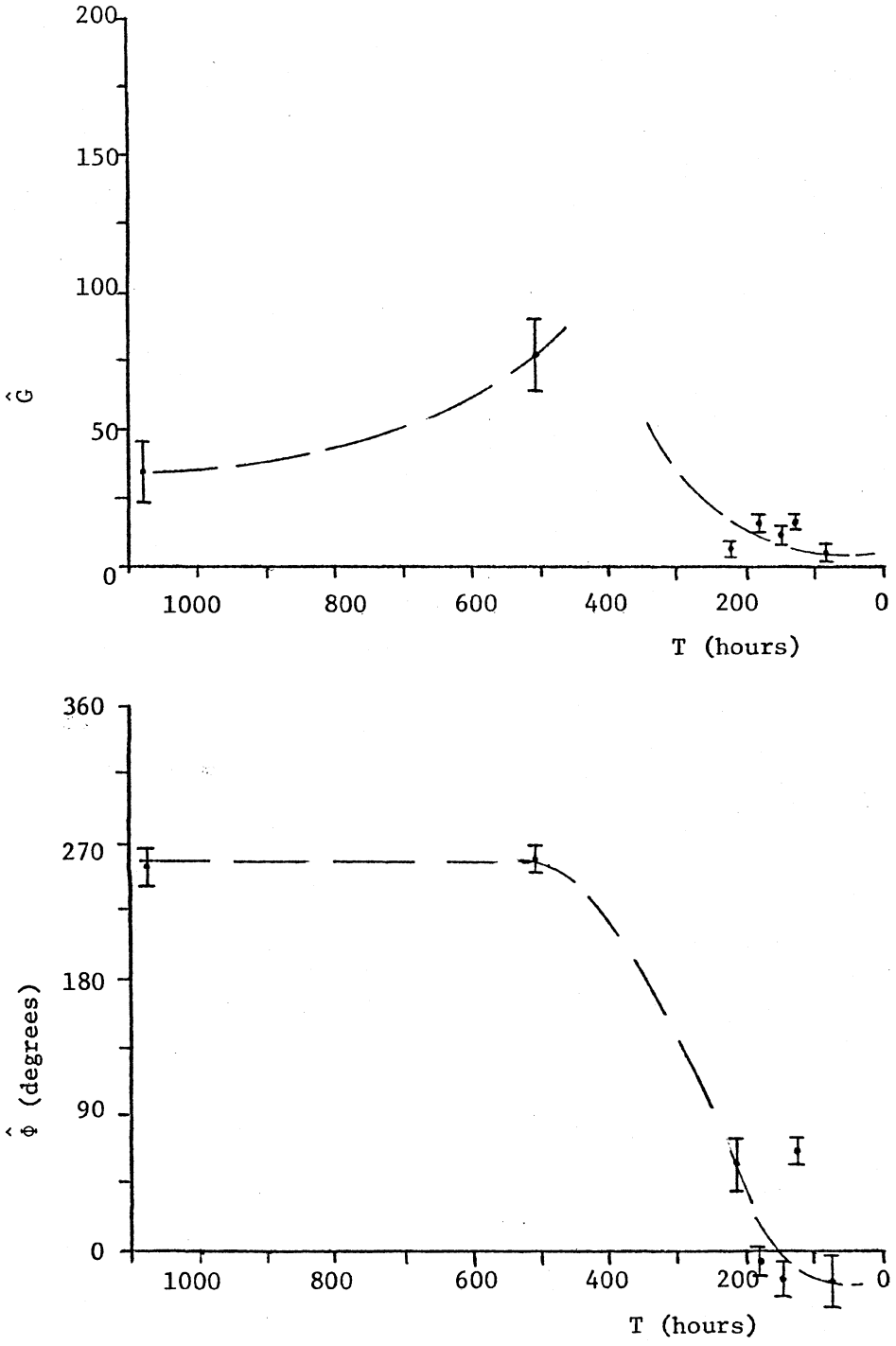

Figure 5.6 Estimates of ORB 94 Tilt Response To Atmospheric Pressure with 95 % Confidence Intervals.

agreement with our extrapolated estimates using the smoothed response functions (see Figures 5.3 and 5.4).

The smoothed tilt response to pressure and temperature was formed as numerical functions on the basis of the smoothed response functions following the procedure described in Chapter 4 (equation 4.28). This was done for both pendulums ORB 95 and ORB 94, for two cases: for the first case we did not include an (extrapolated) 24 hour period for temperature response, for the second we did. The resulting numerical functions were then forced as systematic noise in the observed tilt (along with the eight diurnal and semi-diurnal major tidal constituents, a linear trend and datum biases). The resulting test coefficients ($\hat{c}_f$) of these numerical functions which were identical for both above mentioned cases, are given in Table 5.5 along

Pendulum	c_f (temperature)	c_f (pressure)
ORB 95	0.97 $\pm$ 0.02	0.95 $\pm$ 0.02
ORE 94	0.79 $\pm$ 0.02	1.19 $\pm$ 0.02

Table 5.5. Estimated coefficients of smoothed tilt response numerical functions and their estimated standard deviations.

with their estimated standard deviations. We see that the test coefficients for ORB 95 are, at the 95% confidence level, not significantly different from unity since unity lies within the 95% confidence intervals given by 1.96 $\hat{\sigma}$. This indicates both the numerical integrity of the computer program used for these computations and the fact that our smoothed response estimates do not

depart significantly from their least squares estimates. However the test coefficients for ORB 94 are significantly different from unity which reflects the departure of our smoothed response function from the least square estimates (see Figures 5.4 and 5.6).

Let us now compare the estimated amplitudes and phases of the M_2, O_1 and S_1 tidal constituents for the cases of ignoring or modelling the smoothed tilt responses to pressure and loading. These results are given in Table 5.6; for the case of modelling these smoothed responses we have not considered here the extrapolated 24 hour temperature response. In Table 5.7 we give the estimated

Pendulum	Constituent	Temp. and Press. Effects Ignored		Temp. and Press. Smoothed Responses Removed (except 24 hour temp. response)	
		amplitude (msec)	phase (degrees)	amplitude (msec)	phase (degrees)
ORB 95	M_2	17.54±3.56	19.2±11.6	17.66±2.18	20.7±7.1
	O_1	5.63 ±3.56	82.8±36.2	6.06±2.18	76.6±20.6
	S_1	8.20±1.76	280.9±12.2	12.15±2.19	280.9±10.3
ORB 94	M_2	12.03±3.61	59.8±17.2	12.81±2.61	56.4±11.7
	O_1	0.73±3.63	344.7±284.6	2.32±2.58	285.9±63.5
	S_1	0.70±0.56	326.1±45.4	4.07±2.72	299.4±38.2

Table 5.6 Comparison of Estimated Amplitudes and Phases of M_2, O_1 and S_1 tilt constituents for ignoring or removing smoothed pressure and temperature responses (except 24 hour temp. response).

amplitudes and phases of the same three constituents for the case of including the smoothed (extrapolated) response to the 24 hour temperature constituent. We see that our response estimates are in general

not good: we are deteriorating our results (as witnessed by the increase in S_1 amplitude) instead of improving them when we force our response estimates. However, we note that we have significantly reduced the variance of tilt series as indicated by the smaller standard deviations of the estimated amplitudes and phases. Note that, as mentioned in Section 3.3, a simple regression of tilt on temperature and pressure did not reduce the variance of the tilt. This indicates that our frequency dependent modelling is at least partially successful.

It is felt that the main inadequacy of our response estimates lies in the limitations imposed in their interpretation by the limited available data. For the case of the temperature induced tilt we cannot, for example, attempt to separate instrumental tilt response to

Pendulum	Constituent	Temp. and Press. Smoothed Responses Removed (including the 24 hour temp. smoothed response.	
		amplitude (msec)	phase (msec)
ORB 95	M_2	17.66 ± 2.18	20.7 ± 7.1
	O_2	6.06 ± 2.18	76.6 ± 20.6
	S_1	47.55 ± 2.25	217.3 ± 2.6
ORB 94	M_2	12.81 ± 2.61	56.4 ± 11.7
	O_1	2.32 ± 2.58	285.9 ± 63.5
	S_1	13.74 ± 2.76	130.5 ± 11.3

Table 5.7 Estimated Amplitudes and Phases of M_2, O_1 and S_1 tilt constituents for the case of removing the smoothed pressure and temperature response (including the 24 hour temperature constituent).

pendulum chamber temperature variations from tilts arising from temperature induced deformations of the bedrock, without having records of the chamber temperature variations. In the case of atmospheric pressure, assuming the pressure induced tilts are caused by regional elastic bending of the crust, by measuring pressure variations only at the station itself we are subject to observing phase lags which are dependent on the relative location of the locus of the centre of the pressure high or low and the station. A simple idealized example will demonstrate this point. Suppose we have a circular high pressure area moving from north to south whose centre passes directly over the station. At the time when the centre of this high pressure area is directly over the station we would get, because of symmetry, a zero tilt response. this corresponds to a 90 degree phase lag of tilt response to pressure. However if the centre of the pressure high is moving from north to south but having its centre offset somewhat from the station we would get a maximum tilt in the east-west direction at the same time as we observe a maximum in the atmospheric pressure. This corresponds to a zero degree phase lag of tilt response to pressure. This illustrates the necessity, in order to meaningfully model the pressure induced tilts, to observe pressure variations at, for example, a grid of points surrounding the station.

The complexity of our smoothed response functions (for example the apparent resonances) may be questioned. However, when examining the possibility of simpler response functions by choosing other smooth response functions, which departed significantly from our least squares estimates of response, the results deteriorated even more. This also indicates the possibility of the response functions

appearing complex simply because of interpretation limitations imposed by our limited available data. In order to further study the tilt response to local phenomena at the Fredericton station it thus appears that, in order to arrive at meaningful results, we must include more information in our analysis in the form of, for example, chamber and bedrock temperature measurements and atmospheric pressure measurements at locations other than at the station itself.

Another major cause of difficulty in estimating response gains and phases from the tilt data is the backlash effect. Because no attempt has been made to measure the amount of freedom of movement of the light spots across the liight spot followers, and no record was kept when adjustments were made to the light spott followers, it is impossible to reliably correct the tilt measurements for this effect.

CHAPTER 6

CONCLUSIONS AND RECOMMENDATIONS

We have set out to model the observed tilt response to observed atmospheric pressure and surface temperature variations at the Fredericton tiltmetric station. Taking the empirical approach of attempting to model these interactions on the basis of our observed time series we were confronted with the problem of estimating response functions from noisy, gappy data. This led to the development, after an evaluation of the existing cross-spectral and time domain convolution approaches showed their inadequacy for our purposes, of a least squares response method having its basis in the least squares spectral analysis (Vanicek, [1971]). The application of this method has been demonstrated through a numerical example consisting of generated time series with gaps and superimposed noise. The success of the method in

the case of noise to signal ratios up to 2, with noise superimposed both on input and output, has been demonstrated by Merry and Vanicek [1981] whose results are summarized in Appendix III of this report.

The least squares response method has been applied to the Fredericton tiltmetric station data in an attempt to model the atmospheric pressure and surface temperature induced tilts. The limited success of this application, as summarized in Chapter 5, is believed to be due basically to two reasons. First of all we have considered only surface temperature and atmospheric pressure as input forcing phenomena; we have ignored all other local perturbances such as ground water variations, precipitation, pendulum chamber temperature, etc. This of course results in distortion of our estimates of tilt response to surface temperature and atmospheric pressure. Secondly, because of restrictions imposed by the limited available data, we have not considered, in our modelling, a physical interpretation of the estimated responses of tilt to temperature and pressure. We have shown, for example, that the phase response of tilt to pressure depends on the spatial relationship of the paths of the centres of high or low pressure areas as they move across the region.

On the basis of this study of the Fredericton tiltmetric station the following recommendations and suggestions for future work are offered.

1. A more complete observation programme should be initiated. This has been partially affected already by continuous observations of tiltmeter chamber and bedrock temperature variations which will allow both a determination of the characteristics of temperature penetration in the overburden and the identification of possible

temperature induced instrumental tilts. Observations of precipitation and ground water fluctuations should be also made at the station since, as indicated by Bower [1981], tilts induced by these phenomena can be significant.

2. We have shown that physical and spatial interpretations of tilts induced by local phenomena are necessary. Perhaps with synoptic records of atmospheric pressure variations, along with the observations of pressure at the station, a spatial interpretation of pressure induced tilts can be attempted.
3. Once it becomes available, all data collected at the Fredericton station should be included in the analysis. This will require a calibration of the 1977-79 tilt data and digitization of the observed temperature and pressure records.
4. The Verbaandert-Melchior horizontal pendulums are operating well but have limited operating ranges causing the reflected light spot to move off the recording limits of the light spot follower much too often, especially during times of large atmospheric pressure changes. Without frequent visits to the station by the attendant, whose presence also perturbs the recorded tilt, the recorded tilt series are thus necessarily gappy. This can be alleviated by replacing the Verbaandert-Melchior pendulums by the Stacey mercury level tiltmeters (Stacey et al [1969]) which have larger operating ranges. It is felt that this measure would greatly improve the quality of tilt recordings at the station and is therefore strongly recommended.

5. We have shown that atmospheric pressure induced tilts have magnitudes in excess of the tidal tilts. Assuming that these tilts are a result of regional elastic crustal bending it is obvious that corrections for this effect must be applied to, for example, precise geodetic levelling. Consideration of this effect may shed some light on the evasive, approximately 2 metre, discrepancy in results of trans-Canadian levelling.

APPENDIX I

ANALYTICAL AND GRAPHICAL REPRESENTATIONS OF PERIODIC TILT VARIATIONS

Because they could not be found collectively elsewhere and for the sake of completeness, descriptions of methods commonly used to represent tilt variations are given here.

I.1 Analytical Representations of Tilt

Tilt of the local gravity vector is a two-dimensional phenomenon and we can therefore completely describe or represent it in terms of tilt along two nonparallel plane coordinate axes in the astronomic horizon plane. Usually these two axes are chosen to be mutually orthogonal. Figure I.1 illustrates this representation. Each coordinate, T_p^1 and T_p^2, is thus time varying. The periodic variations of these coordinates can be represented by a sum of trigonometric terms of the form:

$$\phi_i(t) = a_i \cos \omega_i t + b_i \sin \omega_i t \ , \qquad (I.1)$$

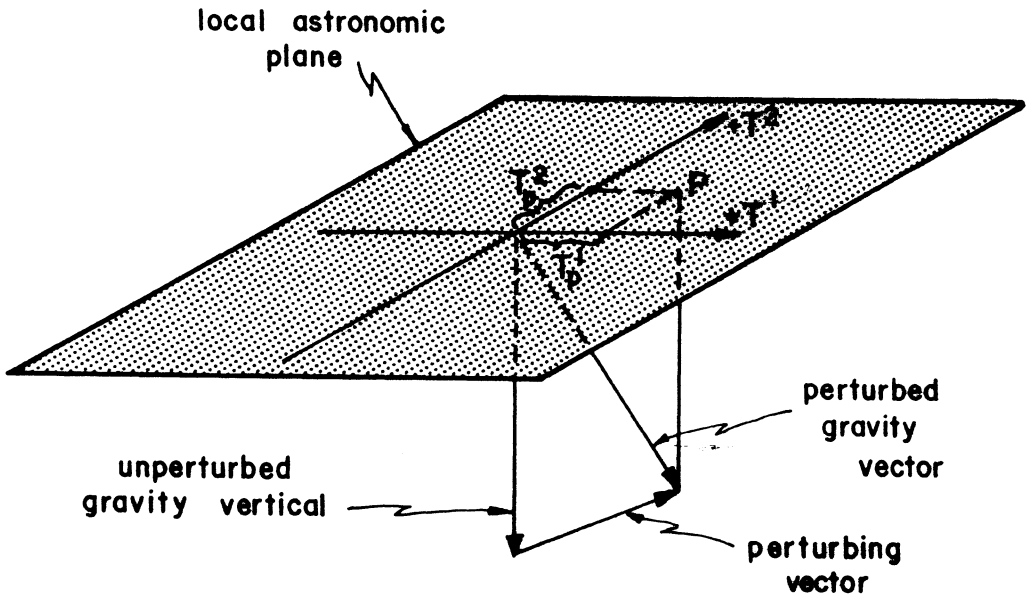

Figure I.1 Plane Representation of Tilt.

where ω is angular frequency, t is time and a_i and b_i are scalar coefficients. This can also be written as

$$\phi_i(t) = c_i \cos(\omega t - \phi_i) \qquad (I.2)$$

with amplitude

$$c_i = (a_i^2 + b_i^2)^{1/2} \qquad (I.3)$$

and phase lag

$$\phi_i = \arctan(b_i/a_i) \; . \qquad (I.4)$$

Since equation (I.4) has an ambiguity of π it is preferable to use

$$\phi_i = 2 \arctan\{b_i/(a_i+c_i)\} \qquad (I.5)$$

which is unambiguous.

Note that we have adopted a sign convention for tilt in Figure I.1. We thus define positive tilt in a direction +T to correspond to the case when the projection of the perturbing vector (see Figure I.1) is positive in that direction. This is the most common convention but it is not universally adopted.

Each constituent of Doodson's development [Doodson (1921); Melchior (1966)] of the luni-solar tides may thus be represented by equation (I.1) or (I.2). However in equation (I.2) we have chosen the phase lag ϕ_i to be the lag with respect to the term cos ωt, i.e. with respect to the arbitrary time origin. This is a cumbersome practice when we wish to compare results of analyses based on different time origins. Therefore it is preferrable to use instead the so-called "Greenwich phase lag" which we denote by g.

For a tidal constituent caused by a celestial body B the Greenwich phase lag is defined as the lag of the phenomena, as it occurs at the place in question, behind the upper transit time of B at the Greenwich meridian (both being referred to the same time origin). This requires more explanation in the case of tilt.

Let us consider, as an example, the M_2 constituent of the theoretical body tilt for a rigid Earth (see Chapter 2). For simplicity in our discussion we will consider the situation for north-south and east-west tilt at a latitude of 45°N. At the time of Moon's transit across the Greenwich meridian the tilt in the north-south direction, at the Greenwich meridian, is at its maximum towards south and is zero in the east-west direction. Because of our convention (explained earlier) the north tilt then leads (or lags) Moon's transit

by 180^{o}. Similarly, the east tilt leads Moon's transit by 90^{o}. We will now consider the effect on these Greenwich phase lags of our moving west through a longitude $\Delta\lambda$ away from the Greenwich meridian. Using M_2 as an example, at a specific fixed time, we would, in a change of longitude $\Delta\lambda = 360^{o}$, encounter exactly two tidal bulges (two wavelengths). Thus if we travel through a longitude $\Delta\lambda \leqslant 360^{o}$ we will be moving through a phase of $2\ \Delta\lambda$ with respect to the M_2 tidal bulges.

Thus for a place with west longitude λ (with respect to the Greenwich meridian) we have the following Greenwich phase lags of the theoretical rigid body tilt:

$$g^{E} = \eta\lambda - 90^{o} \qquad \text{(I-6)}$$

for the east component and

$$g^{N} = \eta\lambda - 180^{o} \qquad \text{(I-7)}$$

for the north component (where η is the "species" number of the constituent; 1 for diurnal, 2 for semi-diurnal, etc.).

Consider finally an observed phenomenon at a place P, with west longitude λ_p, whose east and north components lag the corresponding rigid body components at P by $\Delta\phi^{E}$ and $\Delta\phi^{N}$ respectively. (It is a simple matter to determine the phase lags of the rigid body tilt, with respect to an arbitrary time origin, using for example, a computer program written by Harrison [1971]). The Greenwich phase lags g_p^{E} and g_p^{N} of the observed phenomenon are thus given by

$$g_p^{E} = g^{E} + \Delta\phi^{E} \qquad \text{(I-8)}$$

and

$$g_p^{N} = g^{N} + \Delta\phi^{N}\ . \qquad \text{(I-9)}$$

We now consider briefly the transformation of Tilt T^O, observed in an arbitrary direction, to its east and north components. This situation is illustrated in Figure I-2 for an azimuth α. Expressing T^O as

$$T^O(t) = a^O \cos \omega t + b^O \sin \omega t \qquad \text{(I-10)}$$

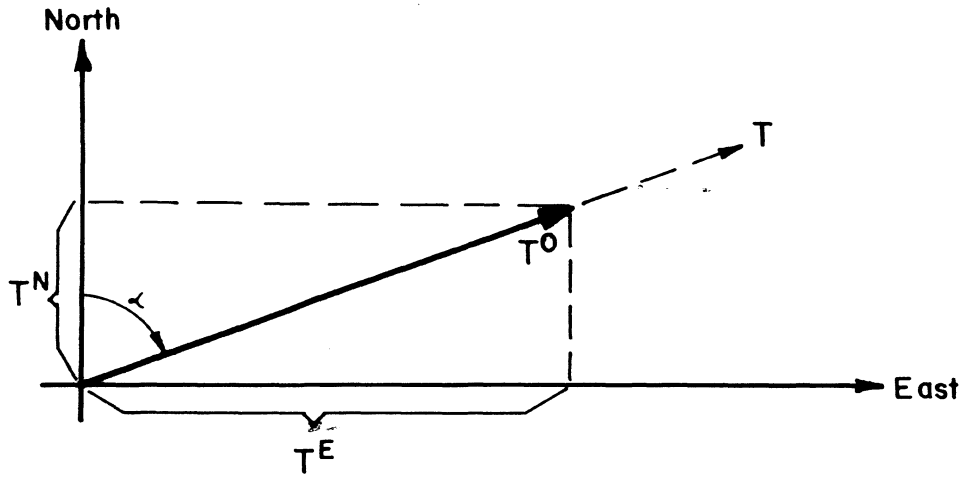

Figure I.2 Transformation of Tilt in Arbitrary Azimuth to East and North Components.

we have, from Figure I-2,

$$T^E(t) = T^O(t) \cdot \sin \alpha \qquad \text{(I-11)}$$

and

$$T^N(t) = T^O(t) \cdot \cos \alpha \qquad \text{(I-12)}$$

Substituting for $T^O(t)$ from (I-10) we have more explicitly

$$T^E(t) = a^E \cos \omega t + b^E \sin \omega t \qquad \text{(I-13)}$$

and

$$T^N(t) = a^N \cos \omega t + b^N \sin \omega t \qquad \text{(I-14)}$$

with

$$a^E = a^o \sin \alpha \qquad \text{(I-15)}$$

$$b^E = b^o \sin \alpha \qquad \text{(I-16)}$$

$$a^N = a^o \cos \alpha \qquad \text{(I-17)}$$

$$b^N = b^o \cos \alpha \qquad \text{(I-18)}$$

A similar approach can be used to transform tilt from one orthogonal system to another. This is illustrated in Figure I-3. For this case we get, when transforming T^o from (T_1, T_2) to (T_1', T_2'),

$$T_1 = \{a^{T_1'} \sin \alpha + a^{T_2'} \cos \alpha\} \cos \omega t + \{b^{T_1'} \cos \alpha - b^{T_2'} \sin \alpha\} \sin \omega t \qquad \text{(I-19)}$$

and

$$T_2 = \{a^{T_1'} \sin \alpha + a^{T_2'} \cos \alpha\} \cos \omega t + \{b^{T_1'} \sin \alpha + b^{T_2'} \cos \alpha\} \sin \omega t \qquad \text{(I-20)}$$

I.2 Graphical Representation of Tilt

We now turn to graphical methods for representing periodic tilt variations. The simplest graphical representation, although not the most revealing, is the simple vector or phasor plot (one for each of the two coordinate axes) showing the magnitude c and phase lag ϕ (or g). However it is difficult to merge these vector plots mentally in order to visualize the total character of the tilt variation. A more useful method is a plot of the "tilt ellipse" or "hodograph".

The tilt ellipse is simply a plot of the coordinates given by, for example, equations I-11 and I-12 which describes the motion of the projection of the gravity vector in the horizon plane. One complete revolution thus occurs in a time interval equal to the period of the constituent being considered. An example of the tilt ellipse is found in Chapter 3.

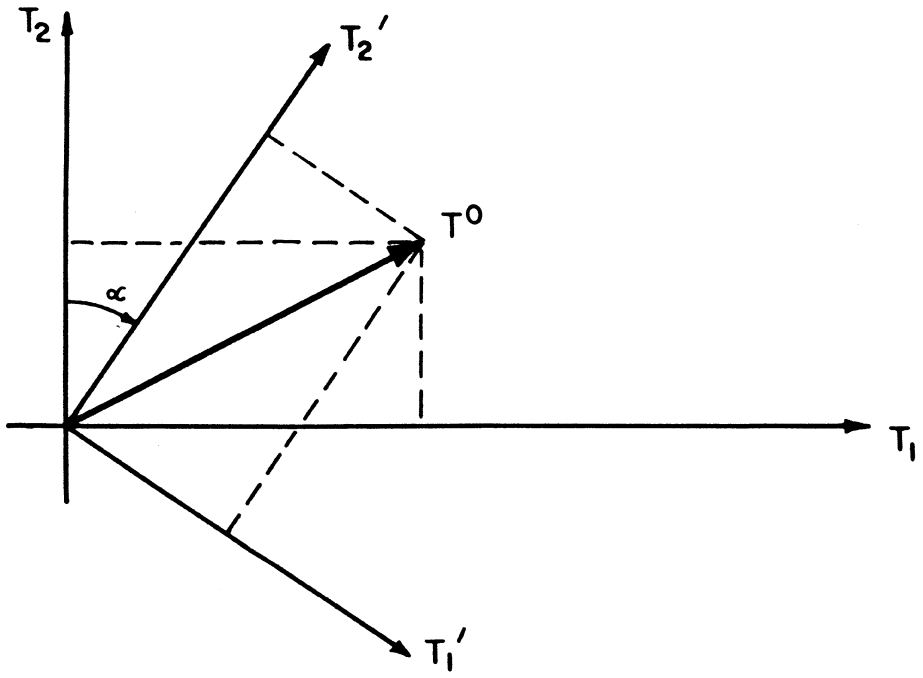

Figure I.3 Transformation of tilt from one Orthogonal Coordinate System to Another.

APPENDIX II

BACKLASH ERROR AND ITS EFFECT ON PHASE AND AMPLITUDE DETERMINATIONS.

A major source of systematic error in the determination of the phases and amplitudes of periodic constituents of an observed time series, using photo cell light spot followers, is the backlash error. In the case of the Fredericton tiltmetric station this error is caused by a small freedom of movement of the reflected light spot (causing no movement of the light spot follower) across the centre of the photo-cells of the light spot follower (see Chapter 3). The effect of this delayed response of the recording system is illustrated in Figure II-1.

One effect of this backlash error is a shifting of the wave ahead in time by 1/2 Δt (see Figure II-1). If the wave is given by $c \cos \omega t$ we see that the time Δt is related to Δh by

$$c - c.\cos (\omega \cdot \Delta t) = \Delta h \cdot \qquad \text{(II-1)}$$

Using the substitution

$$\Delta t = 2\Delta\phi/\omega \qquad \text{(II-2)}$$

we get

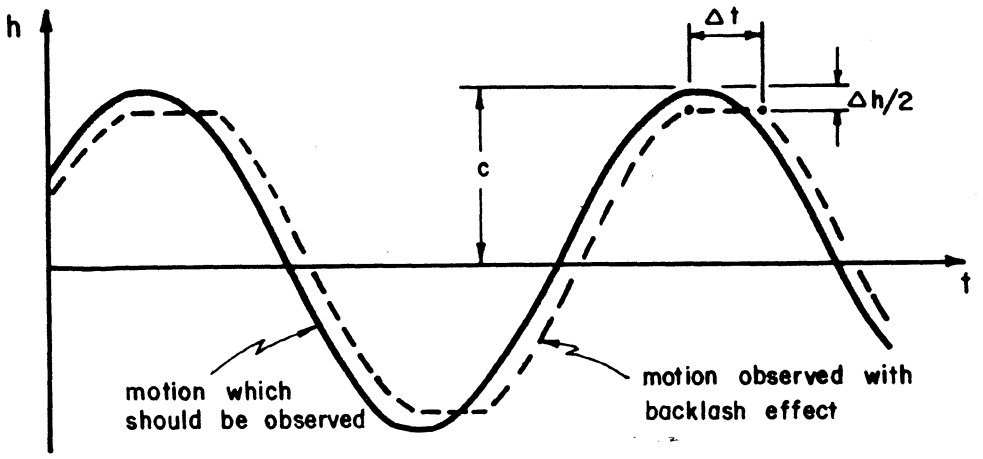

Figure II.1 Effect of Backlash Error.

$$\Delta\phi = \frac{1}{2} \arccos\left(1 - \frac{\Delta h}{c}\right). \qquad \text{(II-3)}$$

The phase shift caused by backlash is thus a function of the ratio $\Delta h/c$. For a given Δh we can therefore reduce the effect by increasing c, i.e. by increasing the sensitivity of the pendulums. Figure II-2 shows this effect for various Δh and c. We see that it is critical that the light spot follower is properly adjusted so that Δh approaches zero. Even for Δh = 0.1 mm we get a phase shift of 5.7 degrees for a recording amplitude of 5 mm. (A 5 mm recording amplitude for M_2 is the maximum practicable at the Fredericton station.

The other effect of the backlash error is its effect on amplitude. Assuming the actual wave is given by c . cos ωt and that the digitized time series is the "clipped" form

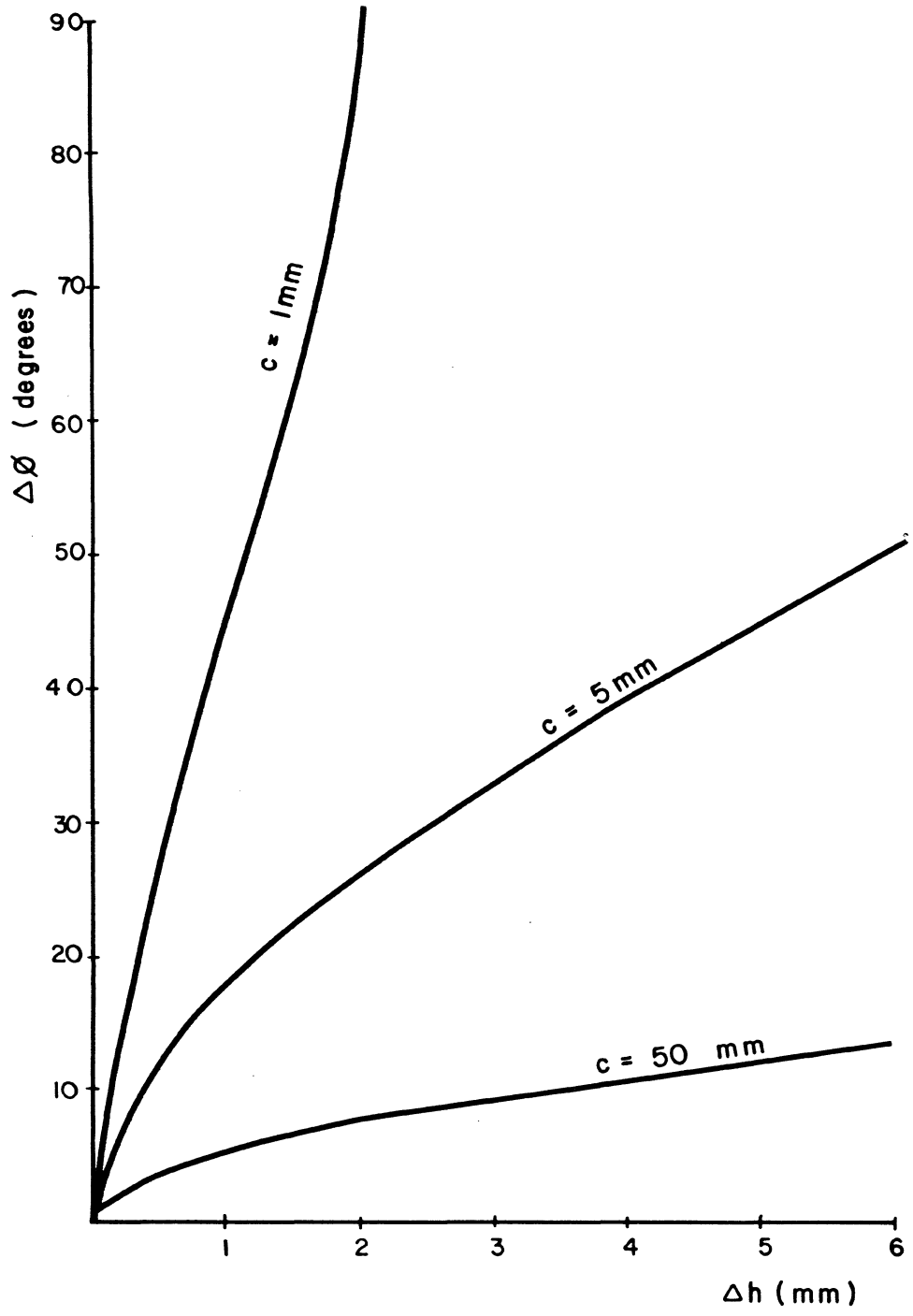

Figure II.2 Effect of Backlash Error on Phase

$$f_i = \min \{c \cdot \cos \omega t_i, f^{max}\} \cdot \text{sign} \{c.\cos \omega t_i\} , \qquad \text{(II-4)}$$

$i = 1, 2, \ldots, n$ where

$$f^{max} = c - \Delta h/2 \qquad \text{(II-5)}$$

we can compute the least squares estimate for c from

$$\hat{c} = \frac{\sum_{i=1}^{n} \{\cos (\omega t_i) \cdot f_i\}}{\sum_{i=1}^{n} \cos^2 \omega t_i} . \qquad \text{(II-6)}$$

This effect is illustrated in Figure II-3. Hourly values for t = 1, 2, ..., 30 were used in equation II-6 for the M_2 frequency. For n > 30 change in $\hat{c}$ is insignificant. Also, variations in the absolute magnitude of c, from c = 1 mm to c = 10 mm, cause no significant variation of Figure II-3.

Note that for c = 5 mm and Δh = 0.5 mm we get phase shift of 13 degrees and an amplitude distortion of only 1 per cent. It is clear then that significant phase distortion can be caused by backlash with corresponding imperceptible amplitude distortions.

The results of this Appendix are considered in Chapter 3 for the analysis of the data collected at the Fredericton station.

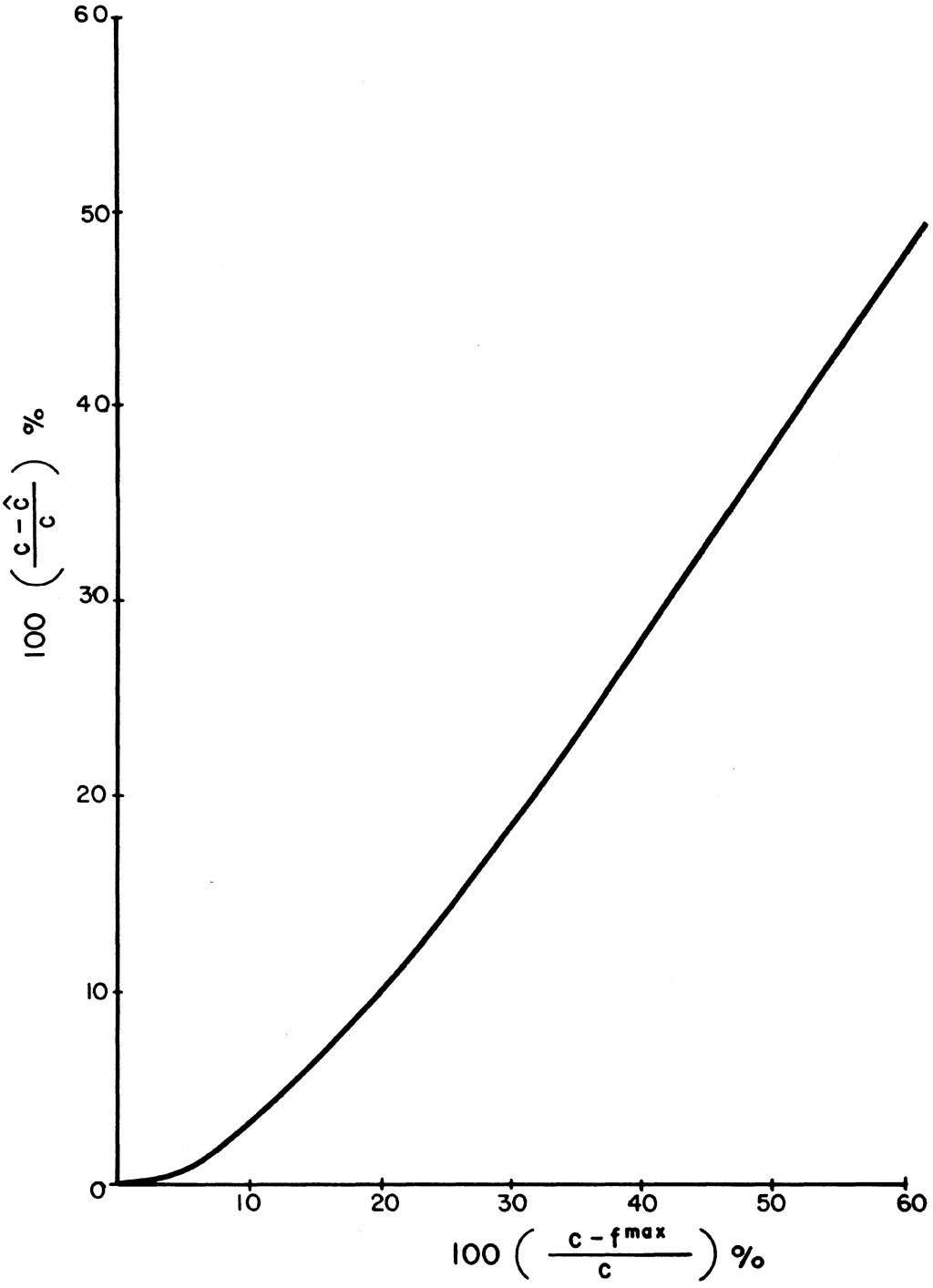

Figure II.3 Effect of Backlash Error on Amplitude.

APPENDIX III

REVIEW AND EVALUATION OF THE CROSS-SPECTRAL AND CONVOLUTION METHODS OF RESPONSE ESTIMATION

In order to evaluate existing methods of response estimation as a function of frequency for application to the Fredericton tiltmetric station data we give a brief review of these methods here. We begin by introducing the linear system representation using the well known convolution integral.

III.1 The Linear System Principle

The term "system" is used to signify a process which transforms an "input" x(t) into an "output" y(t); this process is illustrated in Figure III-1. A linear system is one which can be completely described by a linear operator $\mathcal{L}$ which has the homogeneous property

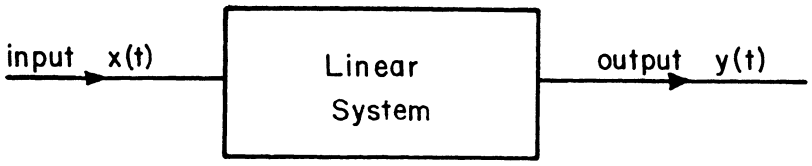

Figure III.1 Schematic Representation of a Single Input Linear System.

$$\mathcal{L}(c.x(t)) = c.\mathcal{L}(x(t)) \qquad \text{(III.1)}$$

where c is an arbitrary constant, and the additive property

$$\mathcal{L}\left(\sum_{i=1}^{n} c_i.x_i(t)\right) = \sum_{i=1}^{n} c_i.\mathcal{L}(x_i(t)) \ , \qquad \text{(III.2)}$$

where c_i, i = 1, 2, ..., n are arbitrary constants. The linear system output is related to its input by the convolution integral (e.g. Bendat and Piersol [1971])

$$y(t) = \int_{-\infty}^{\infty} w(\tau) \ . \ x(t-\tau) \ d\tau \ . \qquad \text{(III.3)}$$

For physically realizable systems the lower limit of integration in equation (III.3) becomes zero. We assume the system is stable, that

is every bounded input produces a bounded output (op cit). Note also the assumption of constant parameters embedded in equation (III.3), i.e. the weighting function, or impulse response function, $w(\tau)$ is not a function of time t but only a function of time lag τ.

For constant parameter, linear, physically realizable systems the response function, which is here defined as the Fourier transform of the weighting function, is given by (op cit)

$$W(\omega) = \int_0^\infty w(\tau).e^{-j\omega\tau} d\tau \qquad \text{(III.4)}$$

where ω is angular frequency and $j = (-1)^{1/2}$. Taking the Fourier transform of both sides of equation (III.3) yields

$$Y(\omega) = W(\omega) \; . \; X(\omega) \qquad \text{(III.5)}$$

where $Y(\omega)$ and $X(\omega)$ are Fourier transforms of an output $y(t)$ and corresponding input $x(t)$ respectively. $W(\omega)$ can be written in complex polar notation as

$$W(\omega) = \left|W(\omega)\right|.e^{-j\phi(\omega)} \qquad \text{(III.6)}$$

where $\left|W(\omega)\right|$ is called the gain (i.e. the ratio of the amplitude of an output sinusoid of frequency ω to the amplitude of the corresponding input sinusoid) and $\phi(\omega)$ the phase (i.e. the output phase minus the input phase) of the response.

By considering the lagged product $y(t).y(t+\tau)$ it can be shown (e.g. Jenkins and Watts [1968]; Bendat and Piersol [1971]) that cross spectral analysis can be used to estimate the response function. The fundamental result is the relation

$$G_{xy}(\omega) = W(\omega) \; . \; G_x(\omega) \qquad \text{(III.7)}$$

where the spectral density functions $G_{xy}(\omega)$ and $G_x(\omega)$ are the Fourier transforms of the input-output cross correlation functions and the input auto correlation functions respectively. We must note that a significant assumption is made in the development of equation (III.7), namely that the inputs are records from stationary random processes [Bendat and Piersol, 1971].

Estimates $\hat{G}_{xy}(\omega)$ and $\hat{G}(\omega)$, not detailed here, can be thus used in computing the estimate $\hat{W}(\omega)$ of the response function using equation (III.7), i.e.,

$$\hat{W}(\omega) = \frac{\hat{G}_{xy}(\omega)}{\hat{G}_x(\omega)} \quad . \tag{III.8}$$

III.2 Evaluation of Response Estimation Based on Cross Spectral Analysis

As already noted in the previous section, the cross spectral analysis approach to response estimation is based on the assumption of stationary inputs. Other considerations for linear system analysis are as follows (op cit).

1) The estimate $\hat{H}(\omega)$ is biased. According to Bendat and Piersol [1971] this bias error is "usually negligible compared to other bias and random errors in practice".
2) The spectral density estimates $\hat{G}_{xy}(\omega)$ and $\hat{G}_x(\omega)$ are themselves biased. This source of bias can be "quite significant at frequencies where spectral peaks occur" (op cit).

3) Measurement noise on the input causes bias in $H(\omega)$. For a spectral density of the measurement noise at the input which is 10% of the spectral density of the signal the resulting estimate $H(\omega)$ is biased downward by approximately 10% (op cit).

We note also that the computation of the cross and auto correlation functions for determining $G_{xy}(\omega)$ and $G_x(\omega)$ require that the data are equally spaced in time. Also, gappy data present obvious problems in computing these estimates of the correlation functions.

III.3 Evaluation of Response Estimation Based on the Convolution Method in the Time Domain

Discretization of equation (III.3) for application to equispaced discrete values of input and output results in

$$y(t) = \sum_{s=-S}^{S} W \cdot x(t - s.\Delta\tau) \qquad \text{(III.8)}$$

where $\Delta\tau$ is some preselected time interval. With preselected S and $\Delta\tau$, least squares estimates of the weights W_s, $s = -S, -S+1, \ldots, S$ can be computed on the basis of the given input and output. Once the weights are determined, the response estimate can be computed using the discrete Fourier transform (analogous to equation III.4). This method of estimating the response function is the basic approach employed by Munk and Cartwright [1966] for the analysis of sea level variations.

We note that this method, as it is thus far developed, is not designed for treating the case in which we have observation noise on

the inputs. Also the method cannot handle the case of unequally spaced data. Although this method is apparently used successfully in sea-level analysis an inherent requirement is the initial specification of both the lag interval $\Delta\tau$ and the number of weights to be used. In sea-level analysis using this method, a "credo of smoothness" is imposed on the response characteristics of the ocean (op cit) by selecting a small number of weights. This may or may not be realistic in other applications. In general the number of weights needed to characterize a system may be large and also the estimates of the weights are highly correlated in the same way that the estimates of the auto and cross-correlation estimates are highly correlated [Jenkins and Watts, 1968].

As shown by Yaramanci [1978], the method of this section is very closely related to the cross spectral analysis method, i.e. it uses the Wiener-Hopf integral (op cit) directly to determine the weights and the cross spectral method uses the Fourier transform of the Wiener-Hopf integral. We note also that equation (III.4) is based on the assumption that our data is stationary and infinite [Bendat and Piersol, 1971].

III.4 Numerical Comparisons of Cross-Spectral, Time Domain Convolution and Least Squares Response Estimation Methods

In this section a summary of numerical comparisons made by Merry and Vanicek [1981] of these three methods is given. For these comparisons one input series x(t) and one output series y(t) were generated according to

$$x(t_j) = c_o^x + \sum_{i=1}^{3} c_i^x \cos(\omega_i^x t_j - \phi_i^x) + n^x(t_j) \qquad \text{(III.9)}$$

$$y(t_j) = c_o^y + \sum_{i=1}^{3} c_i^y \cos(\omega_i^y t_j - \phi_i^y) + n^y(t_j) \qquad \text{(III.10)}$$

$j = 1, 2, \ldots, 1024$ with two of the three frequencies common to $x(t)$ and $y(t)$. The noise terms $n^x(t)$ and $n^y(t)$ were calculated using a zero mean random number generator. The scale factors of the noise terms were varied to arrive at various noise to signal ratios defined by

$$r = \left\{ \frac{\sum_{i=1}^{1024} (n^x(t_i))^2}{\sum_{i=1}^{1024} (x(t_i) - n^x(t_i))^2} \right\}^{1/2} \qquad \text{(III.11)}$$

Fast Fourier transform routines (IMSL package at the U.N.B. Computing Centre) were used for computing the spectral density estimates $G_{xy}(\omega)$ and $G_x(\omega)$ for the cross spectral analysis.

For the convolution approach in the time domain, equation (III.8) was programmed with the summation restricted to $s = 0, 1, \ldots, S$, i.e. causality was enforced. Values of $\Delta\tau = \Delta t = t_{i+1} - t_i$ and $S > 9$ ($S = 12$ was used) were found to give best results. For both the cross spectral analysis and the time domain convolution approaches, the datum biases c_o^x and c_o^y had to be removed before the analysis. In the least squares response estimation these biases were treated as systematic noise (see section 4.2).

Average percentage errors of the response amplitudes and phases were computed for various noise to signal ratios for all three methods in two cases: i) noise on the output only (Figure III.2) and ii) noise on both input and output (Figure III.3). For the first case

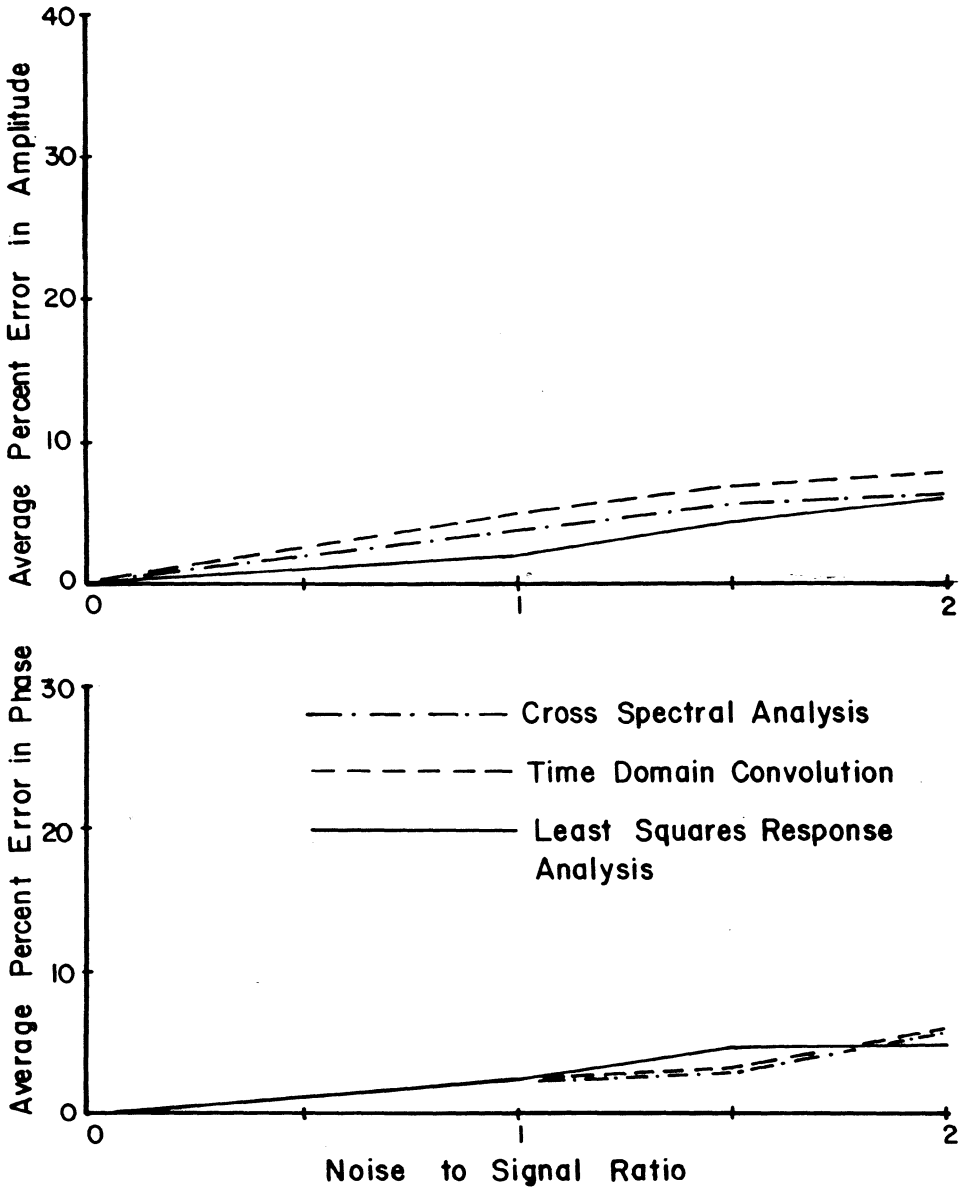

Figure III.2 Percentage Error of Response Estimates for the Case of Noise on Output Only (from Merry and Vaníček [1981]).

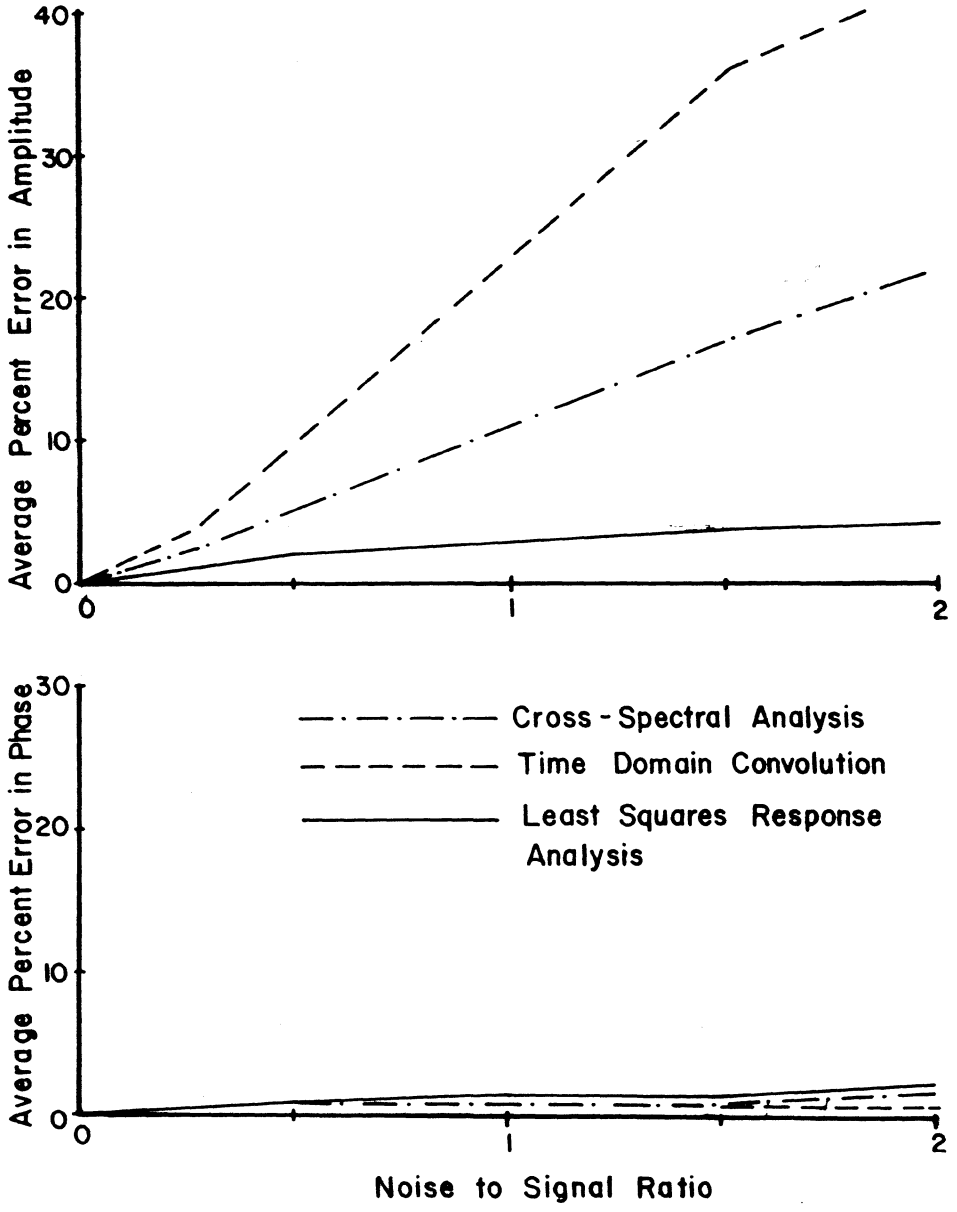

Figure III.3 **Percentage Error of Response Estimates for the Case of Noise on Both Input and Output** (from Merry and Vaníček [1981]).

all three methods perform equally well. However, for noise on the input the results deteriorate rapidly for the cross-spectral analysis method and even more so for the convolution method. On the other hand the least squares response method performs well even in the case of high noise to signal ratios.

REFERENCES

Baker, T.F. (1979). Tidal Tilt at Llanrwst, North Wales: Tidal Loading and Earth Structure. Geophys. J.R. Astr. Soc. 62, pp. 262-290.

Beaumont, C. (1980). Personal communication.

Beaumont, C.; R.D. Hyndman and M.J. Keen (1970). A New Technique for the Installation of Tiltmeters. Earth and Planetary Science Lettters 8, pp. 337-340.

Beaumont, C. and A. Lambert (1972). Crustal Structure from Surface Load Tilts, Using a Finite Element Model. Geophys. J.R. Astr. Soc. 29, pp. 203-226.

Beaumont, C. and R. Boutilier (1978). Tidal loading in Nova Scotia: results from improved ocean tide models. Canadian Journal of Earth Sciences 15, No. 6, pp. 981-983.

Bendat, J.S. and A.G. Piersol (1971). Random Data: Analysis and Measurement Procedures. Wiley-Interscience.

Bower, D.R. (1973). A sensitive water-level tiltmeter. Phil. Trans. R. Soc. Lond. A.274, pp. 223-226.

Bower, D.R. (1980). Personal communication.

Bower, D.R. (1981). Personal communication.

Bower, D.R. and K.C. Heaton (1976). Response of an Unconfined Aquifer to Atmospheric Pressure, Earth Tides and a Large Earthquake. Proc. of the Seventh International Symposium on Earth Tides, pp. 155-164.

Burke, K. (1972). Investigations of Potential Sites for Earth Tide Measurements in Central New Brunswick. Unpublished Report, Department of Geology, U.N.B., Fredericton, N.B.

Director, S.W. and R.A. Rohrer (1972). Introduction to System Theory. McGraw-Hill Book Company.

Doodson, A.T. (1921). The Harmonic Development of the Tide-Generating Potential. Proc. Royal Soc. A.100, No. A704.

Farrell, W.E. (1972). Deformation of the Earth by Surface Loads. Reviews of Geophysics and Space Physics, Vol. 10, No. 3, pp. 761-797.

Harrison, J.C. (1971). New Computer Programs for the Calculation of Earth Tides. Report of the Cooperative Institute for Research in Environmental Sciences, University of Colorado.

Harrison, J.C. (1976). Cavity and Topographic Effects in Tilt and Strain Measurements. Journal of Geophysical Research, Vol. 81, No. 2, pp. 319-328.

Harrison, J.C. and K. Herbst (1977). Thermoelastic Strains and Tilts Revisited. Geophysical Research Letters, Vol. 4, No. 11, pp. 535-537.

Herbst, K. (1979). Interpretation of Tilt Measurements in the Period Range Above that of the Tides. Technical Report 79-0093 of the Air Force Systems Command, USAF.

Jenkins, G.M. and D.G. Watts (1968). Spectral Analysis and Its Applications. Holden-Day Pub.

Jeudy, L. (1981). Theorie du Gyrocompas Suspendu et ses Applications a la Geodesie. Ph.D. Thesis, Dept. de Geodesie et de Cartographie, Universitie Laval, Quebec.

Lecalozet, R. (1977). Address to the Eighth International Symposium on Earth Tides. Proc. of the Eighth International Symposium on Earth Tides, 1977, pp. 23-29.

Lennon, G.W. and T.F. Baker (1973). The Earth Tide Signal and Its Coherency. Quarterly Journal of the Royal Astronomical Society 14, pp. 161-182.

Melchior, P. (1966). The Earth Tides. Pergammon Press.

Melchior, P. (1978). The Tides of the Planet Earth. Pergammon Press.

Merry, C.L. and P. Vanicek (1981). The Zero Frequency Response of Mean Sea Level to Meteorological Influences. Unpublished Technical Report of the Surveying Engineering Department, U.N.B., Fredericton.

Mikhail, E.M. (1976). Observations and Least Squares. IEP - A Dun Donnelley Publisher.

Munk, W.H. and D.E. Cartwright (1966). Tidal Spectroscopy and Prediction. Phil. Trans. of the Royal Society of London, A.259, No. 1105, pp. 533-581.

Peters, J.A. (1977). Results from a New 20 Metre Baselength Mercury Tiltmeter. Proc. of the Eighth International Symposium on Earth Tides, pp. 248-257.

Petrie, B. and R. Lively (1979). Offshore Meteorological Measurements with a CODS Discus Buoy. Atmosphere-Ocean 17 (2), pp. 169-176.

Skalsky, L. (1969). Determination of Azimuths of Simple Horizontal Pendula. Studia geoph. et geod. 13, pp. 400-416.

Stacey, F.D.; J.M.W. Rynn; E.C. Little and C. Croskell (1969). Displacement and Tilt Transducers of 140 dB range. Journal of Scientific Instruments Series 2, pp. 945-949.

Steeves, R.R. (1981). A Statistical Test for Significance of Peaks in the Least Squares Spectrum. Paper submitted for publication to Manuscripta Geodaetica, Dept. Surveying Engineering, U.N.B., Fredericton.

Taylor, J. and S. Hamilton (1972). Some Tests of the Vanicek Method of Spectral Analysis. Astrophysics and Space Science 17, pp. 357-367.

Vanicek, P. (1971). Further Development and Properties of the Spectral Analysis by Least Squares. Astrophysics and Space Science 12, pp. 10-33.

Vanicek, P. (1980a). Tidal Corrections to Geodetic Quantities. NOAA Technical Report NOS 83 NGS 14, U.S. Dept. of Commerce.

Vanicek, P. (1980b). Personal communication.

Wells, D.E. and P. Vanicek (1978). Least Squares Spectral Analysis. Bedford Institute of Oceanography, Dartmouth, N.S., Canada, Report Series BI-R-78-8.

Yaramanci, U. (1978). A Unified Approach To Signal Analysis in Earth Tides. Ph.D. Thesis, University of Liverpool, England.

Zschau, J. (1976). The Influence of Air Pressure Variations on Tilt Measurements With the Askania Borehole Pendulum at the Station Kiel-Rehmsberg. Proc. of the 7th International Symposium on Earth Tides, pp. 779-796.

Zschau, J. (1977). Air Pressure Induced Tilt in Porous Media. Proc. of the 8th International Symposium on Earth Tides, pp. 418-433.